ENZYME IMMOBILIZATION USING THE CELLULOSE-BINDING DOMAIN OF THE *CELLULOMONAS FIMI* EXOGLUCANASE

by

EDGAR ONG

B.S., University of Santo Tomas, 1983
M.Sc., Katholieke Universiteit Leuven, 1986

A THESIS SUBMITTED IN PARTIAL FULFILLMENT OF
THE REQUIREMENTS FOR THE DEGREE OF
DOCTOR OF PHILOSOPHY

in

THE FACULTY OF GRADUATE STUDIES
Department of Microbiology

THE UNIVERSITY OF BRITISH COLUMBIA
February 1992

In presenting this thesis in partial fulfilment of the requirements for an advanced degree at the University of British Columbia, I agree that the Library shall make it freely available for reference and study. I further agree that permission for extensive copying of this thesis for scholarly purposes may be granted by the head of my department or by his or her representatives. It is understood that copying or publication of this thesis for financial gain shall not be allowed without my written permission.

Department of MICROBIOLOGY

The University of British Columbia
Vancouver, Canada

Date 26 March 1992

ABSTRACT

A new strategy employing molecular genetic techniques to produce fusion polypeptides was used for enzyme immobilization. The cellulose-binding domain (CBD) of the *Cellulomonas fimi* exoglucanase (Cex) was used as an affinity "tag" by fusing the sequence encoding CBD_{Cex} to the 3'-ends of the genes encoding two ß-glucosidases, Abg and Cbg, from a mesophilic *Agrobacterium* sp. and a thermophilic bacterium, *Caldocellum saccharolyticum*, respectively. The resulting fusion polypeptides, Abg-CBD_{Cex} and Cbg-CBD_{Cex}, were purified to >95% homogeneity in a single step by affinity chromatography on cellulose using water as the desorbing agent. Protein recovery varied from 58-70%. The matrix, pH and temperature affected the reversibility of binding. These parameters can be selected to facilitate either purification or stable immobilization of the polypeptide.

Fusion of the affinity "tag" appeared not to affect the conformation of the fusion partners significantly, since their specific activities were not altered appreciably. Kinetic analyses revealed that the increase in apparent K_m of the immobilized Abg-CBD_{Cex} was not directly related to the fusion, but rather, to external mass transfer resistance. The percentage of activity retained by the immobilized enzyme was inversely related to the amount of fusion polypeptide adsorbed to cellulose. This was affected by the presence of an extra 57 amino acid residues between the fusion partners. Abg-CBD_{Cex} was stably adsorbed to cellulose between 4° to 50°; pH 3 to 8.5; and in the presence of up to 1 M NaCl. The immobilized Abg-CBD_{Cex} column exhibited long-term operational stability (at least 15 days at 37°) and gave 50-70% substrate conversion at the flow rates employed. At 50° Abg-CBD_{Cex} lost activity but remained bound to cellulose. Immobilized Cbg-CBD_{Cex} was stable at 70° for at least 3 days with no apparent

desorption of fusion polypeptide from the column. The use of a more crystalline cellulosic support improved the stability of binding of both fusion polypeptides.

A plasmid that expressed the gene encoding CBD_{Cex} alone was also constructed to facilitate biochemical analysis of the binding mechanism. CBD_{Cex} was purified from culture supernatant to > 98% homogeneity in a single step by batch affinity chromatography on cellulose. Unlike the fusion polypeptides, it was not desorbed with water. The presence of xylan in the CBD_{Cex} preparation affected its susceptibility to cleavage by pepsin. CBD_{Cex} bound stably to both amorphous and crystalline cellulose, and under a wide range of temperatures, pHs and detergent concentrations.

TABLE OF CONTENTS

LIST OF TABLES

LIST OF FIGURES

LIST OF ABBREVIATIONS

2F-DNPG	2',4'-dinitrophenyl-2-deoxy-2-fluoro-ß-D-glucopyranoside
$[N_o]$	Concentration of binding sites in the absence of protein
[P]	Protein concentration
$[P_o]$	Initial protein concentration
a	Number of lattice units occupied by a protein
Abg	*Agrobacterium* sp. ß-glucosidase
Abg-CBD_{Cex}	Fusion polypeptide between Abg and CBD_{Cex}
BMCC	Bacterial microcrystalline cellulose
BME	ß-mercaptoethanol
BSA	Bovine serum albumin
CBD	Cellulose-binding domain
CBD_{CenA}	CBD of CenA
CBD_{Cex}	CBD of Cex
Cbg	*Caldocellum saccharolyticum* ß-glucosidase
Cbg-CBD_{Cex}	Fusion polypeptide between Cbg and CBD_{Cex}
CD	Catalytic domain
CenA	*Cellulomonas fimi* endoglucanase A
Cex	*Cellulomonas fimi* exoglucanase
dH_2O	Distilled water
DNP	Dinitrophenolate
DTNB	5,5'-dithionitrobenzoic acid
DTT	Dithiothreitol
ε_{280nm}	Extinction coefficient at 280nm
FPLC	Fast protein liquid chromatography
GdmCl	Guanidinium chloride
IPTG	Isopropyl-ß-D-thiogalactoside

K_a	Equilibrium association constant
kbp	kilobase pairs
K_{cat}	Enzyme turnover number
kDa	kilodaltons
K_m	Michaelis-Menten constant
LB	Luria-Bertani
LP	Leader peptide
MUG	Methylumbelliferyl-ß-D-glucoside
pI	Isoelectric point
PMSF	phenylmethylsulfonylfluoride
pNP	*p*-nitrophenolate
pNPG	*p*-nitrophenyl-ß-D-glucopyranoside
PTH	Phenylthiohydantoin
PTIS	Portable translation initiation site
SDS-PAGE	sodium dodecyl sulfate-polyacrylamide gel electrophoresis
TPCK	*N*-tosyl-L-phenylalanine chloromethyl ketone
V_{max}	Maximum rate of enzyme reaction
X-glu	5-bromo-4-chloro-3-indolyl-ß-D-glucoside

ACKNOWLEDGMENTS

This work was supported by grants from the Natural Sciences and Engineering Research Council of Canada. Many people helped me along the way. I would like to express my sincere appreciation particularly to the following:

Doug Kilburn, my supervisor, for his enthusiasm, patience and excellent supervision, and for believing in my ability to accomplish things;

Tony Warren, Bob Miller and Neil Gilkes for their constant support, creative ideas and direction, and helpful discussion;

Emily Kwan for her technical help and friendship;

Helen Smith for providing every little thing that I needed to complete my experiments;

Don Trimbur for the use of TS Graph (version 2);

Gary Lesnicki and Lando Robillo for growing up cells in the fermentor;

The Wesbrook (now NiCE) Deputies for the friendship, Friday night's out, and informal, but substantial discussion (sciencewise or otherwise);

Everyone else in the Cellulase Labs, the Media Room and the Department for the laughter, care and camaraderie.

I lovingly dedicate this thesis to the memory of my mother, Mrs. Rose Ong (1931-1990), for her love and sacrifice up to the very end.

1. INTRODUCTION

1.1 Enzyme immobilization

Enzyme immobilization is an important aspect of biotechnology. It is a process by which movement of enzymes is restricted physically or chemically. It is a part of the much broader area of immobilization technology wherein proteins, other than enzymes (e.g., antibodies, receptors, etc.), and cells are fixed to or entrapped within a matrix. Enzymes can be immobilized by either binding or physical retention (Hartmeier, 1988). Binding to a support can be accomplished either directly by adsorptive, ionic or covalent attachment, or by cross-linking enzymes to the support using glutaraldehyde and similar agents. Enzymes can be retained physically either by matrix entrapment or by membrane enclosure. In most enzyme immobilization processes, the mechanisms overlap somewhat and several could function concurrently.

Enzymes are immobilized for the following reasons: (1) substrate conversion can proceed continuously rather than batchwise; (2) the products of bioconversion are free of enzymes; (3) the product yield per unit volume and time is increased; (4) the potential problem of substrate and/or product inhibition is substantially reduced especially in a column technique; (5) the immobilized enzyme often shows improved pH and temperature stability, and catalytic efficiency (Gianfreda *et al.*, 1985; Webster *et al.*, 1985; Baker *et al.*, 1988; Kimura *et al.*, 1989; Mozhaev, 1990; Reiken *et al.*, 1990; Mattiasson & Kaul, 1991). Efficiency and stability are the two most important parameters for a successful immobilized enzyme process (Monsan & Combes, 1988). The immobilized enzyme should maintain its native conformation, or, if changed, should retain a significant proportion of the catalytic activity of the soluble enzyme. The immobilized enzyme should remain bound and maintain its

catalytic activity for prolonged periods in continuous operation without the need for enzyme replenishment.

In 1916, Nelson and Griffin reported the first immobilization process in which invertase from yeast was bound to activated charcoal and still maintained catalytic activity. Significant advances in enzyme immobilization did not begin until the 1960s. In 1969, the first large-scale industrial application of an immobilized enzyme was demonstrated with the production of L-amino acids using bound L-aminoacylase (Chibata, 1978). Since the 1970s, immobilization technology has advanced beyond the simple one-enzyme type of hydrolytic/ isomeric reactions to include many novel immobilization processes utilizing a great variety of natural and chemically-modified supports. Recent examples include the use of immobilized cells/proteins for multi-step enzymatic reactions (Karkare, 1991; Kimura *et al.*, 1990a); for biochemical synthesis (Jayakumari & Pillai, 1990; Yoshida *et al.*, 1990; Kimura *et al.*, 1990b); for clinical diagnosis (Roda *et al.*, 1991; Chien *et al.*, 1991) and analytical biosensors (Guilbault, 1984; Lowe, 1984; Guilbault, 1988; Guilbault *et al.*, 1991; Huang *et al.*, 1991; Taylor, 1991); for detoxification of pesticides (Caldwell & Raushel, 1991); and for purification of target proteins (Baneyx & Georgiou, 1989; Greenwood *et al.*, 1989; Chen *et al.*, 1991). Several excellent reviews and monographs deal with the various aspects of immobilization technology (Chibata, 1978; Buchholz, 1979; Bernath & Venkatasubramanian, 1987; Hartmeier, 1988; Taylor, 1991).

Carbohydrases have been immobilized on a large number of supports by various modes with varying success in terms of the amount of activity retained after immobilization, i.e. the immobilization yield (Table 1.1).

Various supports have been used for immobilizing proteins. The ideal support should be (1) stable, insoluble and chemically inert, (2) porous and permeable, yet rigid and resistant to compression, and (3) cheap and reusable. Natural cellulose satisfies most of these requirements, and is readily available in

Table 1.1 Immobilization of carbohydrases

Enzyme	Support	Mode	IY[1]	Reference
ß-amylase	polystyrene/Al^{3+}	ionic	7	Roy & Hegde, 1987
ß-galactosidase	alumina	covalent/GA[2]	25	Nakanishi *et al.*, 1983
ß-galactosidase	hydrophobic cotton cloth	adsorption	50	Sharma & Yamazaki, 1984
ß-galactosidase	alginate	covalent/CD[3]	42	Domínquez *et al.*, 1988
ß-glucosidase	Sepharose	covalent	44	Kierstan *et al.*, 1982
ß-glucosidase	ConA-Sepharose	adsorption	93	Lee & Woodward, 1983
ß-glucosidase	alginate	covalent	30	Hahn-Hägerdal, 1984
ß-glucosidase	hydrophobic cotton cloth	adsorption	50	Sharma & Yamazaki, 1984
ß-glucosidase	PHSA[4]/PHEMA[5]	entrapment	50/26	Alfani *et al.*, 1987
ß-glucosidase	alginate	covalent/GP[6]	38	Fujikawa *et al.*, 1988
ß-glucosidase	acrylamide	entrapment	51	Roy *et al.*, 1989
ß-glucosidase	Sepharose	covalent	33	Roy *et al.*, 1989
ß-glucosidase	ConA-Sephadex	adsorption/GA	95/71	Husain & Saleemuddin, 1989
ß-xylosidase	alumina/$TiCl_4$	covalent	70	Oguntimein & Reilly, 1980
Cellulases	ConA-Sepharose	adsorption/ covalent-CNBr	9	Woodward & Zachry, 1982
Glucoamylase	DEAE-cellulose	ionic	61	Tomar & Prabhu, 1985
Glucose isomerase	porous glass beads	covalent	47	Strandberg & Smiley, 1972
Glucose isomerase	DEAE-cellulose	adsorption/ ionic	70	Chen *et al.*, 1981
Invertase	poly(ethylene-vinyl alcohol)	ionic	13	Imai *et al.*, 1986
Maltohexao-hydrolase	acrylamide	copolymeri-zation/radiation	75	Nakakuki *et al.*, 1983

[1] Immobilization yield (percentage of activity retained by immobilized enzyme);
[2] Glutaraldehyde; [3] Carbodiimide; [4] Genipin; [5] poly-human serum albumin; [6] poly-hydroxyethylmathacrylate

a variety of different forms (fibres, powders and papers). Reactive sites in cellulose may be generated for the covalent attachment of proteins (Chen *et al.*, 1981; Cannon *et al.*, 1984; Tomar & Prabhu, 1985; Jin & Toda, 1988; Dumitriu *et al.*, 1989). The principal disadvantages of this approach involving covalent attachment are the extra expense of the derivatized support, and the potential for conformational changes in the protein as a consequence of immobilization, which ultimately result in decreased catalytic activity.

1.2 Fusion polypeptides for enzyme immobilization

This thesis demonstrates the use of a new strategy for enzyme immobilization on cellulose in which a cellulose-binding domain (CBD) from a bacterial exoglucanase is fused to a heterologous enzyme by molecular genetic techniques (Ong *et al.*, 1989a). The hybrid polypeptide produced by this process binds to cellulose and retains the catalytic activity of the fused enzyme. The fusion of genes using molecular genetic techniques allows the production of hybrid polypeptides comprised of two or more separate functional domains (Bülow & Mosbach, 1991). In this way one can custom-design any desired protein, whose gene is available, fused to an affinity "tag". This affinity "tag" can be located at either the N- or C-terminus of the fusion partner, depending on whether fusion at one end inactivates the partner (Greenwood *et al.*, 1989; Ong *et al.*, 1989a). There are numerous examples in the literature describing the use of various affinity "tags" for purification of proteins (Sassenfeld, 1990). The design is basically similar for all of these hybrid polypeptides: the polypeptide of interest is fused to a peptide with high affinity for an appropriate ligand. A protease recognition site can be incorporated between the two partners allowing for the precise cleavage of the fusion protein to release the protein of interest. Under

appropriate conditions, the hybrid polypeptide can also be left adsorbed to the matrix for use in an immobilized enzyme reactor (Table 1.2).

Table 1.2 Immobilization of fusion polypeptides

Enzyme	Affinity tag	Support	Mode	Stability[1]	Reference
ß-glucosidase	CBD[2]	Cellulose	adsorption	70% > 15 days	Ong *et al.*, 1989a; 1991
ß-lactamase	Protein A	IgG on Sepharose 4B	adsorption	ND[3]	Baneyx *et al.*, 1990
GlcDHcys[44]*	Cysteine	Thiopropyl-Sepharose	adsorption	ND	Persson *et al.*, 1991
	+LDH[4]	Hollow fibre (< 15 K)	entrapment	56% at 2.5 days	Persson *et al.*, 1991
Bacterial luciferase	Protein A	IgG on Sepharose 4B	adsorption	ND	Lindbladh *et al.*, 1991

[1] continuous mode; [2] cellulose-binding domain; [3] not determined; [4] lactate dehydrogenase; * glucose dehydrogenase with Asp44Cys

1.3 Cellulose-binding domains

Cellulomonas fimi is a Gram-positive, aerobic, mesophilic, rod-shaped bacterium that produces a cellulase system composed of multiple enzyme components - some of which bind tightly to cellulose. The genes for the major cellulase components in *C. fimi* have been cloned, sequenced, characterized and expressed in *E. coli* (O'Neill *et al.*, 1986; Wong *et al.*, 1986; Owolabi *et al.*, 1988; Coutinho *et al.*, 1991; Meinke *et al.*, 1991). Two of the most well-characterized cellulases of *C. fimi* are endoglucanase A (CenA) and an exoglucanase (Cex)

(Figure 1.1). Both enzymes are glycoproteins with molecular masses of 53 kDa and 49.3 kDa, respectively. When produced in *E. coli* their molecular masses, determined by SDS-PAGE analysis, are 48.7 kDa and 47.3 kDa, respectively,

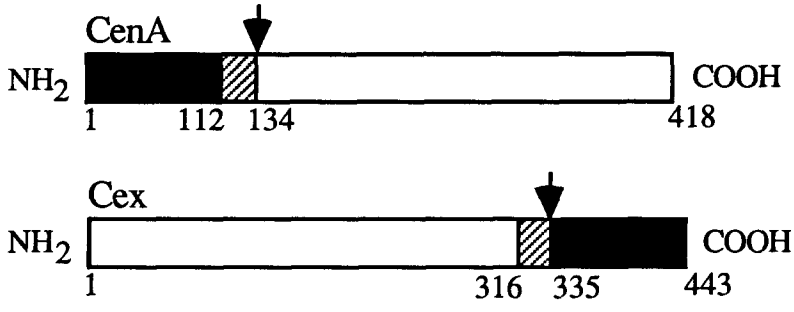

Figure 1.1 Domain arrangement in CenA and Cex. The catalytic domain (unshaded area) is separated from the cellulose-binding domain (shaded area) by a Pro-Thr linker (striped area). The numbers refer to the amino acid residues of the mature protein. The arrows refer to cleavage site by a *C. fimi* serine protease.

reflecting the lack of glycosylation in the recombinant forms. CenA and Cex are both composed of two domains, the catalytic domain (CD) and the cellulose-binding domain (CBD), separated from each other by a short linker composed principally of prolyl and threonyl residues, the Pro-Thr linker. The CD of Cex is found at the N-terminus and the CBD at the C-terminus. This arrangement is reversed in CenA. Proteolysis of recombinant CenA and Cex with a *C. fimi* serine protease releases a core peptide that retains enzymatic activity but no longer binds to cellulose (Figure 1.1; Gilkes *et al.*, 1988). The shorter peptide bearing the CBD could be selectively removed by adsorption to Avicel™ (Gilkes *et al.*, 1988). CenA and Cex are therefore enzymes containing two functionally independent domains separated by a linker sequence.

The CBDs of Cex and CenA are 108 and 111 amino acids long, respectively, and their sequences share more than 50% identity (O'Neill *et al.*, 1986; Wong *et al.*, 1986). Similar sequences are found in many cellulases and xylanases (Gilkes *et al.*, 1991b). The amino acid sequences of the *C. fimi*-type bacterial CBDs are highly conserved, with low numbers of charged amino acids, high contents of hydroxyamino acids, and conserved tryptophan, asparagine and glycine residues (Ong *et al.*, 1989b; Gilkes *et al.*, 1991b). Two conserved cysteine residues, which participate in disulfide bond formation in CenA and Cex, are found at the N- and C-termini in all CBDs but one (endoglucanase1 of *Butyrivibrio fibrisolvens*). Tryptophan residues are a feature of other proteins which interact with polysaccharides: the starch-binding domain of a glucoamylase from *Aspergillus niger* (Svensson *et al.*, 1989); the pilus-associated adhesion proteins in *E. coli* (Lund *et al.*, 1988), and an animal lectin carbohydrate-recognition domain (Drickamer, 1988). At present the only cellulase catalytic domain for which the three-dimensional structure has been solved is that of cellobiohydrolase II (CbhII) from *Trichoderma reesei* (Rouvinen *et al.*, 1990), but this and other fungal CBDs are structurally distinct from the *C. fimi* type.

Small-angle X-ray scattering analyses of CenA and Cex show that the molecules are tadpole shaped. The catalytic domain forms an ellipsoidal head region and the Pro-Thr linker and CBD forms an extended tail region (Pilz *et al.*, 1990; Shen *et al.*, 1991; Gilkes, unpublished results). The CBD of CbhI was synthesized chemically and shown by two-dimensional nuclear magnetic resonance spectroscopy to be wedge-shaped with two disulfide bridges (Kraulis *et al.*, 1989).

The mechanism and significance of binding of a CBD to cellulose are poorly understood. In a number of sugar-binding proteins found in the periplasm of Gram-negative bacteria, charged and aromatic amino acids are the

principal residues participating in the formation of an extensive hydrogen bond network and van der Waals interaction between the protein and the carbohydrate substrate (Quiocho, 1986; Johnson *et al.*, 1988). Tryptophan in particular is thought to play a role in substrate specificity by restricting the binding of sugar epimers because of steric hindrance or polarity of the hydroxyl groups (Quiocho, 1988). Some water molecules also participate in hydrogen bond formation. Other amino acid residues, especially the hydroxyamino acids, form a secondary shell around the principal amino acids, thereby allowing more hydrogen bond formation (Spurlino *et al.*, 1991).

1.4 Cellulose structure

Cellulose is the principal polysaccharide found in the cell walls of plants. It is a linear polymer of ß-D-glucopyranosyl units linked by ß-1,4-glucosidic bonds. Cellulose molecules have up to 10,000 glucopyranosyl units linked to form long chains of molecular weight up to 1.62 million.

Native cellulose, or cellulose I, has a very ordered and regular structure. It forms fibrils composed of long, threadlike bundles of molecules that are stabilized laterally by hydrogen bonds between hydroxyl groups. Cellulose I exhibits a parallel-chain structure, with each repeating cellobiosyl unit forming two intramolecular hydrogen bonds and linked by intermolecular bonds to its neighbors (Figure 1.2). When native cellulose is swollen with acid or alkali, or regenerated from solution by precipitation, cellulose I is converted to cellulose II in which the molecules are in an anti-parallel arrangement. This affords increased intermolecular hydrogen bonding resulting in a more stable and lower-energy structure than cellulose I. There is still a controversy as to the nature of the transformation between cellulose I and II (Blackwell, 1981; Sarko, 1986). Crystalline cellulose resists the entry of water or enzyme molecules, making it

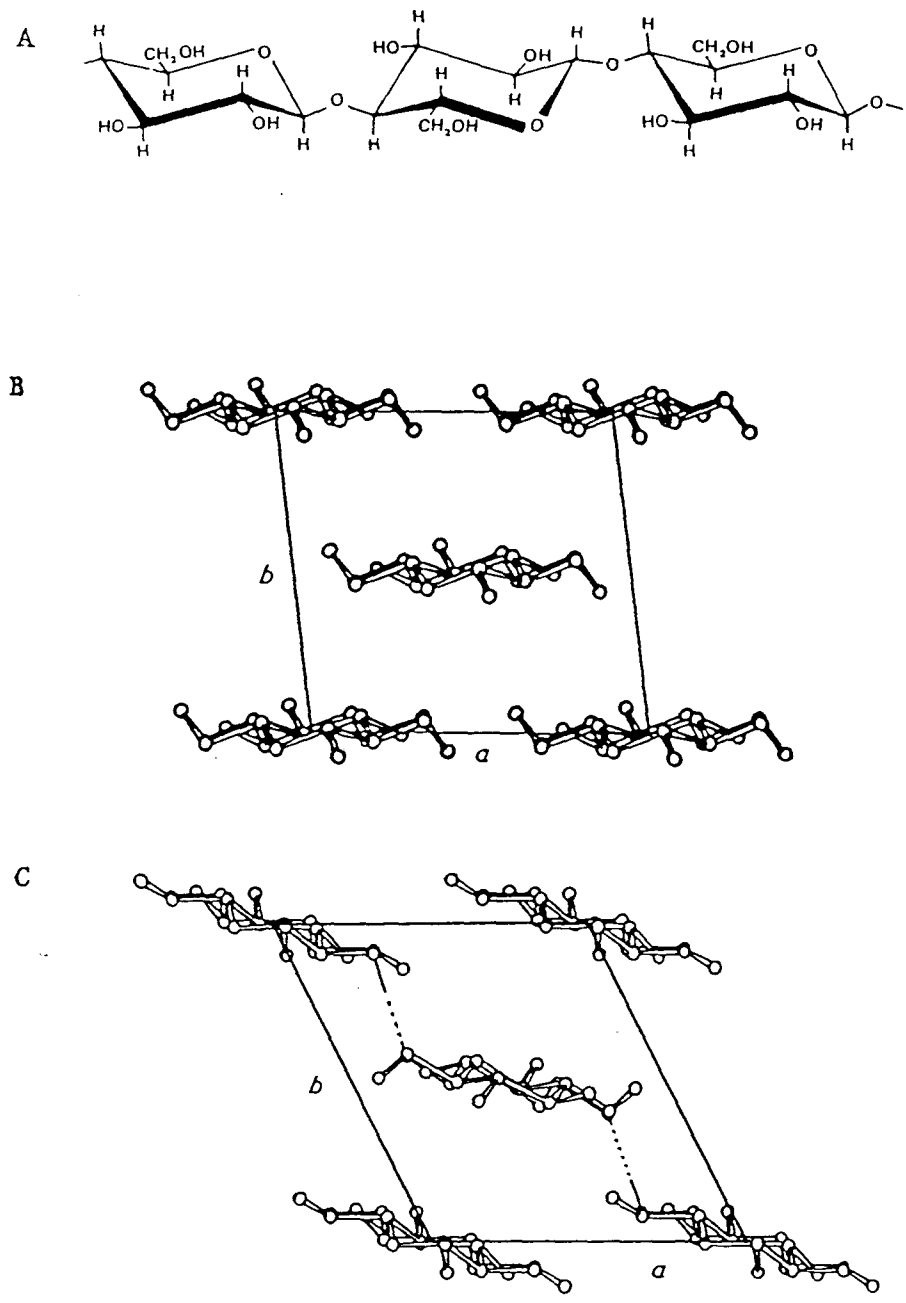

Figure 1.2 Structures of cellulose (A), cellulose I (B), and cellulose II (C). Solid lines, *a* and *b*, axial plane projections; dotted line, intermolecular H-bond. Adapted from Blackwell (1981).

resistant to biological hydrolysis. However, interspersed with the regular crystalline regions are paracrystalline or amorphous regions of a less ordered nature which are more susceptible to enzymatic hydrolysis. Treatment of cellulose with acid or alkali can reduce the degree of crystallinity, thereby facilitating enzymatic hydrolysis.

1.5 Objectives of the study

The general objective of this study was to explore the feasibility of using the cellulose-binding domain (CBD) of the *C. fimi* exoglucanase Cex for enzyme immobilization. The specific objectives included: (1) the construction of fusion polypeptides to serve as model systems for enzyme immobilization on cellulose; (2) the functional characterization of the isolated CBD_{Cex} and fusion polypeptides, especially with respect to their pH and temperature stability, and binding to various types of cellulose; (3) the operation of immobilized enzyme columns in a continuous mode.

2. MATERIALS AND METHODS

2.1 Chemicals, media components, buffers and enzymes

All chemicals used were of analytical or HPLC grade. Media components were from Difco. Buffers were prepared as described previously (Gomori, 1955; Stoll & Blanchard, 1990). Restriction and modifying enzymes were used according to manufacturers' recommended procedures. Bacterial microcrystalline cellulose (BMCC) was prepared from cultures of *Acetobacter xylinum* (Hestrin, 1963). Phosphoric acid swollen cellulose or regenerated cellulose was prepared as described previously (Wood, 1988). Avicel™ PH-101, α-chitin, Cellufine™, and CF1™ cellulose were purchased from FMC International (Ireland), Sigma, Grace Co. (Amicon), and Whatman, respectively.

2.2 Bacteria, plasmids, growth media and conditions

Escherichia coli was the host bacterium for recombinant DNA work and protein production. The *E. coli* strains plus their relevant genotypes, and the plasmids plus their associated genetic characters used in the study are listed in Tables 2.1 and 2.2, respectively. The medium used for growing *E. coli* strains carrying recombinant DNA was Luria-Bertani (LB) medium (tryptone, 10 $g.L^{-1}$; yeast extract, 5 $g.L^{-1}$; NaCl, 10 $g.L^{-1}$) supplemented with 100 μg ampicillin (Sigma). mL^{-1} (Sambrook *et al.*, 1989). All recombinant *E. coli* strains were grown under inducing conditions (0.1 mM final concentration of isopropyl-ß-D-thiogalactoside [IPTG; Sigma]) at 37° for approximately 16-18 h unless stated otherwise.

Table 2.1 *Escherichia coli* strains

Strain	Genotypes	Reference
CAG440	*lacZ*am *trp*am *pho*am *sup*C^{ts} *mal* *rps*L *phe rel*	Baker *et al.*, 1984
CAG456	CAG440, *rpo*H165 (*htp*R165)	Baker *et al.*, 1984
JM101	F' *tra*D36 *lac*I^{q} Δ(*lacZ*)M15 *pro*AB/*sup*E *thi* Δ(*lac-pro*AB)	Yannish-Perron *et al.*, 1985
JM109	F' *tra*D36 *lac*I^{q} Δ(*lac*Z)M15 *pro*AB/*rec*A1 *end*A1 *gyr*A96 (NaI^{r}) *thi hsd*R17 (r_K-m_K+) *sup*E44 *rel*A1 Δ(*lac-pro*AB)	Yannish-Perron *et al.*, 1985
PM191	*dra drm thr leu thi lac*Y *rec*A56 *sup*E	Meacock & Cohen, 1980
RZ1032	HfrKL16 PO/45 [*lys*A(61-62)] *dut*1 *ung*1 *thi*1 *rel*A1 Zbd-279::Tn*10* *sup*E44	Kunkel *et al.*, 1987

Table 2.2 Plasmids

Plasmid	Genetic characters	Reference
pABG5	*bla* p*lac abg*	Wakarchuk *et al.*, 1986
pEO1	*bla* p*lac abg-CBD*$_{cex}$	Ong *et al.*, 1989
pNZ1070	*bla* p*lac* f1*ori cbg*	Love *et al.*, 1988
pTZ18R	*bla* p*lac* f1*ori*	Pharmacia
pTZ18R-*cbg*	*bla* p*lac* f1*ori cbg*	D. Trimbur, unpublished work
pTZEO1	*bla* p*lac* f1*ori abg-CBD*$_{cex}$1	This study
pTZEO2	*bla* p*lac* f1*ori abg-CBD*$_{cex}$2	This study
pTZEO3	*bla* p*lac* f1*ori abg-CBD*$_{cex}$3	This study
pTZEO4	*bla* p*lac* f1*ori CBD*$_{cex}$	This study
pTZEO6	*bla* p*lac* f1*ori cex*	This study
pTZEO7	*bla* p*lac* f1*ori CBD*$_{cex}$	This study
pTZEO7 (PTIS)	*bla* p*lac* f1*ori CBD*$_{cex}$	This study
pTZEO8	*bla* p*lac* f1*ori cbg*	This study
pTZEO10	*bla* p*lac* f1*ori cbg-CBD*$_{cex}$	This study
pUC12	*bla* p*lac*	Vieira & Messing, 1982
pUC12-1.1*cex*	*bla* p*lac cex*	O'Neill *et al.*, 1986

2.3 Recombinant DNA work

All protocols for recombinant DNA work were described previously (Sambrook *et al.*, 1989) unless stated otherwise. Double-stranded plasmid DNA was prepared by the alkaline-lysis method. It was purified by cesium chloride/ ethidium bromide ultracentrifugation if required. Plasmid DNA for double-stranded sequencing was prepared as described previously (Kraft *et al.*, 1988). Single-stranded M13 phage DNA was prepared by extraction with phenol-chloroform. Uridine-containing single-stranded DNA was prepared as described previously (McClary *et al.*, 1989).

After restriction endonuclease digestion of the desired plasmid, DNA fragments were separated by agarose gel electrophoresis and purified by the GeneClean™ method (Bio101, La Jolla, CA). Following ligation of the desired insert(s) and vector with T_4 DNA ligase, the ligated mixture was transformed into competent *E. coli* cells (Hanahan, 1982). Transformed cells were selected on LB-ampicillin plates.

Oligodeoxyribonucleotides for mutagenesis (Kunkel *et al.*, 1987) and DNA sequencing (Sanger *et al.*, 1977) were synthesized using an Applied Biosystems automated DNA synthesizer model 380A (Oligonucleotide Synthesis Facility, University of British Columbia, Vancouver, B.C.). They were purified by polyacrylamide gel electrophoresis and reversed-phase chromatography on Sep-Pak™ columns (Millipore)(Atkinson & Smith, 1984).

Single- or double-stranded DNA was sequenced by the dideoxyribo-nucleotide chain-terminating method (Sanger *et al.*, 1977) using modified T_7 DNA polymerase and ^{35}S-α–dATP (Tabor & Richardson, 1987).

2.4 Screening for gene expression

Transformants were screened by plating on LB plates supplemented with ampicillin, IPTG and either 100 μM methylumbelliferyl-ß-D-glucoside (MUG; Sigma) or 100 μM 5-bromo-4-chloro-3-indolyl-ß-D-glucoside (X-glu; Sigma). After incubation overnight at 37°, ß-glucosidase activity was detected by the production of either fluorescent (MUG) colonies when observed under long-wavelength UV light, or blue (X-glu) colonies.

Transformants were also screened by colony immunoblotting (Hanahan & Meselson, 1983) and Western blot analysis (Harlow & Lane, 1988). Primary polyclonal antisera against *Agrobacterium* ß-glucosidase (Abg) and *C. fimi* exoglucanase (Cex) were raised in rabbits. Goat anti-rabbit IgG-alkaline phosphatase conjugate (BRL) was used as secondary antibody. The detection reagents were 5-bromo-4-chloro-3-indolyl-phosphate (Sigma) and nitroblue tetrazolium dye (Sigma).

2.5 Production of polypeptides

2.5.1 Small-scale production of polypeptides

E. coli cells were grown in 25 mL LB supplemented with ampicillin and IPTG in a 125-mL flask. The culture was grown overnight at 37° (30° for *E. coli* CAG456), 150 rpm (New Brunswick Scientific G-25 incubator shaker). Cells were harvested by centrifugation at 17,400g, 4° for 10 min, washed in 5 mL of 50 mM potassium 50 mM potassium phosphate buffer, pH 7, pH 7 and recentrifuged. The cell pellet was resuspended in 3 mL 50 mM potassium phosphate buffer, pH 7 supplemented with 3 mM EDTA. Cells were homogenized using a 5-mL French press cell (Aminco). The cell extract was

clarified by centrifugation at 17,400g, 4° for 20 min. Cell extract was stored at 4° in the presence of 0.02% NaN_3, 1 mM phenylmethylsulfonyl-fluoride (PMSF; BDH), and 1 μM pepstatin A (Sigma).

2.5.2 Large-scale production of fusion polypeptides

E. coli cells were grown in 60 L LB supplemented with ampicillin and IPTG in a 110-L fermentor (L.H. Fermentation). Growth conditions were the same as in 2.5.1. Cells were separated from the culture medium by centrifugation at 31,000g (Sharples Inc.). Cells were washed in 500 mL of 50 mM potassium phosphate buffer, pH 7, centrifuged at 4,000g, 4° for 10 min and resuspended in 800 mL of 50 mM potassium phosphate buffer, pH 7 supplemented with 3 mM EDTA. Cells were homogenized in 40 mL batches using a 50-mL French press cell. PMSF and pepstatin A were added immediately to prevent proteolysis. Cell debris was removed by centrifugation at 17,400g, 4° for 25 min. Nucleic acids were precipitated from the supernatant by addition of streptomycin sulfate (Sigma) to a final concentration of 1.5% (wt/v) and incubating the mixture overnight. The precipitate was removed by centrifugation at 17,400g, 4° for 20 min. The supernatant was then centrifuged at 150,000g, 4° for 40 min, using a Beckman Ti 50.2 rotor, so as to remove membrane-associated debris and loaded onto cellulose columns as described below.

CF1™ cellulose was washed extensively with distilled H_2O (dH_2O) to remove fines and then packed into a column in 50 mM potassium phosphate buffer, pH 7. Two column sizes were routinely used: a 30 cm x 5 cm diameter column (~ 400 mL bed volume; Pharmacia XK50/30) and a 60 cm x 5 cm diameter column (~ 800 mL bed volume; Pharmacia XK50/60). After equilibration of the column with 50 mM potassium phosphate buffer, pH 7 at 4°, the sample was loaded into the column at a flow rate of 1 $mL.min^{-1}$. The

column was washed with 5 bed-volumes of 1 M NaCl in 50 mM potassium phosphate buffer, pH 7 followed by 2 bed-volumes of 50 mM potassium phosphate buffer, pH 7. Desorption was effected using a concave descending gradient of 50 mL 50 mM potassium phosphate buffer, pH 7 and 2 L of dH_2O. For Cbg-CBD_{Cex} further desorption was achieved using a 0-8 M gradient of guanidinium chloride (GdmCl) in 50 mM potassium phosphate buffer, pH 7. The column run was controlled and monitored with an FPLC™ (fast protein liquid chromatography) system (Pharmacia). Peak fractions were identified by on-line absorbance readings at 280 nm, pooled and concentrated by ultrafiltration through a 10 kDa-cutoff membrane (Amicon PM-10). If necessary, the polypeptide sample was further purified by MonoQ anion-exchange chromatography using the FPLC™ system. Enzyme preparations were stored at 4° in the presence of 0.02% NaN_3.

2.5.3 Large-scale production of CBD_{Cex} from culture supernatant

E. coli cells were grown as in 2.5.2. The cells were removed by centrifugation at 31,000g (Sharples) and the supernatant was transferred to 3 x 20-L jugs (Pyrex) - each containing 330 g of Avicel™ or CF1™ cellulose. The suspension was stirred periodically for 3 to 5 h at room temperature to allow binding of protein to cellulose. After the cellulose settled, the supernatant was aspirated. Each 330 g of cellulose was resuspended in 1 L of 1 M NaCl in 50 mM potassium phosphate buffer, pH 7, stirred for 30 min at room temperature and filtered through a GF/C glass fibre filter (Whatman). The NaCl wash was repeated, followed by two washes with 1 L of 50 mM potassium phosphate buffer, pH 7. Bound proteins were desorbed from the cellulose with 500 mL of 8 M GdmCl in 50 mM potassium phosphate buffer, pH 7. The eluate was concentrated and exchanged with dH_2O by ultrafiltration using a 2 kDa-cutoff

membrane (Amicon YM-2). The polypeptide was either lyophilized or stored in solution at 4° in the presence of 0.02% NaN_3. The material purified from Avicel™ was contaminated with xylan (see 3.1.2) and was used for all subsequent experiments except when noted.

Contaminating xylan (see pp. 37, 39 & 48) was removed from purified CBD_{Cex} by cation-exchange chromatography on MacroprepS beads (Bio-Rad) using a pH gradient consisting of 20 mM formic acid/trimethylamine buffer, pH 4 and 20 mM trimethylamine/formic acid, pH 7.

2.6 Determination of protein and carbohydrate concentrations

Protein concentrations in cell extract and partially purified preparations were determined by dye binding (Bradford, 1976). Bovine serum albumin (BSA) was used as the standard. Protein concentrations in purified preparations were determined by absorbance at 280 nm using the extinction coefficient obtained for the purified polypeptides (Scopes, 1974).

The carbohydrate contents of purified polypeptides were determined by the phenol-sulfuric acid method (Chaplin, 1986). D-Glucose was used as the standard.

2.7 Gel electrophoresis - staining for protein

Polypeptides were resolved by sodium dodecyl sulfate-polyacrylamide gel electrophoresis (SDS-PAGE) (Laemmli; 1970; Schägger & von Jagow, 1987). Non-denaturing PAGE was performed in the same manner except for the omission of SDS, ß-mercaptoethanol (BME) and heat treatment; the pH of the system was 8.8; the stacking gel was 3%, the resolving gel 7.5%; the running buffer was Tris-Tricine without SDS (Schägger and von Jagow, 1987).

Isoelectric focusing PAGE was performed using a Phast gel system (Pharmacia). Protein bands were visualized by either Coomassie blue staining (Merril, 1990) or silver staining (Merril, 1990). Quantification of protein bands was done using a densitometer (Molecular Dynamics ImageQuant version 3.0, Sunnyville, CA). The following proteins were used as molecular weight markers: myosin (205-212 kDa); ß-galactosidase (116-130 kDa); phosphorylase B (97.4 kDa); bovine serum albumin (66-68 kDa); catalase (57.5 kDa); glutamate dehydrogenase (53 kDa); alcohol dehydrogenase (43-45 kDa); ovalbumin (41 kDa); glucose-3-phosphate dehydrogenase (36 kDa); carbonic anhydrase (29 kDa); soybean trypsin inhibitor (20.1 kDa); lysozyme (14 kDa); and cytochrome C (12.3 kDa).

2.8 Gel electrophoresis - *in situ* detection of enzymatic activity

Polypeptides were resolved by non-denaturing PAGE. The gel was then incubated in 50 mM potassium phosphate buffer, pH 7 for 15 min at room temp. ß-glucosidase activity was detected by immersing the gel in 2 mM MUG for 2-5 min at room temp. Fluorescent protein bands were detected under long-wavelength UV light.

2.9 Amino acid sequence determinations

Polypeptides were resolved by SDS-PAGE, then electroblotted (0.5 amperes, 30 min) onto a poly(vinylidine difluoride) membrane (Immobilon™; Millipore) (Matsudaira, 1987; 1990). Stained bands corresponding to the peptide of interest were excised from the blots and sequenced directly by automated Edman degradation using an Applied Biosystems 470A gas-phase sequenator with on-line PTH analyzer and 900A system controller and data analyzer (Protein Sequencing Facility, University of Victoria, Victoria, B.C.).

2.10 Protease digestion of CBD_{Cex}

The following proteases were used: endoproteinase Lys-C (Boehringer-Mannheim); endoproteinase Asp-N (Sigma); TPCK-treated trypsin (Cooper); papain (Sigma); pepsin (Sigma) and a *C. fimi* serine protease (Gilkes *et al.*, 1988). Each of the proteases was used at its optimum pH and temperature in either the presence or absence of urea and/or dithiothreitol (Aitken *et al.*, 1989; Matsudaira, 1989). The protease to CBD_{Cex} weight ratio varied from 1:5 to 1:30. Digestion was monitored by SDS-PAGE.

2.11 Determination of disulfide bonds in CBD_{Cex}

Purified CBD_{Cex} was analyzed by SDS-PAGE in the absence of BME. Reaction of 5,5'-dithionitrobenzoic acid (DTNB) with free thiol groups in CBD_{Cex} was determined as described previously (Creighton, 1989).

2.12 Binding analysis

Purified polypeptides (0.15-90 μM) were mixed with either 5 mg of Avicel™, 1 mg of BMCC, 1 mg α-chitin or 1 mg regenerated cellulose equilibrated in 1 mL of 50 mM potassium phosphate buffer, pH 7 contained in 1.7 mL micro-centrifuge tubes. Tube contents were mixed continually by rotation at 2 rpm on a Labquake Shaker™ (Labindustries, Inc., Berkeley, CA). After equilibration at the desired temperature for 3 to 24 h, substrate and bound polypeptides were removed by centrifugation at 14,800g for 10 min. The supernatant was removed and assayed either for ß-glucosidase activity (Abg-CBD_{Cex}) or by absorbance at 280 nm (CBD_{Cex}).

2.13 Enzyme kinetics

Purified Abg-CBD_{Cex} or Cbg-CBD_{Cex} was diluted in 50 mM potassium phosphate buffer, pH 7 containing 0.2 mg BSA.mL^{-1} as a stabilizer. ß-glucosidase activity was estimated by measuring the initial rate of *p*-nitrophenolate (pNP) formation from *p*-nitrophenyl-ß-D-glucopyranoside (pNPG; Sigma). One unit of ß-glucosidase or pNPGase activity releases one µmole of pNP per min from pNPG in either 50 mM potassium phosphate buffer, pH 7 at 37° (Abg-CBD_{Cex}) or phosphate-citrate buffer, pH 6.2 at 70° (Cbg-CBD_{Cex}) (standard conditions).

The Michaelis-Menten kinetic parameters of Abg and soluble Abg-CBD_{Cex} were determined using pNPG concentrations from approximately 0.1 x K_m to 20 x K_m. The V_{max} for Abg-CBD_{Cex} bound to cellulose and resuspended in a stirred cell was determined by active site titration using 2',4'-dinitrophenyl-2-deoxy-2-fluoro-ß-D-glucopyranoside (2F-DNPG) as a substrate analogue (Withers & Street, 1988). 2F-DNPG inactivated the bound, active ß-glucosidase fusion polypeptide by the rapid formation of a covalent glycosyl-enzyme intermediate at the active site with concomitant release of an equimolar quantity of dinitrophenolate (DNP) (Withers & Street, 1988). The amount of DNP produced was directly proportional to the number of active sites of the bound fusion polypeptide. The phenol product was measured at a wavelength of 400 nm.

The column flow characteristics and the apparent K_m of immobilized Abg-CBD_{Cex} in a continuous column reactor were determined as described previously (Lilly *et al.*, 1966; Ford *et al.*, 1972). The filter holder (see 2.14) containing fusion polypeptide adsorbed to cellulose acetate membranes was equilibrated with 50 mM potassium phosphate buffer, pH 7 at room temperature for 30 min. pNPG was perfused through the column and the appearance of pNP

in the column effluent was measured by absorbance at 405 nm. The absorbance was plotted against the column effluent volume to obtain a time distribution of pNP in the column. The apparent K_m was determined using a similar procedure and a pNPG concentration range of 150-10,000 µM. Reaction was carried out at 37°, 60 $mL.h^{-1}$ flow rate.

2.14 Immobilization of Abg-CBD_{Cex} and Cbg-CBD_{Cex}

The following cellulosic adsorbents were used: dewaxed, absorbent cotton (Fisher); CF1™ cellulose; Avicel™, Cellufine™, and cellulose acetate membranes (Memtek).

Cellulose was first resuspended in dH_2O and centrifuged or filtered under vacuum. This procedure was repeated once with dH_2O and twice with 50 mM potassium phosphate buffer, pH 7. Finally, the cellulose was resuspended to a fixed volume in 50 mM potassium phosphate buffer, pH 7. Sufficient Abg-CBD_{Cex} was then added to saturate the cellulose. After brief mixing, the suspension was incubated at 4° for 3 h with gentle agitation, then centrifuged. The supernatant was assayed for ß-glucosidase activity and the activity of the enzyme bound to cellulose was determined from the difference between this value and the original activity in the preparation. The pellet was resuspended in 50 mM potassium phosphate buffer, pH 7, the mixture centrifuged and the supernatant discarded. The moist pellet was then kept at 4° until required.

For Cbg-CBD_{Cex} five cellulose acetate membranes (0.2 mm x 25 mm diameter per membrane) were stacked and installed in a filter holder (Memtek). The membrane was equilibrated by pumping 50 mM potassium phosphate buffer, pH 7 through the holder at a given temperature. A given amount of fusion protein (4 nmoles) was then passed through the holder at a flow rate of 1 $mL.min^{-1}$. The amount of fusion protein bound to cellulose was determined

from the difference between the ß-glucosidase activity found in the flow through and that added initially.

2.15 Stability of CBD_{Cex}, Abg-CBD_{Cex} and Cbg-CBD_{Cex} adsorbed to cellulose

2.15.1 pH

2.15.1.1 CBD_{Cex}

The buffers used were 25 mM citrate, pH 3 and 5; 25 mM phosphate, pH 7; and 25 mM carbonate, pH 9 and 11. Increasing concentrations of purified CBD_{Cex} (0.9-90 μM) were adsorbed to 1 mg of BMCC (2 $mg.mL^{-1}$ made up in the appropriate buffer) in a total volume of 1 mL contained in 1.7 mL micro-centrifuge tubes. After equilibration at the desired pH, at 22° with constant agitation for 18-24 h, the cellulose was pelleted by centrifugation at 17,400g, 22° for 10 min. The concentrations of polypeptides in the supernatant were measured by absorbance at 280 nm.

2.15.1.2 Abg-CBD_{Cex}1

The buffers (50 mM) used were: KCl-HCl (pH 2); glycine-HCl (pH 3); sodium acetate-acetic acid (pH 4 and 5); citrate-phosphate (pH 6 and 6.5); phosphate (mono- and dibasic) (pH 7, 7.5 and 8); glycine-NaOH (pH 9 and 10) and phosphate-NaOH (pH 11). Cellufine™ (3 g) was saturated with Abg-CBD_{Cex}1 (124.1 U). The Cellufine™ was filtered on a glass fibre filter. A 200 mg sample of the Cellufine™ was placed in a vial and 4.8 mL of buffer of the appropriate pH was added to it. The Cellufine™ was resuspended with a vortex mixer. The

suspension was incubated in a shaker bath at 25°, 150 rpm for 3 days. A 0.5 mL sample of the suspension was centrifuged; the Cellufine™ was washed in 50 mM potassium phosphate buffer, pH 7, resuspended in 0.5 mL of 50 mM potassium phosphate buffer, pH 7 and assayed for ß-glucosidase activity under standard conditions. A control sample of Abg-$CBD_{Cex}1$ in solution (0.5 µM) was incubated and assayed as above. Bound fusion polypeptide was also analyzed by SDS-PAGE. A uniform amount of Cellufine™ (2 mg), after incubation at the indicated pH, was extracted with SDS loading buffer. The solution obtained was then loaded onto a 10%T SDS-polyacrylamide gel.

The binding stability was also tested by eluting a column (2.5 cm x 0.5 cm diameter; Pharmacia HR 5/2, containing 0.5 mL of Cellufine™ suspension, 50% v/v) containing 0.03 µmoles of bound Abg-$CBD_{Cex}1$ with a pH gradient of the appropriate constant ionic strength buffers (50 mM sodium acetate, pH 6.9 and 0.2 M HCl + 50 mM KCl, pH 1.2; 50 mM triethanolamine, pH 7.1 and 0.2 M NaOH + 50 mM KCl, pH 12.6) (Elving *et al.*, 1956). Protein desorption was monitored by absorption at 280 nm. Fractions (1 mL) were collected and the pH of each measured at 25°.

2.15.2 Ionic strength

Stability of soluble and bound Abg-$CBD_{Cex}1$ as a function of ionic strength was determined as follows: a 500 mg sample of Abg-$CBD_{Cex}1$-Cellufine™ suspension was placed in a vial to which 4.5 mL of dH_2O or potassium phosphate buffer (pH 7) of the appropriate ionic strength were added. The cellulose was resuspended and incubated at 25°, 150 rpm for 24 h. Subsequently, a 0.5 mL sample of the suspension was taken, washed and analyzed for ß-glucosidase activity as in the pH stability study. A control sample of Abg-$CBD_{Cex}1$ in solution, 1.2 µM, was

prepared in the same manner. Residual ß-glucosidase activities were determined under standard conditions.

The binding stability of the fusion polypeptide at varying ionic strength was also tested using a column flow-through technique. A column (2.5 cm x 0.5 cm diameter; Pharmacia HR5/2) containing 0.5 mL of Cellufine™ suspension (50% v/v) with 0.03 µmoles of bound Abg-CBD_{Cex}1 was eluted with a linear salt gradient. The buffers used for the linear gradient were from 0-1 M NaCl in 50 mM potassium phosphate buffer, pH 7 at a flow rate of 0.1 $mL.min^{-1}$. Protein desorption was monitored by absorption at 280 nm.

2.15.3 Temperature

The buffer used was 25 mM potassium phosphate buffer, pH 7. Increasing concentrations of purified CBD_{Cex} (0.9-90 µM) were adsorbed to 1 mg of BMCC (2 $mg.mL^{-1}$ in 50 mM potassium phosphate buffer, pH 7) in a total volume of 1 mL contained in 1.7 mL micro-centrifuge tubes. After equilibration at the desired temperature with constant agitation for 18-24 h , the cellulose was pelleted by centrifugation at 17,400g, 22° for 10 min. The protein concentrations in the supernatant were measured by absorbance at 280 nm.

2.15.4 Time

Stability of the fusion polypeptide during storage was determined as follows: Abg-CBD_{Cex}1 adsorbed to Avicel™ (0.012 µmoles enzyme.g Avicel™$^{-1}$) was incubated in a final volume of 10 mL (containing 1 g Avicel™) of 50 mM potassium phosphate buffer, pH 7 for 7 weeks at 4° and 37°. A 0.5 mL sample of the suspension was taken weekly and centrifuged to pellet the Avicel™. The Avicel™ was washed once in 50 mM potassium phosphate buffer, pH 7, then

resuspended with 0.5 mL of 50 mM potassium phosphate buffer, pH 7. The suspensions were then assayed for ß-glucosidase activity under standard conditions to determine residual activity. As a control, 4.8 µmoles of Abg-$CBD_{Cex}1$ were incubated in 10 mL of 50 mM potassium phosphate buffer, pH 7, and assayed in the same manner as the immobilized enzyme. In addition, all samples were analyzed by SDS-PAGE. Samples of the soluble Abg-$CBD_{Cex}1$ were first concentrated by lyophilization. After addition of SDS loading buffer into each sample, volumes equivalent to equal original weights of the test protein were loaded onto a 10%T SDS-polyacrylamide gel.

2.15.5 Detergents

Triton X-100, a non-ionic detergent, and SDS, an ionic detergent, were tested at concentrations from 0.002% to 2% (v/v). Nine nmoles CBD_{Cex} were bound to 5 mg Cellufine™. The Cellufine™ was washed and resuspended in a given concentration of detergent. The mixture was incubated at 22° with constant agitation for 4 h, centrifuged and the supernatant discarded. Polypeptides remaining bound to the cellulose was extracted with SDS loading dye and analyzed by SDS-PAGE. An analogous procedure was used to test whether binding could occur in the presence of detergent. In this case binding of CBD_{Cex} to cellulose was done in the presence of detergent for 2 h at 22° with constant agitation.

2.16 Performance of Abg-CBD_{Cex} and Cbg-CBD_{Cex} immobilized enzyme columns

A schematic diagram of the system used to test the performance of immobilized enzymes is shown in Figure 2.1. Cotton fibres were cut to lengths of 0.85 mm or less with a Wiley cutting mill (A. Thomas Co.). One to two grams of the cut cotton were washed twice with dH_2O and once with 50 mM potassium phosphate buffer, pH 7 by filtration and resuspension. The fibres were mixed with Abg-$CBD_{Cex}1$ in 50 mL 50 mM potassium phosphate buffer, pH 7, incubated at 4° with shaking at 200 rpm for 3 h, then centrifuged at 17,400 g, 4° for 15 min. The supernatant was removed and assayed for ß-glucosidase activity. The fibres were resuspended in 50 mM potassium phosphate buffer, pH 7 and packed into a jacketed column (20 cm x 1.6 cm diameter; ~35 mL bed volume; Pharmacia XK16/20). The column was connected to a circulating water bath (Forma) and equilibrated at the desired temperature. Unbound fusion polypeptide was desorbed with 50 mM potassium phosphate buffer, pH 7. Substrate (3 mM pNPG in 50 mM potassium phosphate buffer, pH 7) was then perfused through the column at a constant flow rate using a peristaltic pump (Pharmacia P3). The outflow from the column was collected in 7.5 mL fractions to which an equal volume of 1 M Na_2CO_3 was added by the same peristaltic pump to inactivate any enzyme that might have desorbed from the support. A sample of each fraction was transferred to a microtitre plate and the pNP produced was measured by absorbance at 405 nm. The same protocol was followed when CF1™ cellulose was used as a support instead of cotton except that it was not pretreated mechanically.

Essentially the same protocol was followed for Cbg-CBD_{Cex} except that the enzyme was immobilized on 5 cellulose acetate membranes (0.2 mm x 25 mm

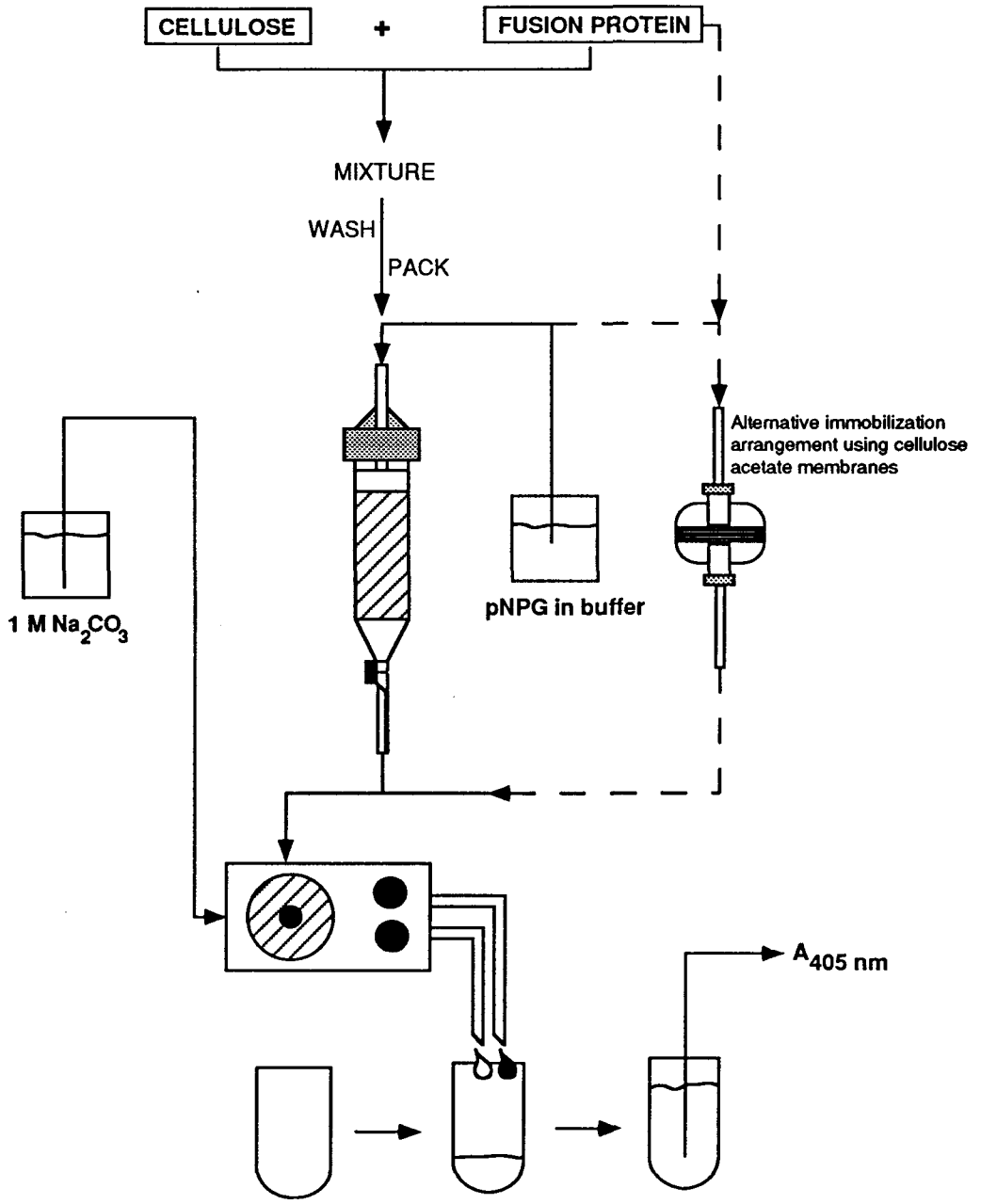

Figure 2.1 Schematic diagram of the system to test performance of Abg-CBD_{Cex} and Cbg-CBD_{Cex} immobilized enzyme columns

diameter per membrane; Memtek) stacked in series in a filter holder. The buffer used was phosphate-citrate buffer, pH 6.2 optimal for Cbg.

3. RESULTS

3.1 The cellulose-binding domain of *C. fimi* exoglucanase Cex (CBD_{Cex}; Figure 3.1)

3.1.1 Construction of plasmids expressing CBD_{cex}

A *C. fimi* serine protease cleaves Cex into two peptides - a core peptide that retains enzymatic activity against *p*-nitrophenyl-ß-D-cellobioside, and a shorter peptide that still adsorbs to cellulose (Gilkes *et al.*, 1988). N-terminal amino acid sequence analysis of this shorter peptide indicated a sequence corresponding to the amino acids immediately after the Pro-Thr linker (Figure 1.1; Gilkes *et al.*, 1988). In this study the cellulose-binding domain of Cex (CBD_{Cex}) corresponded to the same sequence starting at the serine residue immediately after the Pro-Thr linker and extending to the C-terminus of Cex. Two extra amino acids (A & S) were introduced at the N-terminus of CBD_{Cex} corresponding to an NheI site created to facilitate DNA manipulation.

Three plasmids were constructed to express CBD_{cex}: pTZEO7, pTZEO7 (PTIS) and pTZEO4 (Figures 3.2, 3.3 & 3.4). The coding sequence for the Cex leader peptide was directly fused to the sequence encoding CBD_{Cex} in both pTZEO7 and pTZEO7 (PTIS). This allowed the export of the polypeptide to the periplasm of the cells. In the latter plasmid a portable translation initiation site (PTIS) corresponding to the consensus Shine-Dalgarno sequence was introduced upstream of the ATG. The plasmid pTZEO4 was a cloning vector containing the multiple cloning sites of pTZ18R introduced upstream of the CBD_{cex} coding sequence. This vector was made to facilitate cloning of heterologous genes to the CBD_{Cex} coding sequence. In all three plasmids expression was controlled by the

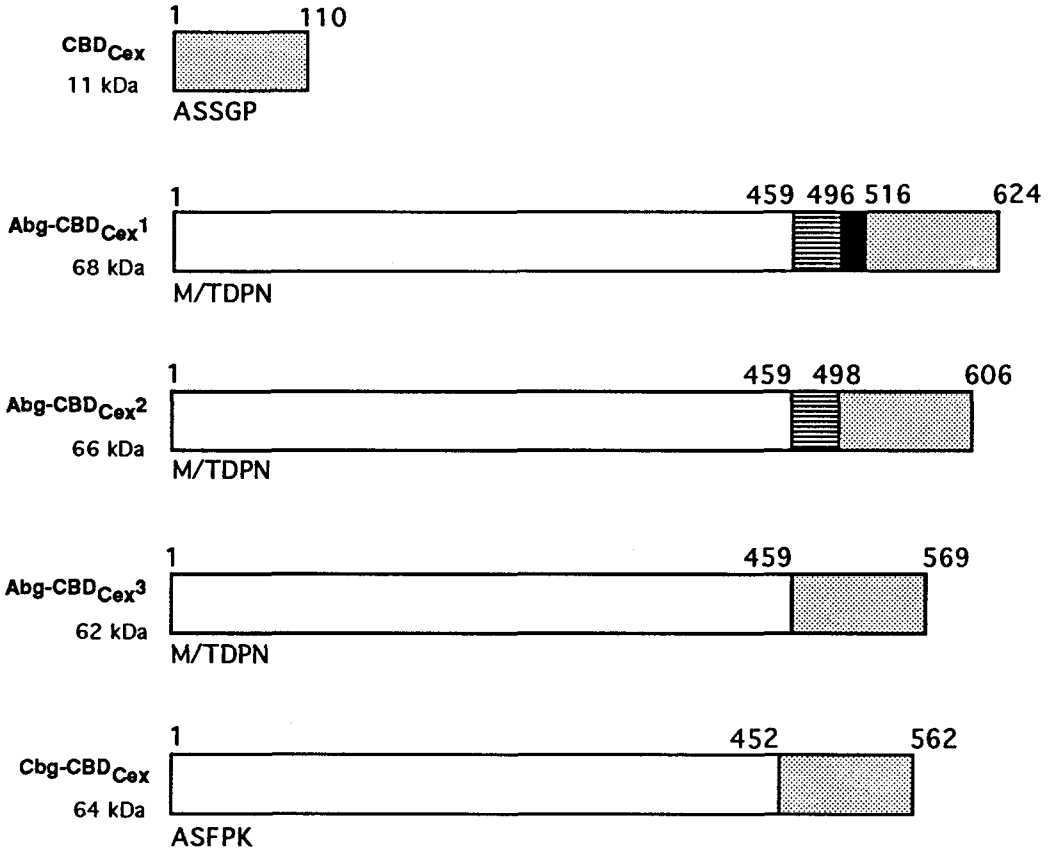

Figure 3.1 Block diagrams of CBD_{Cex} and fusion polypeptides. Abg: *Agrobacterium* ß-glucosidase. Cbg: *Caldocellum saccharolyticum* ß-glucosidase. Sizes in kDa are based on the predicted amino acid sequences. Numbers refer to amino acid residues. The letters give the N-terminal amino acid sequences determined experimentally. □ : Abg or Cbg. ▤ : Cex catalytic domain. ■ : Pro-Thr linker. ▨ : CBD_{Cex}.

Figure 3.2 Construction of pTZEO7. pUC12-1.1*cex* (PTIS) (O'Neill *et al.*, 1986) (see Figure 3.3) was digested completely with BamHI and HindIII. The *cex* insert was isolated and ligated to pTZ18R, which had been digested completely with BamHI and HindIII, to give pTZ1.1*cex*. An NheI site was introduced between the Cex leader peptide (LP) coding sequence and the coding sequence for the Cex catalytic domain by oligonucleotide-directed *in vitro* mutagenesis to give pTZEO6. pTZEO6 was digested completely with ScaI, NheI and SspI and the 1.9 kbp fragment containing the Cex LP coding sequence was isolated. The plasmid pTZEO2 (see 3.2.1) was digested completely with ScaI and NheI, and the 1.8 kbp fragment containing the CBD_{Cex} coding sequence was isolated. The 1.8 kbp and the 1.9 kbp fragments were ligated to give pTZEO7.

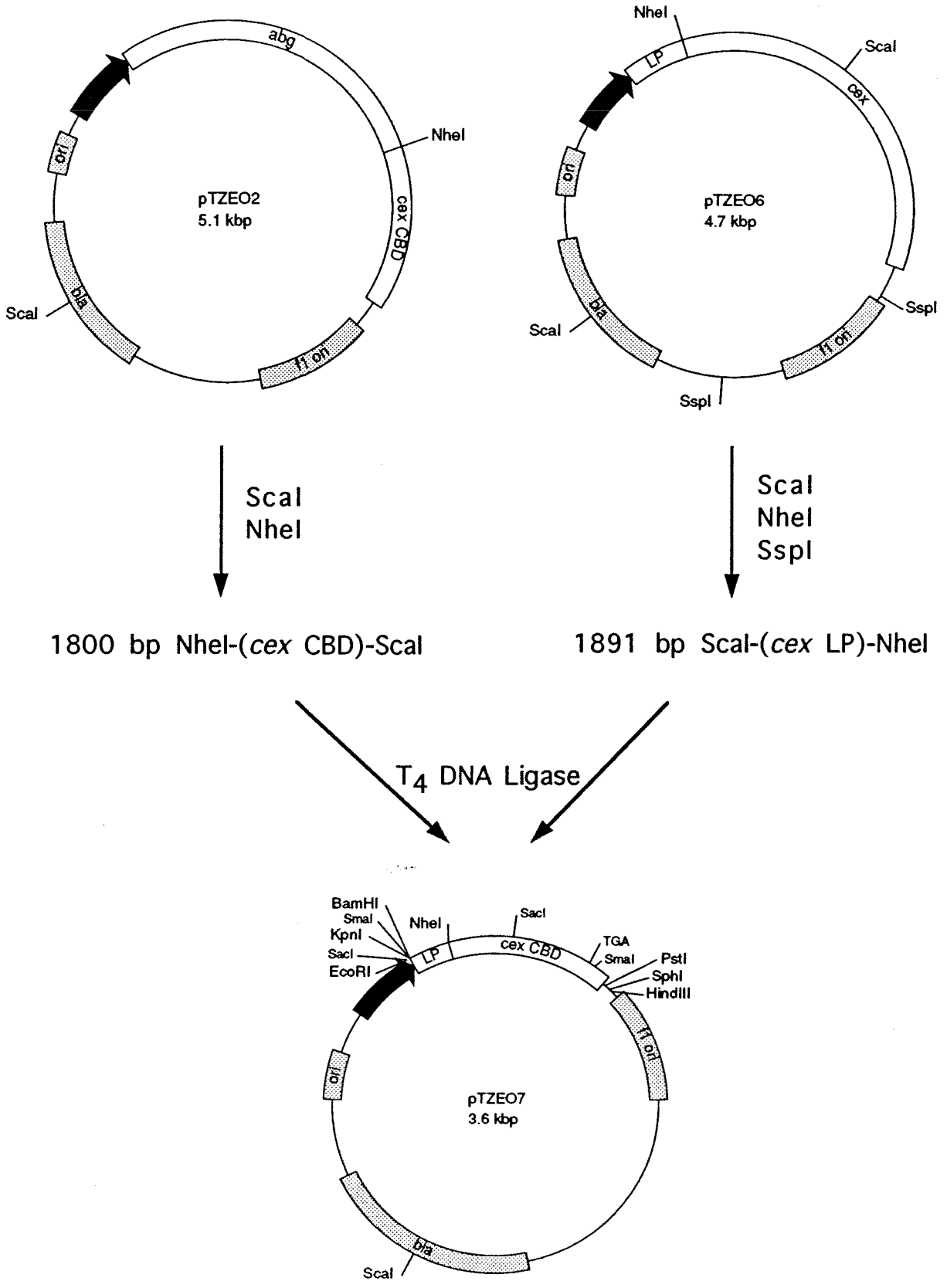
abg
NheI
ori
pTZEO2
5.1 kbp
cex CBD
ScaI
bla
f1 ori
NheI
LP
ScaI
cex
ori
pTZEO6
4.7 kbp
bla
SspI
ScaI
f1 ori
SspI
ScaI
NheI
ScaI
NheI
SspI
1800 bp NheI-(cex CBD)-ScaI
1891 bp ScaI-(cex LP)-NheI
T4 DNA Ligase
BamHI
SmaI
KpnI
SacI
EcoRI
NheI
SacI
LP
cex CBD
TGA
SmaI
PstI
SphI
HindIII
f1 ori
ori
pTZEO7
3.6 kbp
bla
ScaI

Figure 3.3 Construction of pTZEO7 (PTIS). pUC12-1.1*cex* (PTIS) was completely digested with ScaI, BamHI and PstI, and the 1.7 kbp fragment containing the PTIS sequence was isolated. pTZEO7 was digested completely with ScaI, BamHI and PstI, and the 1 kbp and 0.85 kbp fragments were isolated. The 1.7, 1 and 0.85 kbp fragments were ligated to give pTZEO7 (PTIS).

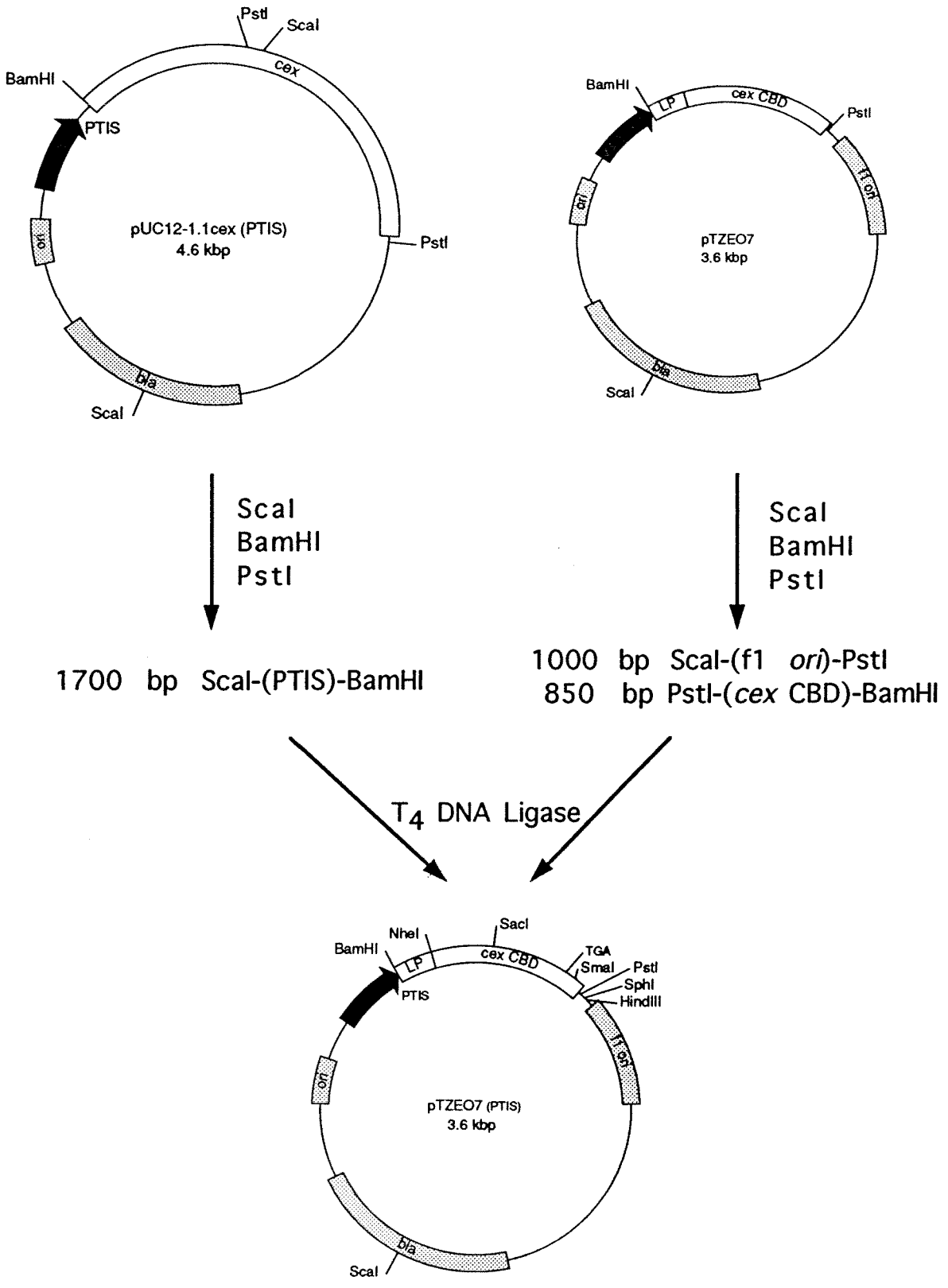
PstI
ScaI
BamHI
cex
PTIS
pUC12-1.1cex (PTIS)
4.6 kbp
PstI
ori
bla
ScaI
BamHI
LP
cex CBD
PstI
f1 ori
ori
pTZEO7
3.6 kbp
bla
ScaI
ScaI
BamHI
PstI
ScaI
BamHI
PstI
1700 bp ScaI-(PTIS)-BamHI
1000 bp ScaI-(f1 ori)-PstI
850 bp PstI-(cex CBD)-BamHI
T4 DNA Ligase
NheI
SacI
BamHI
LP
cex CBD
TGA
SmaI
PstI
SphI
HindIII
PTIS
f1 ori
ori
pTZEO7 (PTIS)
3.6 kbp
bla
ScaI

Figure 3.4 Construction of pTZEO4. pTZEO2 was digested completely with NheI. The fragments were made blunt-ended using kPolI, then digested completely with PstI. The 0.7 kbp fragment containing CBD_{cex} was isolated. pTZ18R was digested with XbaI, made blunt-ended as above, digested with PstI, and ligated to the 0.7 kbp fragment from pTZEO2 to give pTZEO4.

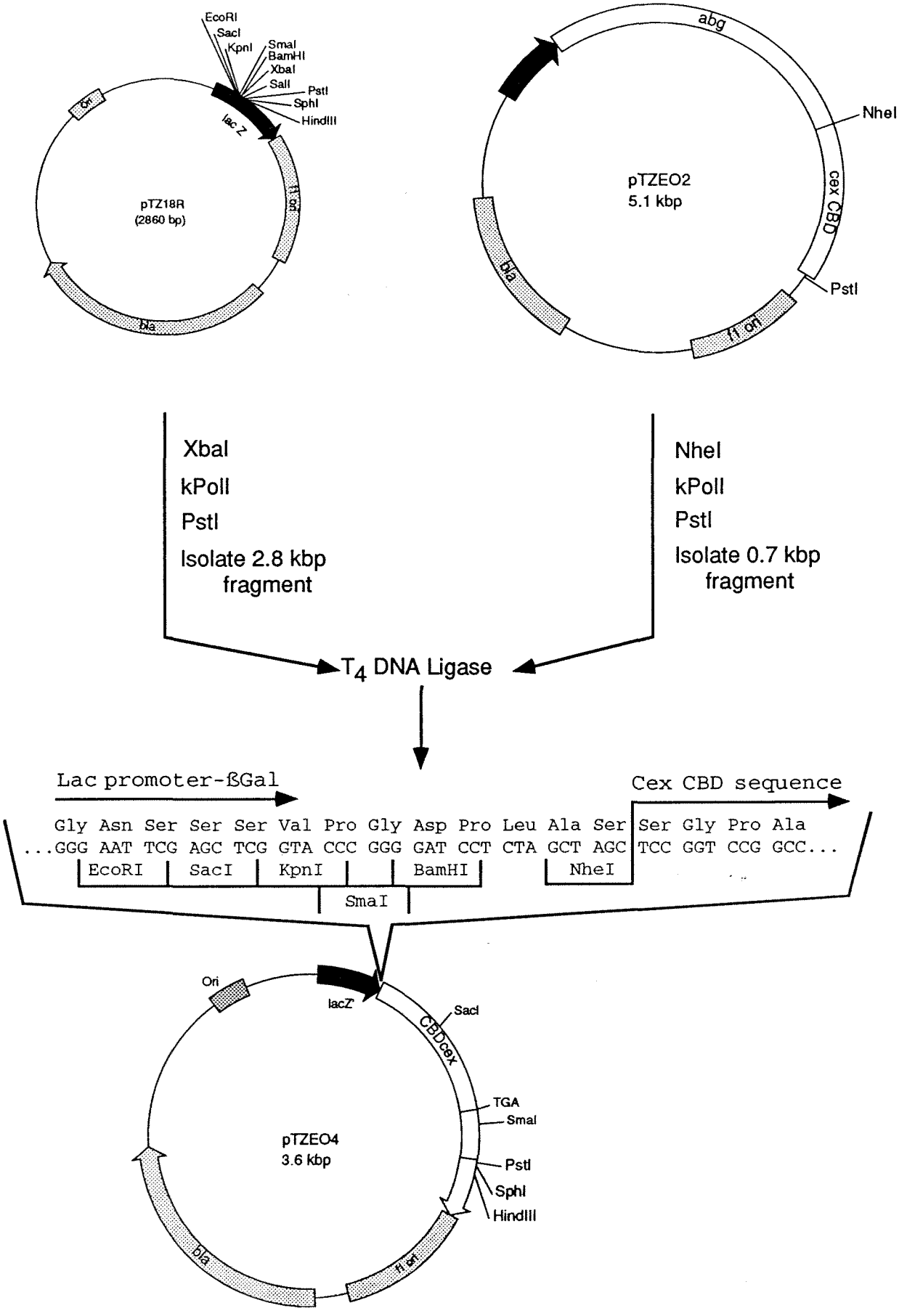
EcoRI
SacI
KpnI
SmaI
BamHI
XbaI
SalI
PstI
SphI
HindIII
ori
lac Z
pTZ18R
(2860 bp)
f1 ori
bla
abg
NheI
pTZEO2
5.1 kbp
cex CBD
bla
PstI
f1 ori
XbaI
kPolI
PstI
Isolate 2.8 kbp fragment
NheI
kPolI
PstI
Isolate 0.7 kbp fragment
T4 DNA Ligase
Lac promoter-ßGal
Cex CBD sequence
Gly Asn Ser Ser Ser Val Pro Gly Asp Pro Leu Ala Ser Ser Gly Pro Ala
...GGG AAT TCG AGC TCG GTA CCC GGG GAT CCT CTA GCT AGC TCC GGT CCG GCC...
EcoRI
SacI
KpnI
BamHI
NheI
SmaI
Ori
lacZ
SacI
CBDcex
TGA
SmaI
PstI
SphI
HindIII
pTZEO4
3.6 kbp
bla
f1 ori

lac promoter. The correctness of the constructs was confirmed by restriction endonuclease analysis and DNA sequencing.

3.1.2 Production of CBD_{Cex}

The production of CBD_{Cex} in *E. coli* JM101/pTZEO7 was detected by Western blot analysis (Figure 3.5). Approximately 30% of the CBD_{Cex} produced by the cell was found in the culture medium. The introduction of the consensus Shine-Dalgarno sequence upstream of the ATG of the coding sequence for the Cex leader peptide increased the production of CBD_{Cex} by 4-fold (Figure 3.6 A).

CBD_{Cex} was purified by batch affinity chromatography on Avicel™. The typical yield was between 10-15 mg $CBD_{Cex}.L^{-1}$ culture medium. Recovery of CBD_{Cex} bound to either Avicel™ or CF1™ cellulose using GdmCl was greater than 90%. The material obtained was >98% pure (Figure 3.6 B). The material purified from Avicel™ was contaminated with xylan (up to 30 K mol. wt.) as determined by proton nuclear magnetic resonance spectroscopy and fast-atom bombardment mass spectrometry (J. Carver, personal communication). The xylan was removed by cation-exchange chromatography (Figure 3.7). The $A_{280\ nm}$ peaks 2 and 3 corresponded to CBD_{Cex}. The reason for two CBD_{Cex} peaks was not clear. Subsequent proteolytic digestion by pepsin (see 3.1.6) involved peak 3 only.

3.1.3 Properties of CBD_{Cex}

The mol. wt. of CBD_{Cex}, deduced from the DNA-derived protein sequence (O'Neill *et al.*, 1986), was 11,081. The M_r of CBD_{Cex} as determined by SDS-PAGE was 11 K. The isoelectric point (pI) for the polypeptide was approximately 8.6. The predicted pI was 8.3 (Skoog & Wichman, 1986). The

Figure 3.5 CBD_{Cex} production in *E. coli* JM101/pTZEO7. Crude cell extracts were prepared from two transformants. A sample (50 µg total protein) was bound to 1.25 mg of Avicel™. The mixture was incubated for 3 h on ice with periodic agitation. After centrifugation the cellulose pellet was washed with 2 x 100 µL of 1M NaCl in phosphate buffer followed by 2 x 100 µL phosphate buffer. Following centrifugation the pellet was resuspended in 20 µL of 2x SDS loading dye, boiled for 2.5 min and centrifuged. Equivalent amounts of proteins were analyzed by SDS-PAGE. Lane 1, cell extract of *E. coli* JM101/pTZ18R. Lane 2, Cex cleaved with a *C. fimi* serine protease. The upper band, p36, is the Cex catalytic domain with the Pro-Thr linker. The lower band is CBD_{Cex}. Lanes 3 and 6, crude cell extracts from two transformants. Lanes 4 and 7, unbound proteins. Lanes 5 and 8, proteins which bound to Avicel™. (A) Coomassie blue-stained gel. (B) Western blot. The primary antiserum used was rabbit anti-Cex.

A

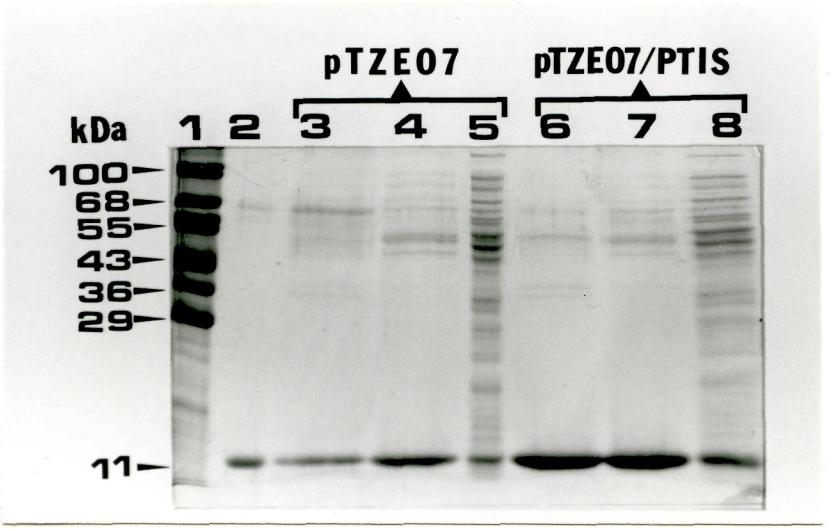

B

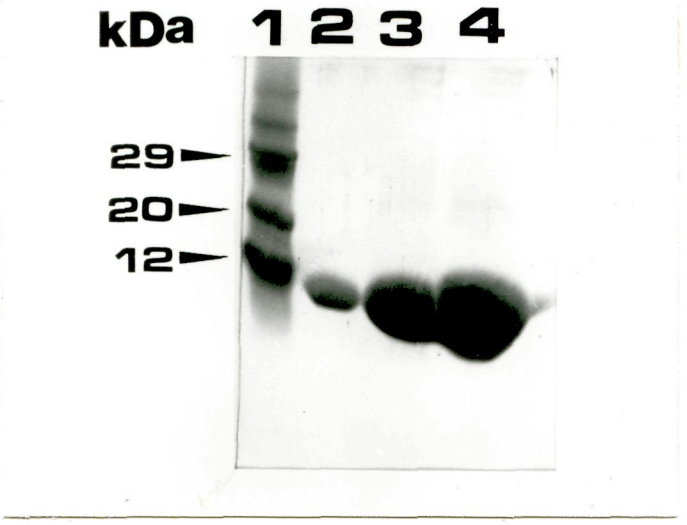

Figure 3.6

A. CBD_{Cex} production by *E. coli* JM101/pTZEO7 and JM101/pTZEO7 (PTIS). Culture medium (500 µL) and crude cell extract (50 µg) were bound separately to 5 mg Avicel™. The mixtures were treated as in the legend to Figure 3.5. The polypeptides were analyzed by SDS-PAGE. Lane 1, molecular weight markers. Lane 2, purified CBD_{Cex}. Lanes 3 and 6, Avicel™-bound proteins from culture medium. Lanes 4 and 7, Avicel™-bound proteins from crude cell extract. Lanes 5 and 8, crude cell extracts corresponding to 1/8th of the amounts loaded in lanes 4 and 7.

B. Purity of CBD_{Cex}. CBD_{Cex} was purified by batch affinity chromatography on CF1™ cellulose, then analyzed by SDS-PAGE. Lane 1, molecular weight markers. Lanes 2-4 are loaded with 12, 60 and 120 µg CBD_{Cex}, respectively.

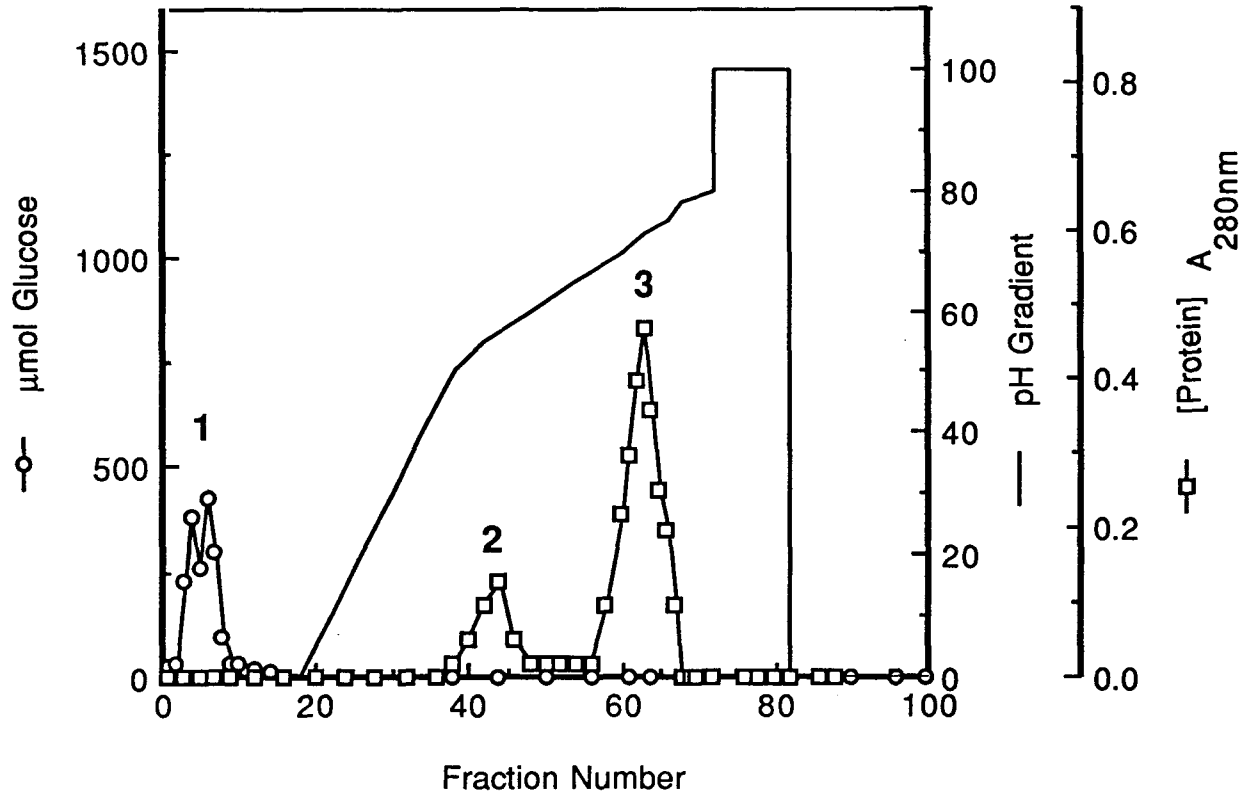

Figure 3.7 Removal of xylan from purified CBD_{Cex}. A 12.5 mg sample of CBD_{Cex} in 20 mM trimethylamine/formic acid, pH 4 was loaded onto a MacroprepS Econocolumn (Bio-Rad). Sensitivity of the UV monitor was set at 2.0 absorbance units. The gradient was formed with 20 mM trimethylamine/ formic acid, pH 4 and pH 7. (○) carbohydrate detected by the phenol-sulfuric acid assay. (□) absorbance at 280 nm. (—) pH gradient.

ε_{280nm} for CBD_{Cex} was 2.3 $mL.mg^{-1}.cm^{-1}$. The predicted ε_{280nm} (Cantor & Schimmel, 1980) was 2.6 $mL.mg^{-1}.cm^{-1}$. The N-terminal amino acid sequence was ASSGP, in agreement with the predicted sequence (O'Neill *et al.*, 1986). The polypeptide reacted with anti-Cex antiserum (Figure 3.5).

3.1.4 Binding of CBD_{Cex}

An adsorption model describing the interaction of a large ligand (protein) with a lattice of overlapping potential binding sites (cellobiosyl units) was used to analyze binding of CBD_{Cex} to cellulose (Gilkes *et al.*, 1992). The dimensions of CBD_{CenA} (Pilz *et al.*, 1990; Shen *et al.*, 1991) are greater than the dimensions of the repeating cellobiosyl unit on the cellulose surface (Henrissat *et al.*, 1988). This results in the CBD occupying several lattice units at any given time. If a binding site is larger than one lattice unit, the surface can be considered as an array of overlapping potential binding sites. The Langmuir adsorption isotherm models a single ligand interacting with only one receptor (Stuart & Ristroph, 1985; Steiner *et al.*, 1988). This model is not valid for the CBD. A probability function must be included to find the concentration of available binding sites (Gilkes *et al.*, 1992). The probability depends on both the concentration and configuration of proteins bound on the cellulose surface. This complication can be avoided if one only considers low concentrations of bound protein where the spacing is such that any two neighboring CBD molecules do not exclude the binding of a third CBD. The modified Langmuir equation (1) can be "linearized" by rearranging it in a double reciprocal form (2) which emphasizes data for the lower concentration range.

$$\text{bound [P]} = \frac{[N_o] \cdot K_a \cdot \text{free [P]}}{1 + a \cdot K_a \cdot \text{free [P]}} \qquad (1)$$

$$\frac{1}{\text{bound [P]}} = \frac{1}{K_a \cdot [N_o]} \cdot \frac{1}{\text{free [P]}} + \frac{a}{[N_o]} \qquad (2)$$

where bound [P] is the concentration of bound protein (μmole.g cellulose^{-1}), free [P] is the concentration of free protein (μmolar), $[N_o]$ is the concentration of binding sites in the absence of protein (μmole.g cellulose^{-1}), K_a is the equilibrium association constant (L.μmole^{-1}) and a is the number of lattice units occupied by a single protein molecule (μmole lattice unit.μmole protein^{-1}).

Bound protein was determined from the difference between the initial protein concentration ($[P_o]$, μM) and the equilibrium concentration of free protein. The adsorption isotherm was derived by plotting bound [P] vs. free [P]. The saturation value was estimated at the highest total protein concentrations. The absolute value of K_a cannot be determined unless $[N_o]$ is known (Gilkes *et al.*, 1992). However, a relative affinity value [$(K_a \cdot [N_o])^{-1}$; L.g cellulose^{-1}] can be used to compare the affinities of various proteins for a given preparation of cellulose (i.e. when $[N_o]$ is constant). The relative affinity was determined from the initial slope of the double reciprocal plot (1/bound [P] vs. 1/free [P]), i.e. slope = $(K_a \cdot [N_o])^{-1}$, at low protein concentrations.

The binding of CBD_{Cex} to Avicel™, BMCC, α-chitin and regenerated cellulose was determined. Regenerated cellulose had the highest capacity for binding CBD_{Cex} (Figure 3.8). It becomes predominantly amorphous in nature after acid treatment. BMCC bound 5-fold more CBD_{Cex} than did Avicel™, suggesting that BMCC had significantly more surface area for adsorption. CBD_{Cex} bound most strongly to BMCC and least strongly to regenerated cellulose (Figure 3.9), indicating a tighter adsorption of the polypeptide to cellulose with a higher crystallinity. The relative affinity and saturation level of CBD_{Cex} adsorbed to α-chitin was about twice that of Avicel™. Adsorption to α-chitin suggests that CBD_{Cex} recognizes a common structural pattern in both cellulose and chitin.

Two operating parameters of importance for immobilized enzyme columns are temperature and pH. CBD_{Cex} bound to BMCC over wide ranges of temperature and pH (Figures 3.10; 3.11). The relative affinities were not markedly influenced by temperature within the range tested, although a lower value was observed at 50°. The relative affinity increased with increasing pH. The highest value was observed at pH 9, around the isoelectric point of CBD_{Cex}. The saturation levels remained essentially the same.

Detergents might block or destabilize the binding of a CBD fusion polypeptide. This would preclude the use of detergents in wash solutions or reaction mixtures. CBD_{Cex} adsorbed to and remained bound to cellulose in the presence of up to 2% Triton X-100, a non-ionic detergent (Figure 3.12). It adsorbed to and remained bound to cellulose in the presence of 0.2% SDS, an ionic detergent (Figure 3.12). Higher concentrations of SDS destabilized the binding.

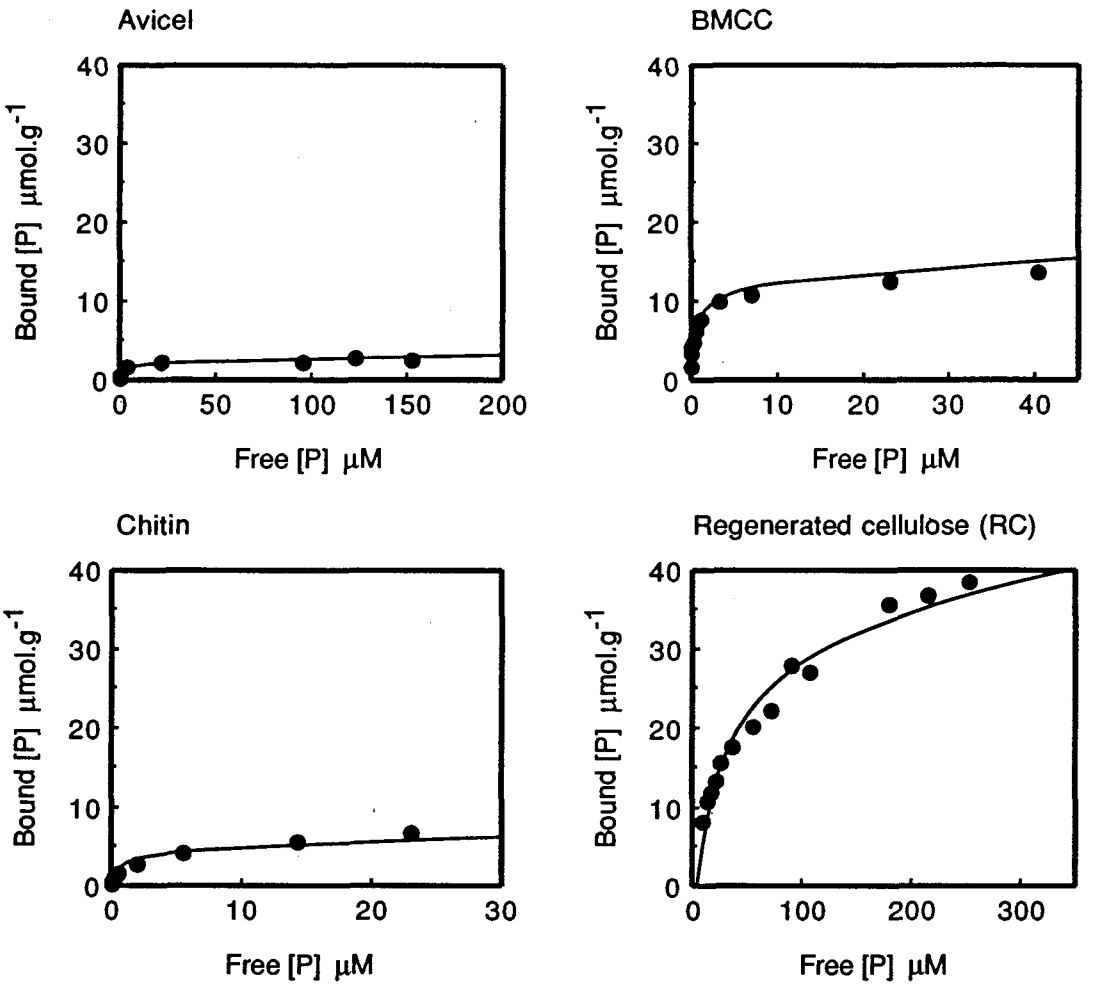

Substrate	Saturation level (µmol.g^{-1})
Avicel	> 3
BMCC	> 15
Chitin	> 7
RC	> 40

Figure 3.8 Adsorption of CBD_{Cex} to cellulose and α-chitin. Avicel™ (5 mg), BMCC (1 mg), chitin (1 mg) or regenerated cellulose (1 mg) was mixed with varying initial concentrations of CBD_{Cex} ($[P_o]$ = 0.9-180 µM for Avicel™ and $[P_o]$ = 1.8-300 µM for BMCC, chitin and regenerated cellulose). Samples were treated as in 2.12.

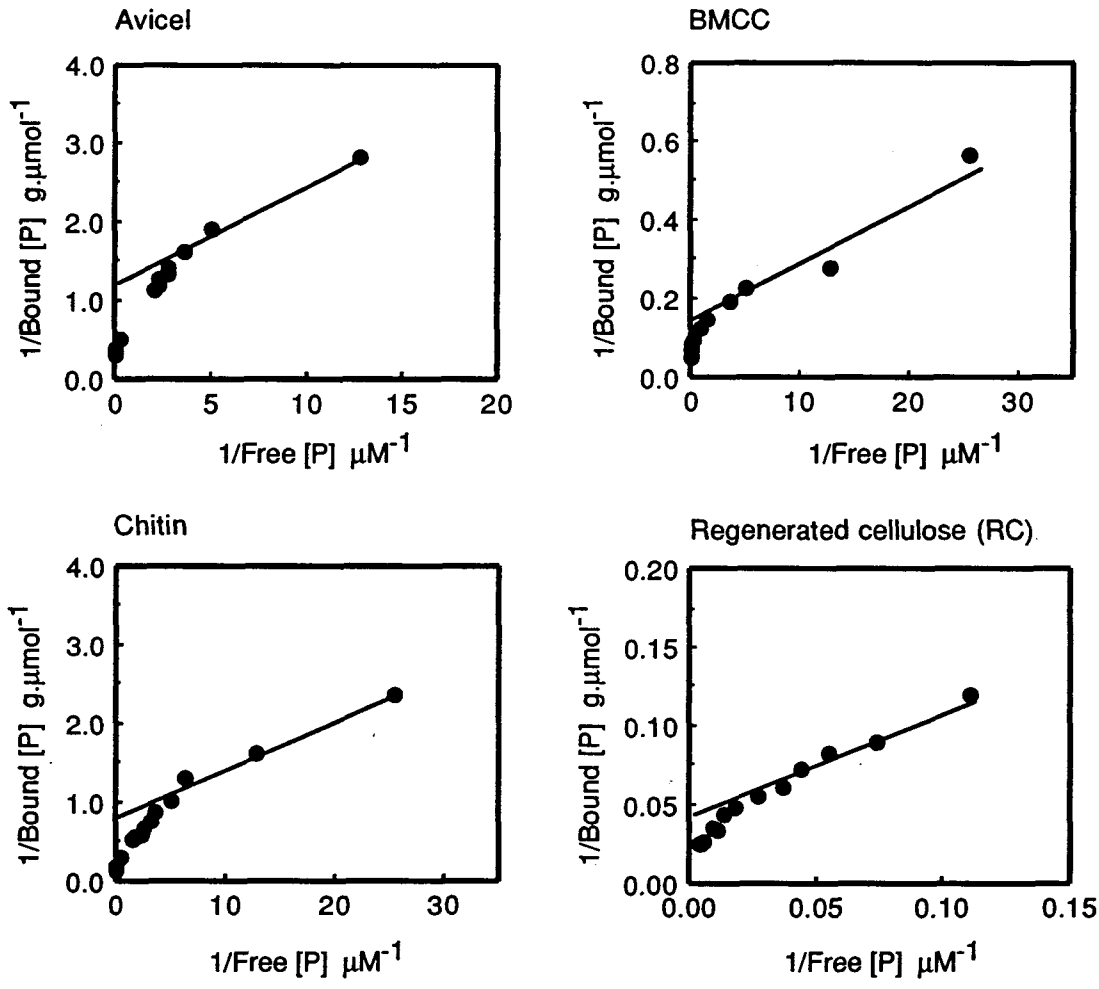

Substrate	Relative affinity ($L.g^{-1}$)
Avicel	8
BMCC	58
Chitin	18
RC	1

Figure 3.9 Relative affinities for the binding of CBD_{Cex} to cellulose and α-chitin. Details are given in the legend to Figure 3.8.

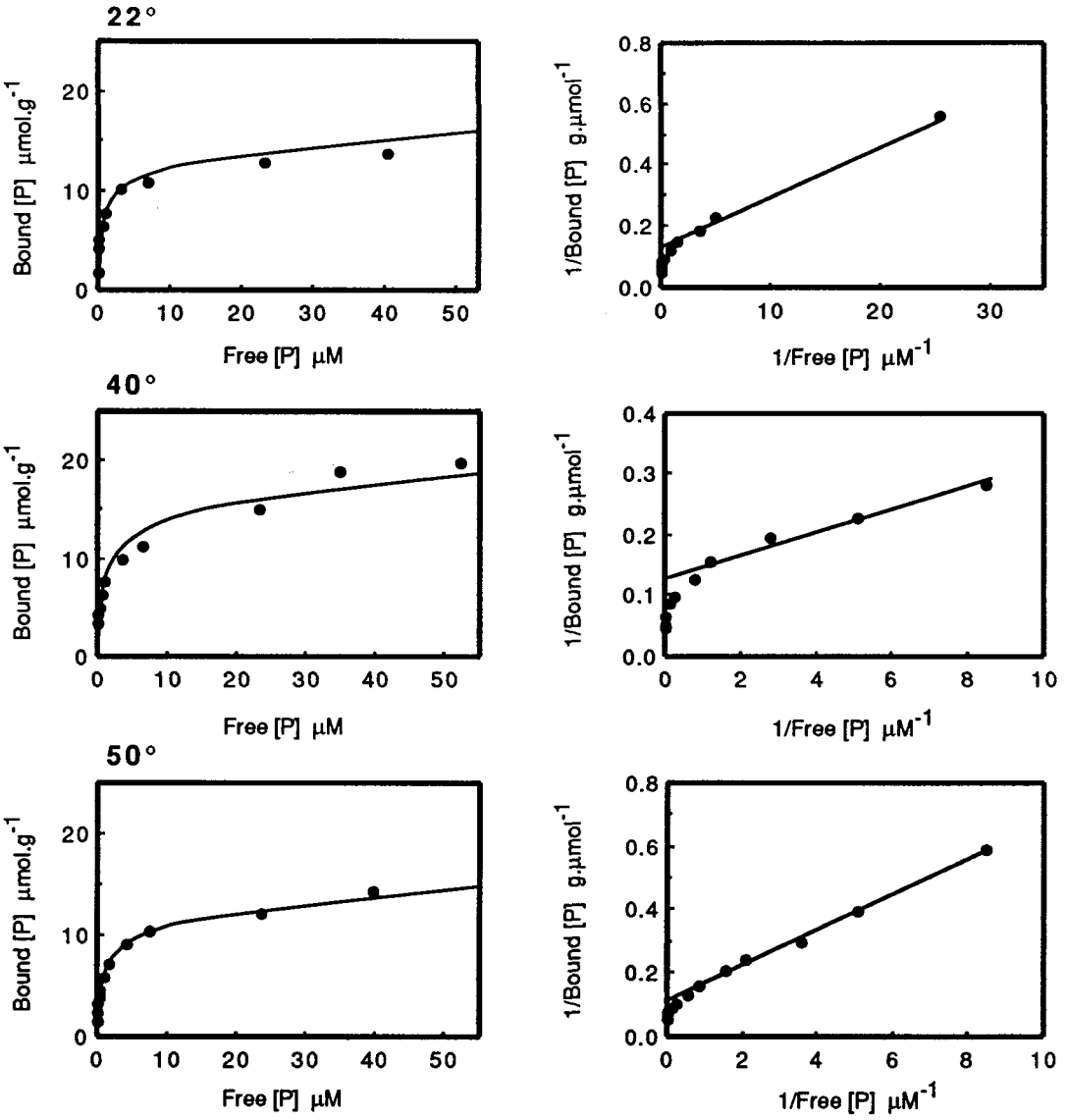

Temperature (°C)	Relative affinity ($L.g^{-1}$)	Saturation level ($\mu mol.g^{-1}$)
22	58	> 15
40	58	> 20
50	18	> 15

Figure 3.10 Adsorption of CBD_{Cex} to BMCC (1 mg) at 22°, 40° and 50°, pH 7. $[P_o]$ = 1.8-90 µM. Details are given in 2.12.

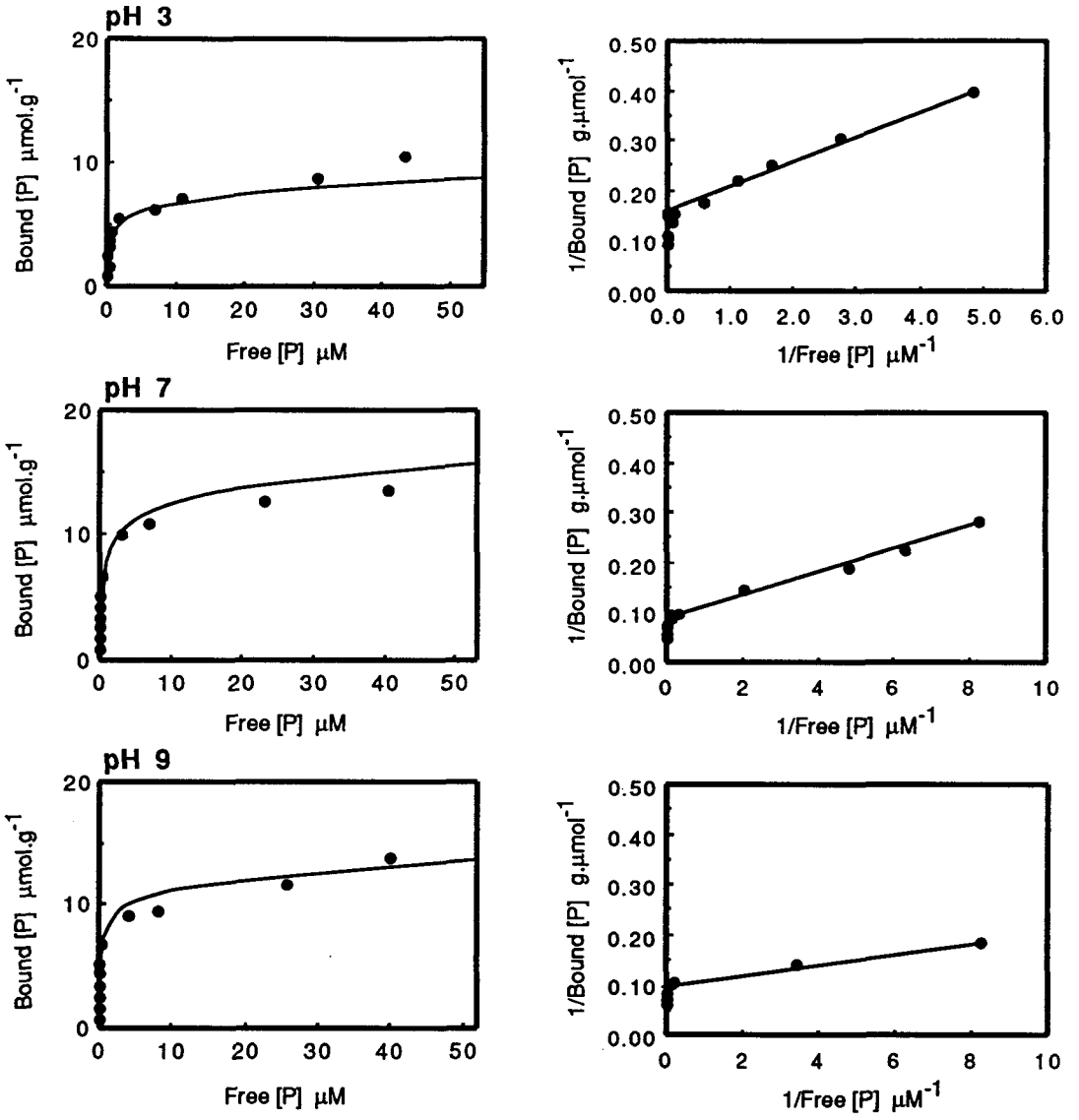

pH	Relative affinity ($L.g^{-1}$)	Saturation level ($\mu mol.g^{-1}$)
3	20	> 10
7	45	> 15
9	108	> 15

Figure 3.11 Adsorption of CBD_{Cex} to BMCC (1 mg) at pH 3, 7 and 9, 22°. $[P_o]$ = 1.8-90 µM. Details are given in 2.12.

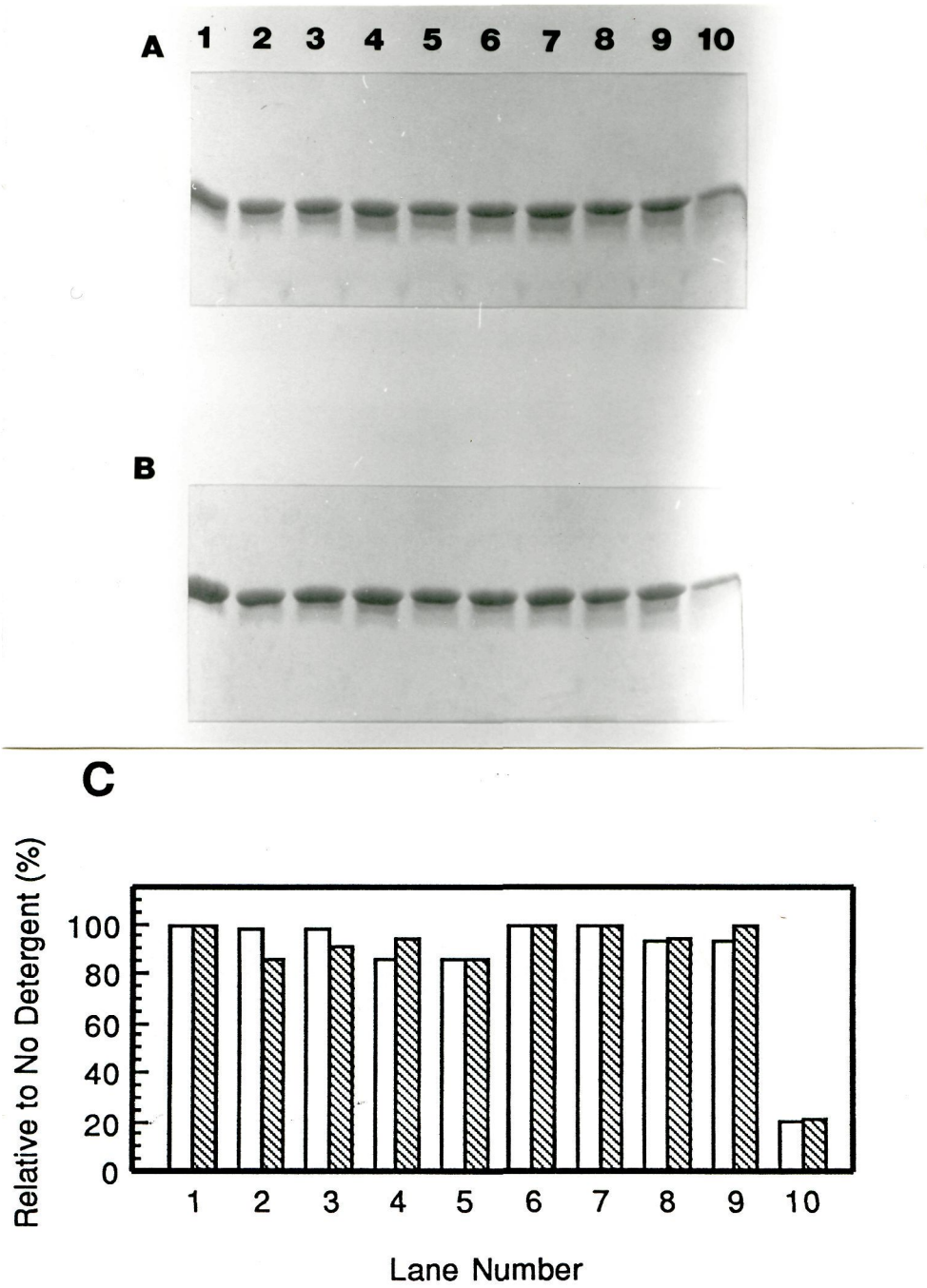

Figure 3.12 The influence of detergents on the binding of CBD_{Cex} to cellulose. Details are given in 2.15.4. The percentage of gel used was 16%T. Protein loading per lane was approximately 1.8 nmoles. The detergent was either added after binding of CBD_{Cex} to cellulose (**A,** □) or present during binding of CBD_{Cex} to cellulose (**B,** ▨). **C**, densitometric scan of protein bands. Lanes 1-5, CBD_{Cex} treated with Triton X-100 (0, 0.002%, 0.02%, 0.2% and 2%, respectively). Lanes 6-10, CBD_{Cex} treated with SDS (0, 0.002%, 0.02%, 0.2% and 2%, respectively).

3.1.5 CBD_{Cex} contains a disulfide bridge

An indirect way of showing the presence of disulfide bonds in a protein is to analyze the migration of the protein in an SDS-polyacrylamide gel in the presence or absence of a reducing agent such as ß-mercaptoethanol (BME) or 1,4-dithiothreitol (DTT). Proteins that are not reduced, i.e. that have disulfide bridges, have a different hydrodynamic behavior and as a result appear to be smaller and therefore migrate further in an SDS-polyacrylamide gel (Creighton, 1989). There are 3 disulfide bridges in Cex, one of which is in the CBD (Gilkes *et al.*, 1991a). CBD_{Cex} migrated more slowly in the presence than in the absence of BME (Figure 3.13), showing that the two cysteine residues in CBD_{Cex} formed a disulfide bridge. The failure of CBD_{Cex} to react with DTNB (Creighton, 1989) confirmed this (data not shown). This is consistent with the finding of Gilkes *et al.* (1991a).

3.1.6 Sensitivity of CBD_{Cex} to proteases

Digestion of a protein with proteases of different specificities often provides information regarding its conformation (Price & Johnson, 1989). Proteolysis pinpoints specific residues that are exposed and susceptible to digestion. Denaturants and reducing agents can be added to monitor changes in protease susceptibility of the protein as a result of unfolding or the reduction of disulfide bridge(s).

CBD_{Cex} purified by affinity chromatography on Avicel™ was resistant to cleavage by papain, endoproteinase Lys-C, endoproteinase Asp-N, trypsin, and a *C. fimi* serine protease. Trypsin hydrolyzed CBD_{Cex}, but only slowly (Figure 3.14). There are two possible trypsin cleavage sites in CBD_{Cex} : K28 and R68. Complete digestion should give fragments of 2.9, 4 and 4.1 kDa; partial digestion

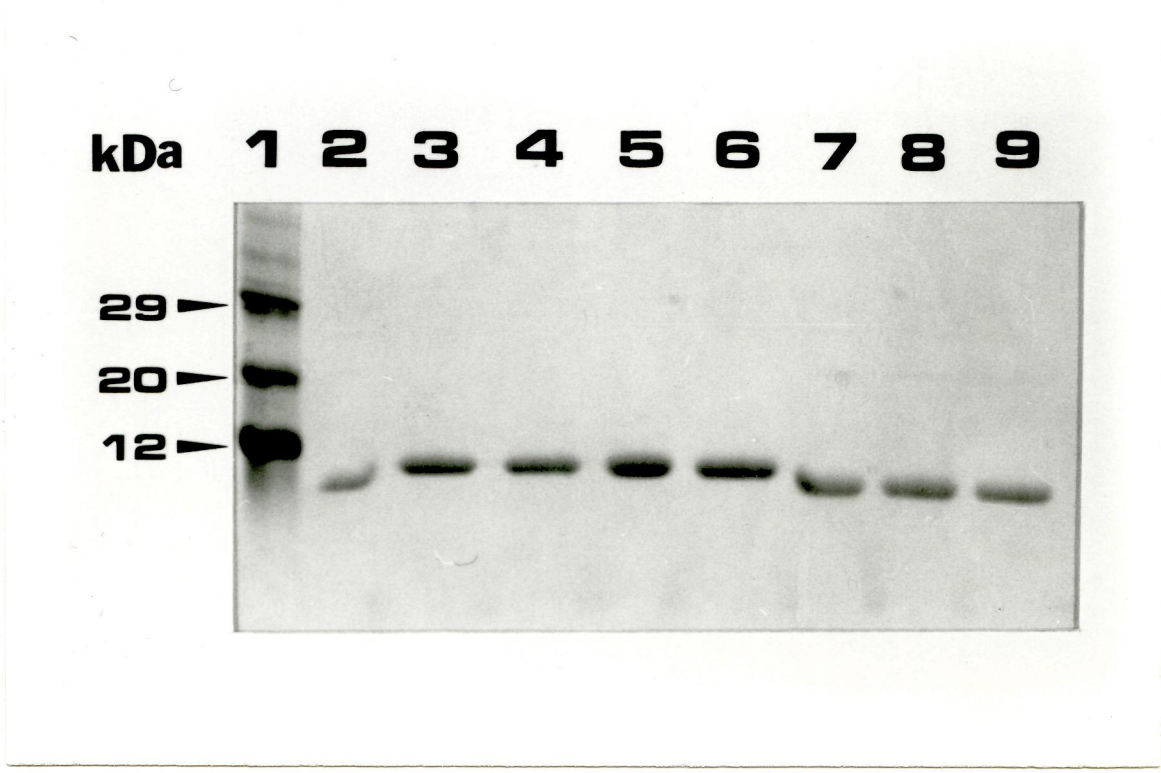

Figure 3.13 The influence of ß-mercaptoethanol (BME) on the mobility of CBD_{Cex}. The percentage of gel used was 15%T. Protein loading per lane was approximately 0.7 nmoles. Lane 1 is molecular weight markers. CBD_{Cex} was electrophoresed either in the presence (lanes 3-6) or absence (lanes 2, 7-9) of BME with no heat treatment (lanes 2 & 3) or incubated for 3 min at 37° (lanes 4 & 7), 60° (lanes 5 & 8) and 100° (lanes 6 & 9).

Figure 3.14 Trypsin sensitivity of CBD_{Cex}

A. Single time-point trypsin digestion of CBD_{Cex}. CBD_{Cex} (554 μg; 50 nmoles) was dissolved in 123 μL of 8 M urea in 0.4 M $NaHCO_3$ and 15 μL of 0.5 M DTT, and incubated at 50° for 15 min. The sample was diluted to 1000 μL with dH_2O supplemented with 20 mM $CaCl_2$. TPCK-treated trypsin (10 $mg.mL^{-1}$ stock in 1 mM HCl) was added to a final weight ratio of 1:30 (trypsin:CBD_{Cex}). The solution was incubated at 37° for 2 h. The reaction was stopped by adding PMSF (10 $mg.mL^{-1}$ stock in 100% isopropanol) to a final concentration of 100 $\mu g.mL^{-1}$. Buffer (0.4 M $NaHCO_3$) replaced either urea or DTT, or both in the other tubes. Samples (each equivalent to 11 μg; 1 nmole) were analyzed by SDS-PAGE.

Lanes 1-6 are + CBD_{Cex}
- Lane 1 is + urea, - DTT, + trypsin.
- Lane 2 is + urea, - DTT, - trypsin.
- Lane 3 is - urea, + DTT, + trypsin.
- Lane 4 is - urea, + DTT, - trypsin.
- Lane 5 is + urea, + DTT, + trypsin.
- Lane 6 is + urea, + DTT, - trypsin.

Lane 7 is - CBD_{Cex}, + urea, + DTT, + trypsin.
Lane 8 is + CBD_{Cex}, - urea, - DTT, - trypsin.
Lane 9 is trypsin (10 μg).

B. Time course digestion of CBD_{Cex} with trypsin. CBD_{Cex} was digested as above in the presence of urea and DTT. Numbers refer to the incubation time in min.

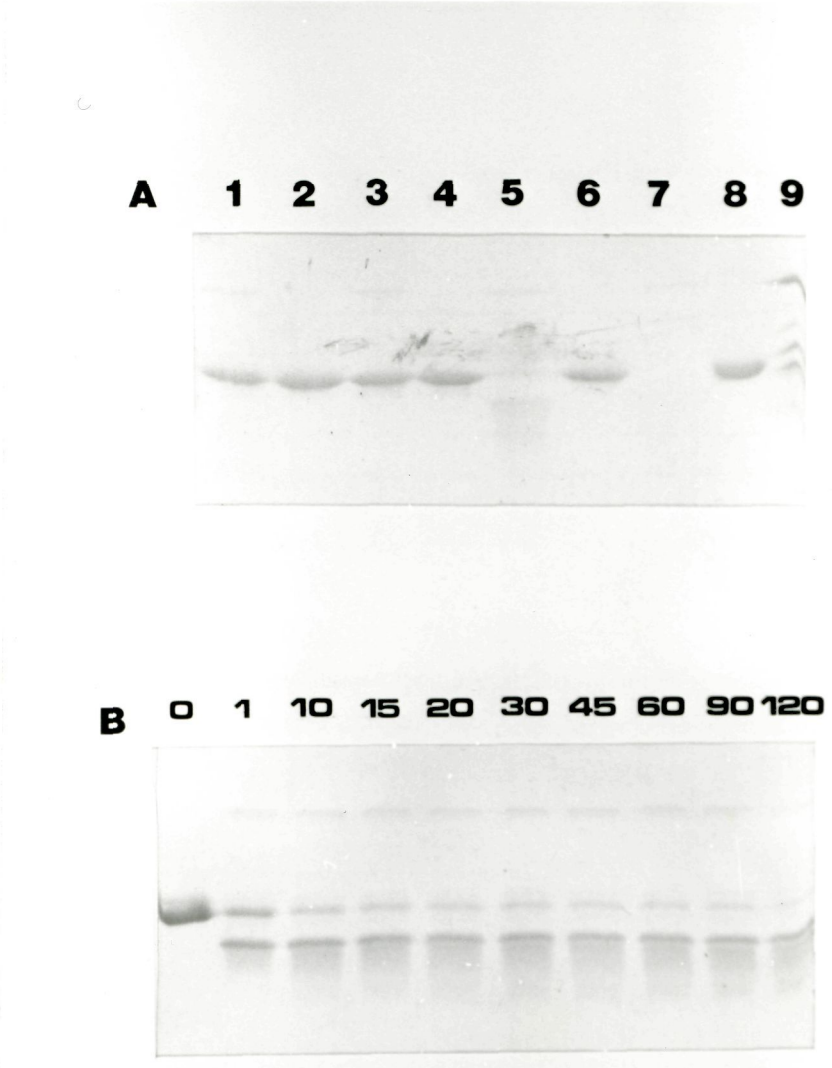
A 1 2 3 4 5 6 7 8 9
B 0 1 10 15 20 30 45 60 90 120

could give fragments of 8.1, 6.9, 4.1, and 2.9 kDa. Since CBD_{Cex} was only cleaved in the presence of both urea and DTT, denaturation appears essential to expose the amino acid residue(s) recognized by trypsin.

Analysis of CBD_{Cex} prepared for two-dimensional nuclear magnetic resonance spectroscopy revealed that the material purified on Avicel™ contained xylan (J. Carver, personal communication). The xylan associated with CBD_{Cex} (see 3.1.2) affected its sensitivity to pepsin. The xylan-free material was resistant to pepsin, whereas the contaminated material was rapidly degraded (Figure 3.15A & B). When the xylan-free material was readsorbed to Avicel™, desorbed with GdmCl and the GdmCl removed, it became susceptible to pepsin (Figure 3.15C). Apparently, the xylan contaminant picked up by CBD_{Cex} from Avicel™ alters the conformation of the polypeptide, making it susceptible to pepsin.

Figure 3.15 Digestion of CBD_{Cex} with pepsin

A. Avicel™-purified CBD_{Cex} (200 μg; 18 nmoles) was diluted to 200 μL with 0.4% acetic acid, pH 3. Pepsin (5 $mg.mL^{-1}$ stock in 1 mM HCl) was added to a final weight ratio of 1:5. The digest was incubated at 37°. Samples were removed at intervals and added to an equal volume of 1 M Tris.Cl buffer, pH 8 to stop the reaction. 10 μg (1 nmole) from each sample were analyzed by SDS-PAGE. Pepsin was replaced with acetic acid buffer in the control digest. Lane 1, molecular weight markers; lanes 2 and 8, no pepsin control at 0 and 1 h, respectively; lanes 3-7 are pepsin digestion of CBD_{Cex} at 0, 5, 15, 30 and 60 min, respectively.

B. Details are as above except CBD_{Cex} was purified further by cation-exchange chromatography on MacroprepS beads (Bio-Rad).

C. CBD_{Cex} from **B** was bound to Avicel™, desorbed with 8 M GdmCl and exchanged with dH_2O. The sample was treated as in **A**. Lane 1, molecular weight markers; lanes 2-4, 5-7 and 8-10, CBD_{Cex} in **B**, CBD_{Cex} in **C**, and CBD_{Cex} in **A**, respectively. Digestion for each sample was 0, 5 and 60 min, respectively.

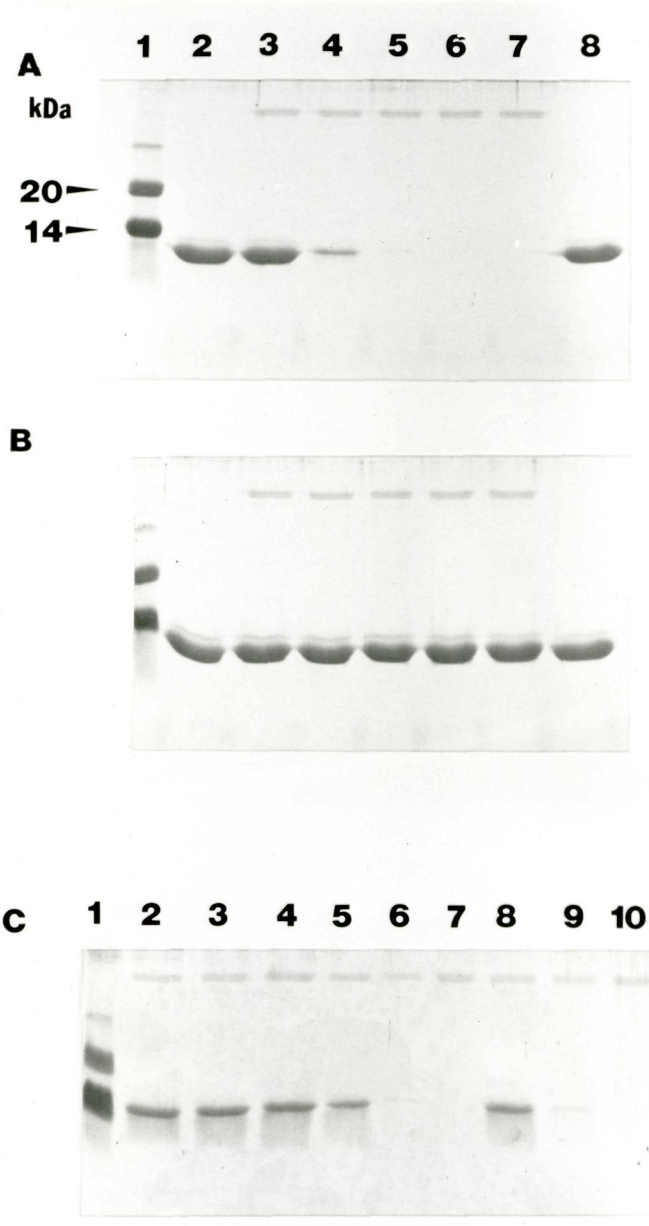
A
1 2 3 4 5 6 7 8
kDa
20
14
B
C
1 2 3 4 5 6 7 8 9 10

3.2 A fusion polypeptide comprising CBD_{Cex} fused to the C-terminus of a ß-glucosidase (Abg) from an *Agrobacterium* sp. (Abg-CBD_{Cex}; Figure 3.1)

3.2.1 Construction of plasmids expressing *abg-CBD_{cex}*

The model enzyme chosen for immobilization work comprised the ß-glucosidase Abg (Han & Srinivasan, 1969) fused at its C-terminus to the N-terminus of CBD_{Cex}. It was designated Abg-CBD_{Cex}. The first plasmid construct (pEO1) expressed the fusion protein Abg-$CBD_{Cex}1$. In this polypeptide 37 amino acids of the C-terminus of Cex catalytic domain and the Pro-Thr linker separated the fusion partners (Figure 3.16). Oligonucleotide-directed *in vitro* "loop out" mutagenesis was used to remove the linker, giving pTZEO2 (Figure 3.17). In a third construct, pTZEO3, the C-terminus of Abg was fused precisely to the N-terminus of CBD_{Cex} (Figure 3.18). Gene expression in all three plasmids was controlled by the *lac* promoter. The correctness of the constructs was confirmed by restriction endonuclease analysis and DNA sequencing. The fusion polypeptides expressed by pEO1, pTZEO2 and pTZEO3 were designated Abg-$CBD_{Cex}1$, Abg-$CBD_{Cex}2$ and Abg-$CBD_{Cex}3$, respectively.

3.2.2 Improved yield of Abg-$CBD_{Cex}1$ in *E. coli* CAG456/pEO1

E. coli CAG456 has an amber mutation in the *htp*R locus and a temperature-sensitive suppressor t-RNA; *E. coli* CAG440 is an *htp*R^+ isogenic variant of CAG456 (Baker *et al.*,1984). The *htp*R locus encodes the sigma factor required for transcription of heat shock and other SOS genes (Grossman *et al.*, 1984).

Figure 3.16 Construction of pEO1. pUC12-1.1*cex* (PTIS) was digested completely with ScaI and NdeI, and the 1.1 kbp fragment was isolated containing the CBD_{cex} coding sequence. pABG5 (Wakarchuk *et al.*, 1986) was first digested completely with NdeI then partially with NcoI. A 3.8 kbp fragment containing the whole vector sequence plus the sequence encoding all but the last six amino acids of Abg was isolated. The 1.1 kbp and 3.8 kbp fragments were ligated using an adapter which encoded the last six amino acids of Abg, to give pEO1.

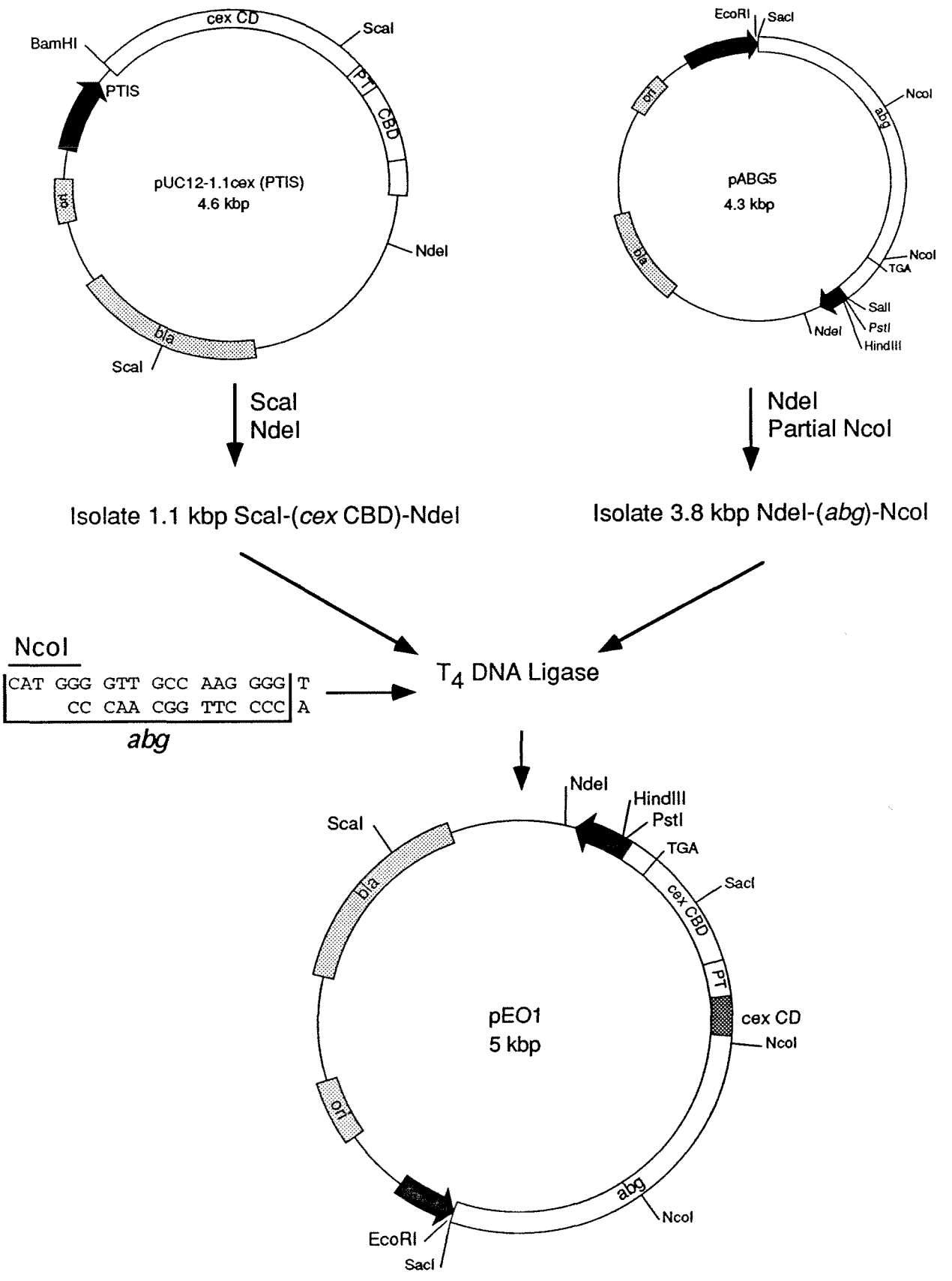
cex CD
ScaI
BamHI
PTIS
PT
CBD
pUC12-1.1cex (PTIS)
4.6 kbp
ori
NdeI
bla
ScaI
EcoRI
SacI
ori
NcoI
abg
pABG5
4.3 kbp
bla
NcoI
TGA
SalI
PstI
NdeI
HindIII
ScaI
NdeI
NdeI
Partial NcoI
Isolate 1.1 kbp ScaI-(cex CBD)-NdeI
Isolate 3.8 kbp NdeI-(abg)-NcoI
NcoI
CAT GGG GTT GCC AAG GGG T
CC CAA CGG TTC CCC A
abg
T4 DNA Ligase
NdeI
HindIII
PstI
TGA
SacI
cex CBD
PT
cex CD
NcoI
ScaI
bla
pEO1
5 kbp
ori
abg
NcoI
EcoRI
SacI

Figure 3.17 Construction of pTZEO1 and pTZEO2. pEO1 was digested completely with SacI and PstI. Two fragments were isolated from the digest: a 1.7 kbp fragment containing *abg*, *cex* catalytic domain (CD), *cex* PT and part of CBD_{cex}, and a 0.6 kbp fragment containing remainder of the CBD_{cex} and *cex* 3' non-coding region. pTZ18R was digested with SacI and PstI, then ligated to the two fragments from pEO1 to give pTZEO1. pTZEO2 was made by replacing the sequence encoding the Pro-Thr linker in pTZEO1 with an NheI site using oligonucleotide-directed *in vitro* "loop-out" mutagenesis.

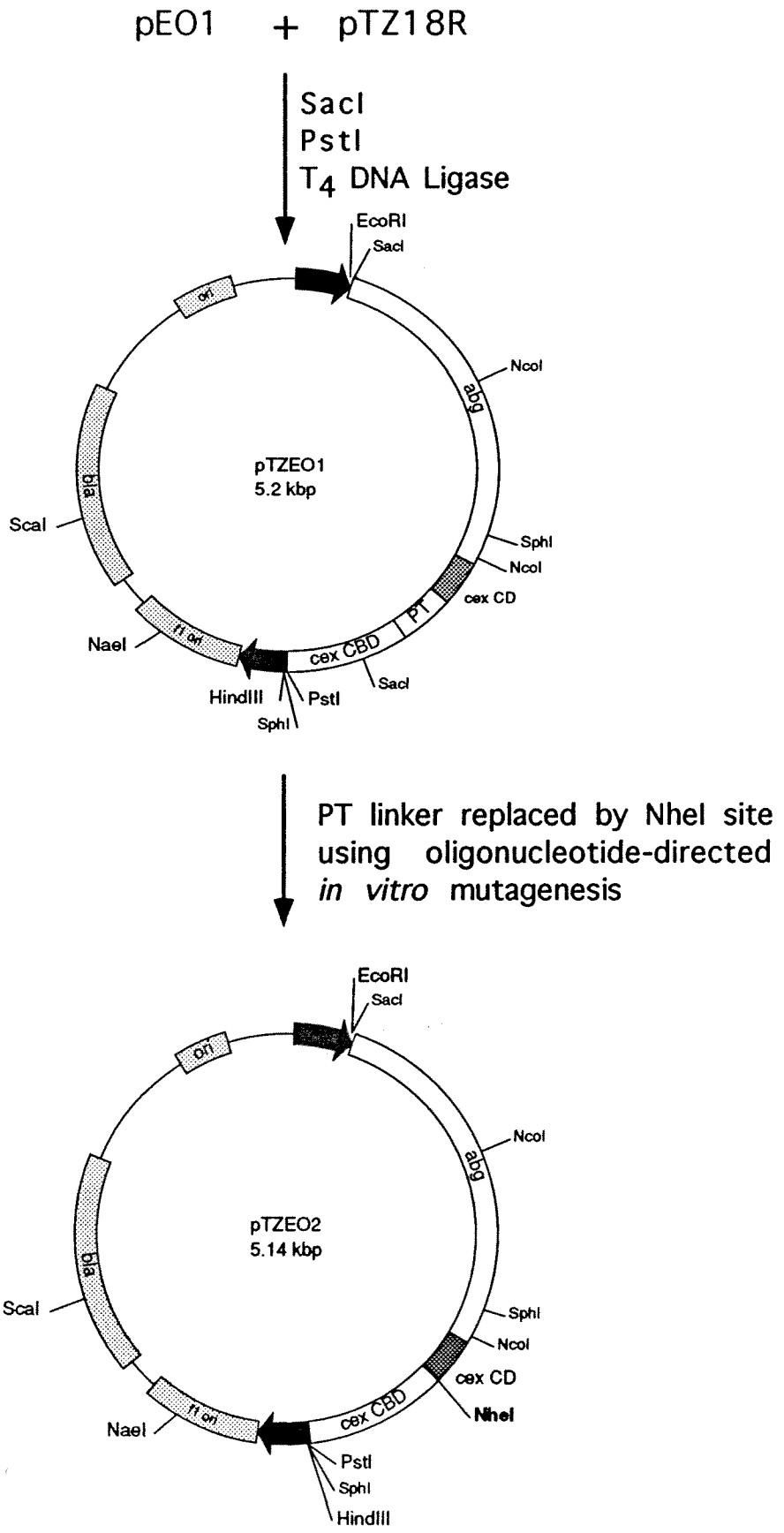
pEO1 + pTZ18R
SacI
PstI
T4 DNA Ligase
EcoRI
SacI
ori
NcoI
egg
pTZEO1
5.2 kbp
bla
ScaI
SphI
NcoI
cex CD
PT
f1 ori
NaeI
cex CBD
SacI
HindIII
PstI
SphI
PT linker replaced by NheI site using oligonucleotide-directed in vitro mutagenesis
EcoRI
SacI
ori
NcoI
egg
pTZEO2
5.14 kbp
bla
ScaI
SphI
NcoI
cex CD
NheI
f1 ori
NaeI
cex CBD
PstI
SphI
HindIII

Figure 3.18 Construction of pTZEO3. pTZEO2 was digested completely with NheI. The NheI sites were filled-in using kPolI. The blunt-ended DNA was digested partially with NcoI. A 5.1 kbp fragment containing all of pTZEO2 except the sequence encoding the last six amino acids of *abg* was isolated. An adapter (see Figure 3.16) was ligated to the 5.1 kbp fragment to give pTZEO3. The NheI site in pTZEO2 was not restored in pTZEO3.

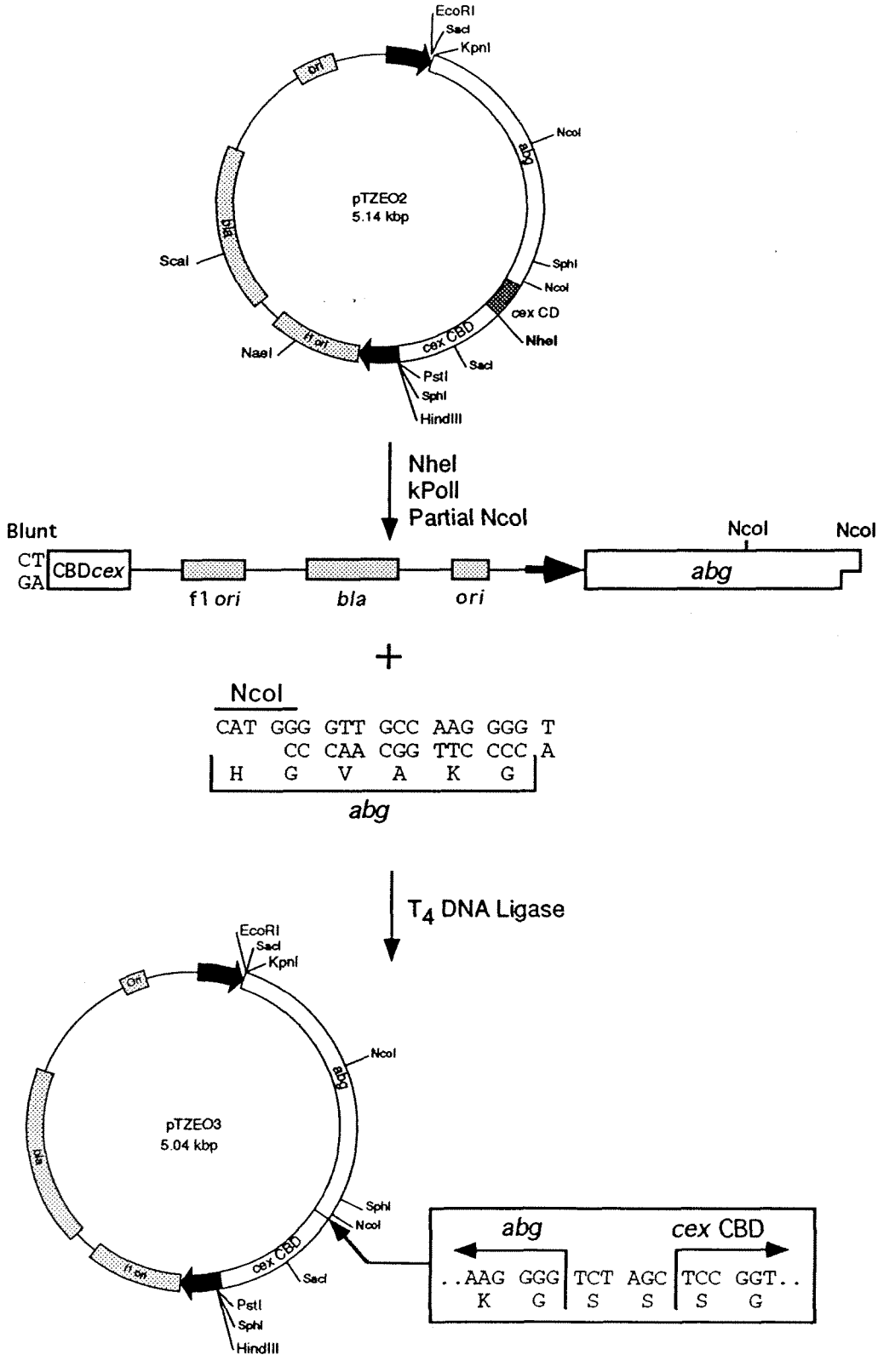
EcoRI
SacI
KpnI
ori
NcoI
abg
pTZEO2
5.14 kbp
ScaI
bla
SphI
NcoI
cex CD
NheI
NaeI
f1 ori
cex CBD
SacI
PstI
SphI
HindIII
NheI
kPoII
Partial NcoI
Blunt
CT
GA
CBDcex
NcoI
NcoI
f1 ori
bla
ori
abg
+
NcoI
CAT GGG GTT GCC AAG GGG T
CC CAA CGG TTC CCC A
H G V A K G
abg
T4 DNA Ligase
EcoRI
SacI
KpnI
Ori
NcoI
abg
pTZEO3
5.04 kbp
bla
SphI
NcoI
f1 ori
cex CBD
SacI
PstI
SphI
HindIII
abg
cex CBD
..AAG GGG TCT AGC TCC GGT..
K G S S S G

Overproduction of foreign proteins by *E. coli* may cause stress to which the cells respond by producing proteases (e.g. Lon protease) which may degrade the overproduced proteins (Goldberg & Goff, 1986). Some proteins are unstable when produced in a wild type strain, but exhibit significantly longer half-lives when produced in an *htp*R strain (Baker *et al.*, 1984). There was a 3-fold increase in total enzyme activity (to 298 pNPGase units) and a 4-fold increase in the specific activity of crude extracts (to 96 units.μmol^{-1}) of Abg-$CBD_{Cex}1$ when it was produced in CAG456 compared to JM109. The specific activities of Abg-$CBD_{Cex}1$ produced in CAG440 and JM109 were comparable. The CAG456 cells also contained more of the intact fusion protein (Figure 3.19). The low molecular weight polypeptides (<30 K) in the cell extracts (4, 5 and 6 in Figure 3.19) represented non-specific antibody binding. The lower molecular weight polypeptides in Abg-$CBD_{Cex}1$ (<55 K; 3 in Figure 3.19) were degradation products formed during storage of the enzyme (Ong *et al.*, 1989a).

3.2.3 Screening of Abg-CBD_{Cex}

The intact fusion polypeptides reacted with both anti-Abg and anti-Cex antisera (Figure 3.20). The degradation product(s) reacted only with anti-Abg antiserum indicating that these corresponded to Abg. The degradation products which were larger than native Abg were probably Abg with some amino acid residues from either the Cex catalytic domain or the CBD_{Cex} attached to its C-terminus, which did not react with the anti-Cex antiserum.

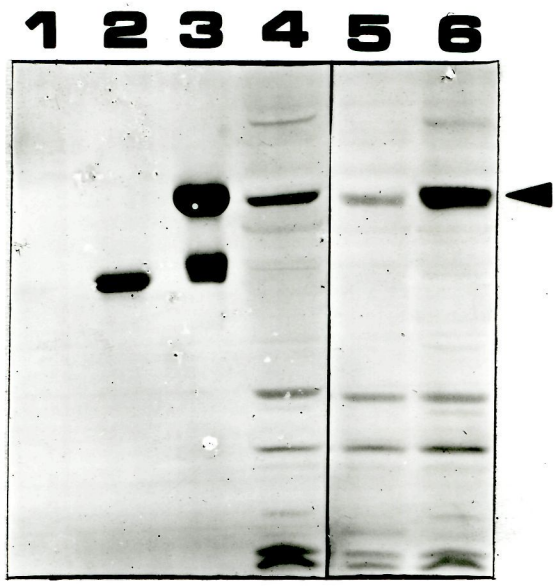

Figure 3.19 Abg-$CBD_{Cex}1$ production by various strains of *E. coli*. Polypeptides were resolved by SDS-PAGE and detected by Western blotting. The primary antiserum used was rabbit anti-Cex. Triangle indicates Abg-$CBD_{Cex}1$. Lanes 2 and 3, cellulose-purified Cex and Abg-$CBD_{Cex}1$, respectively; lanes 1, 4, 5 and 6, equivalent amounts of protein from JM109, JM109/pEO1, CAG440/pEO1, and CAG456/pEO1, respectively.

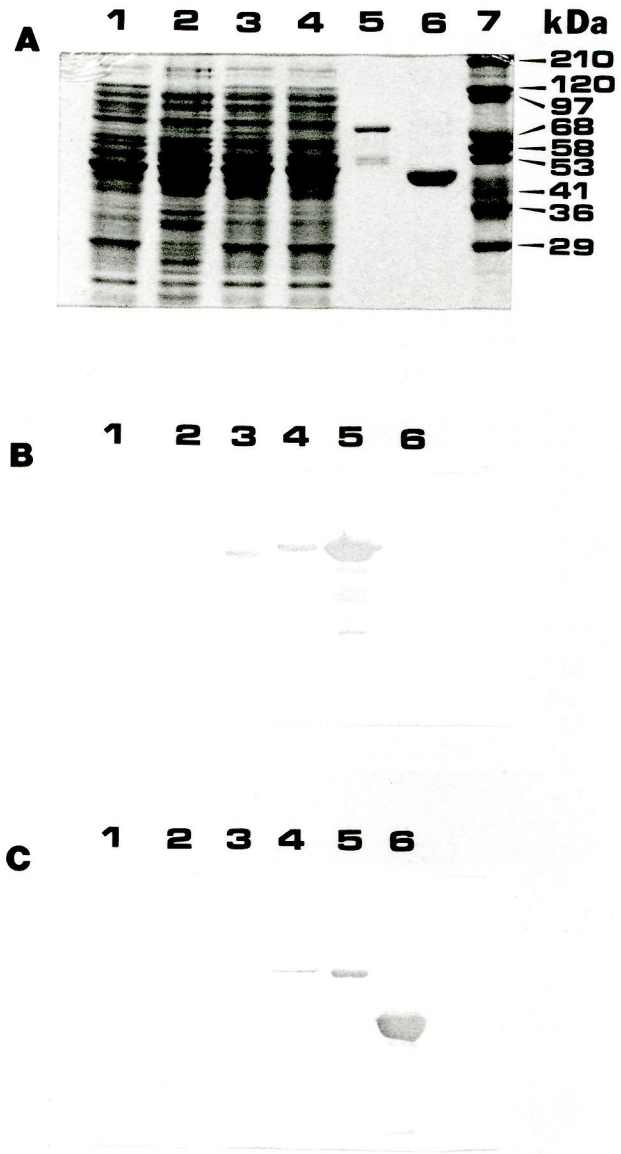

Figure 3.20 Integrity of Abg-CBD$_{Cex}$ produced by various *E. coli* strains. Lane 7, molecular weight markers. Lanes 5 and 6, purified Abg-CBD$_{Cex}$1 and Cex, respectively; lanes 1, 2, 3 and 4, equivalent amounts of cell extracts from JM101/pTZ18R, JM101/pTZEO3, JM101/pTZEO2, and JM101/pTZEO1, respectively. Primary antisera used were rabbit anti-Abg (B) and anti-Cex (C).

3.2.4 Large-scale purification of fusion polypeptides

CBD_{Cex} fusion polypeptides could be purified virtually to homogeneity in a single step by adsorption to and desorption from cellulose. After removal of the nucleic acids from the crude cell extract, the fusion polypeptide was adsorbed to cellulose. Non-specifically adsorbed proteins were desorbed with 1 M NaCl in phosphate buffer. The fusion polypeptide was then desorbed with dH_2O. The rate of desorption became significant when the conductivity of the column effluent decreased to < 1 μmho (Figure 3.21). The nature of the cellulose influenced the stability of adsorption. Only 20% of the bound fusion polypeptide was desorbed from Cellufine™ compared to 70% from CF1™ cellulose (Figure 3.22). This phenomenon is discussed in 3.2.11 and section 4. A typical purification scheme using CF1™ cellulose is summarized in Table 3.1. Column elution is shown in Figure 3.23. Comparable results were obtained using this protocol for Abg-CBD_{Cex}1, 2 and 3 (Table 3.2). The desorption yield was between 58-70%. A 100- to 260-fold purification of the fusion polypeptides was achieved using affinity chromatography on cellulose. The specific activity of the purified Abg-CBD_{Cex}1 was comparable to Abg that was purified using a combination of gel filtration and ion-exchange chromatography (K. Rupitz, personal communication). Large-scale production of CBD_{Cex} and Cbg-CBD_{Cex} is presented in 3.1.2 and 3.3.2, respectively.

3.2.5 Properties of the fusion polypeptides

The M_rs (68, 66 and 62 K) for the 3 fusion polypeptides as determined by SDS-PAGE were very similar to the predicted molecular weights (O'Neill *et al.*, 1986; Wakarchuk *et al.*, 1988). The N-terminal amino acid sequences of intact Abg-CBD_{Cex}1 and its degradation products were identical to that of mature Abg

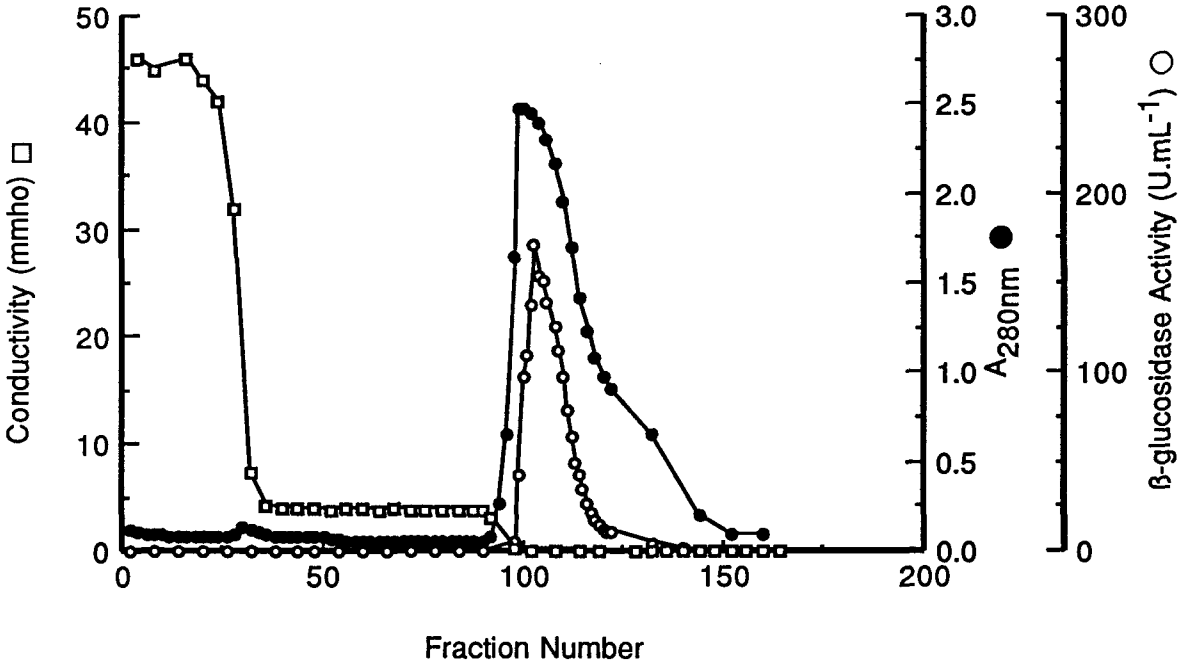

Figure 3.21 Purification of Abg-CBD$_{Cex}$1 by affinity chromatography on CF1 cellulose. Details are given in 2.5.2.

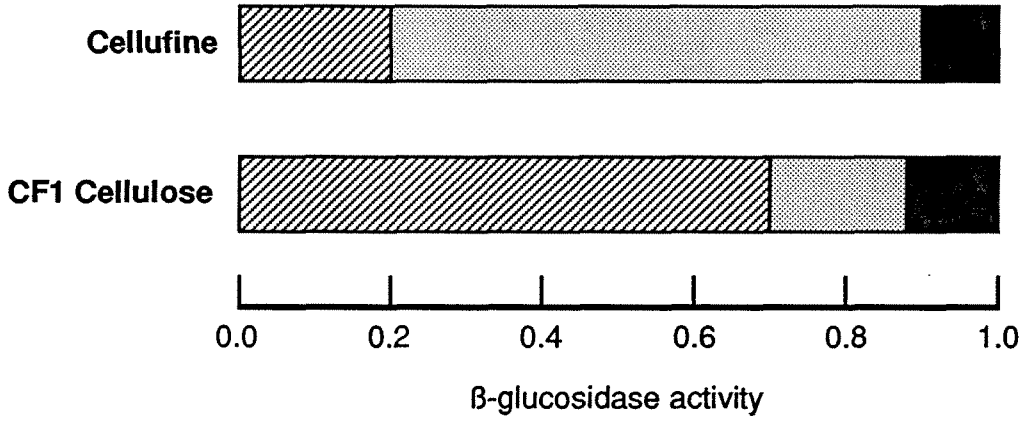

Figure 3.22 The influence of cellulose matrix on the recovery of Abg-$CBD_{Cex}1$. (▨), recovered bound activity; (□), unrecovered bound activity; (■), unbound activity.

Table 3.1 Purification of Abg-$CBD_{Cex}1$ by affinity chromatography on CF1 cellulose

Purifi-cation stage*	Volume (mL)	Activity (Units. mL^{-1})	Total activity (Units)	[Protein] ($mg.mL^{-1}$)	Total [Protein] (mg)	Specific activity ($Units.mg^{-1}$)	Overall yield (%)	Desorption yield (%)	Fold-purification
A	867	21.9	18,987	21.3	18,467	1.02	100		1.0
B	848	17.4	14,755	14.3	12,126	1.22	78		1.2
C	885	0.12	106	0.78	690				
D	1,750	0.98	1,719	6.39	11,179				
E			12,950		257	50.4	68	100	49
F	22	411.1	9,045	3.44	76	119.6	48	70	117.2

*A, French press cell extract; B, Streptomycin sulfate-treated and GF/C-filtered cell extract; C, Column flow through; D, High and low salt buffer washes; E, Cellulose-adsorbed polypeptide; F, d.H_2O-desorbed polypeptide after ultrafiltration

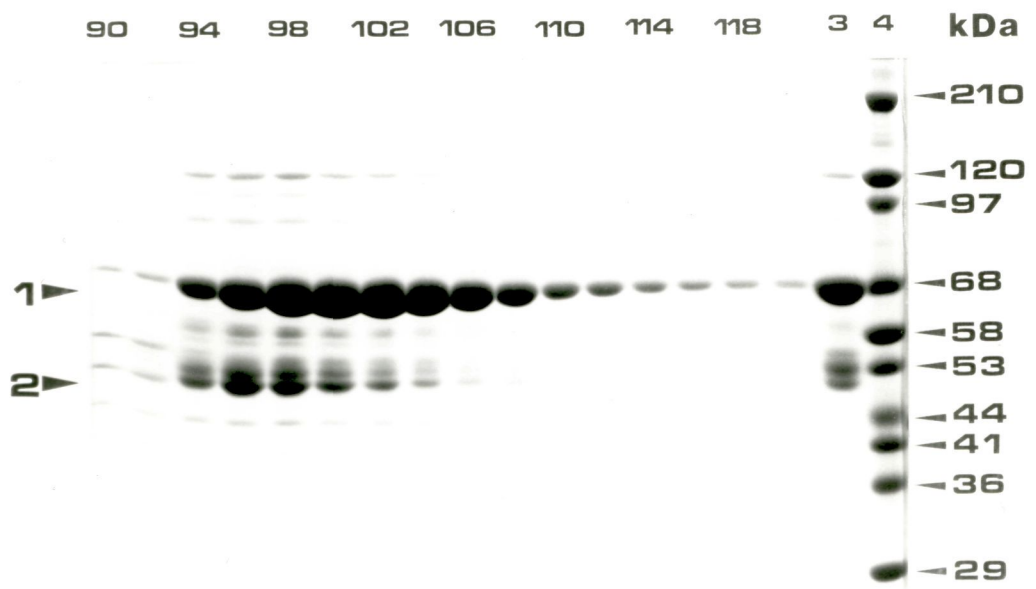

Figure 3.23 Column output of Abg-CBD$_{Cex}$1 purified from CF1™ cellulose. Equal volume of each fraction (90-120) was analyzed by SDS-PAGE. 1, intact fusion polypeptide; 2, degradation product; 3, Abg-CBD$_{Cex}$1 from a previous purification; 4, molecular weight markers.

Table 3.2 Purification of fusion polypeptides

Fusion polypeptide	Step*	Total activity (Units)	Total protein (mg)	Specific activity ($U.mg^{-1}$)	Fold-purification	Yield (%)
Abg-$CBD_{Cex}1$	1	12,947	10,701	1.21	1	100
	2	9,045	76	119	98	70
Abg-$CBD_{Cex}2$	1	3,301	7,709	0.43	1	100
	2	1,911	29	66	153	58
Abg-$CBD_{Cex}3$	1	7,256	15,773	0.46	1	100
	2	4,590	38	121	262	63

*[1]Clarified cell extract prepared by rupture in a French pressure cell and precipitation of nucleic acids with streptomycin sulfate.

[2]Water-desorbed polypeptides using affinity chromatography on CF1™ cellulose and concentrated by ultrafiltration with an Amicon cell.

(M/TDPN). A significant proportion retained the N-terminal methionine residue as found previously for the recombinant Abg (Wakarchuk *et al.*, 1988). The predicted pI for Abg-$CBD_{Cex}1$ was 5.1 (Skoog & Wichman, 1986). The fusion polypeptides reacted with both anti-Abg and anti-Cex antisera (Figure 3.19).

3.2.6 Binding of Abg-$CBD_{Cex}1$ to cellulose

Abg is a dimeric protein (Day & Withers, 1986). Abg-CBD_{Cex}, like CenA and Cex (Gilkes *et al.*, 1988; 1989), is susceptible to proteolysis between the two fusion partners. Analysis of purified Abg-$CBD_{Cex}1$ by non-denaturing PAGE revealed three distinct species, only two of which bound to cellulose (Figure

3.24). All three species hydrolyzed MUG (Figure 3.25). One of the species binding to cellulose contained only the 68 kDa polypeptide, the other contained both the 68 and the 51 kDa polypeptides (Figure 3.25). The species unable to bind to cellulose contained only the 51 kDa polypeptide. This was probably formed by subunit exchange between the two types of cellulose-binding dimers during and after affinity purification on cellulose. Abg-$CBD_{Cex}1$, like Abg itself, forms dimers. Both homodimers (Abg-$CBD_{Cex}1$/Abg-$CBD_{Cex}1$) and heterodimers (Abg-$CBD_{Cex}1$/Abg) bind to cellulose. The observation that dimeric polypeptides can be adsorbed to cellulose if one or both of the monomers carry a CBD suggests that CBD fusion polypeptides might be used to purify the components of protein complexes by linking a constituent polypeptide to cellulose through a fused CBD.

3.2.7 Stability of fusion polypeptides

Increased stability is one benefit of immobilizing an enzyme on a solid matrix (Hartmeier, 1988). Abg-$CBD_{Cex}1$ adsorbed to Avicel™ was stable and remained bound at 4° and 37° for up to 7 weeks. In solution, in contrast, the fusion polypeptide was stable at 4° but not at 37° (Figure 3.26). Clearly, binding to cellulose protects the fusion polypeptide from inactivation.

3.2.8 Enzyme kinetics

Fusion of an enzyme to a CBD might affect its catalytic activity. The specific activities (μmol pNP.min^{-1}.μmol $protein^{-1}$) for the purified fusion polypeptides were 8,296 for Abg-$CBD_{Cex}1$; 4,356 for Abg-$CBD_{Cex}2$ and 7,502 for Abg-$CBD_{Cex}3$ compared to 7,344 for recombinant Abg. Therefore, fusion of Abg to

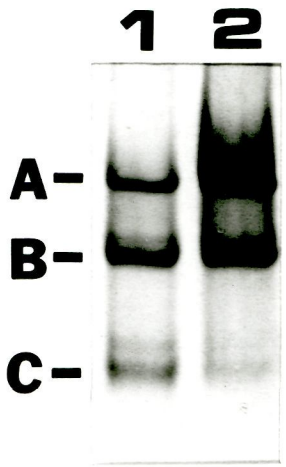

Figure 3.24 Heterogeneity of purified Abg-$CBD_{Cex}1$. Purified Abg-$CBD_{Cex}1$ and the fraction of it binding to Avicel™ were analyzed by non-denaturing PAGE using a 7.5%T gel. Lanes: 1, purified Abg-$CBD_{Cex}1$; 2, fraction binding to Avicel™. A, intact fusion homodimer; B, heterodimer; C, Abg homodimer.

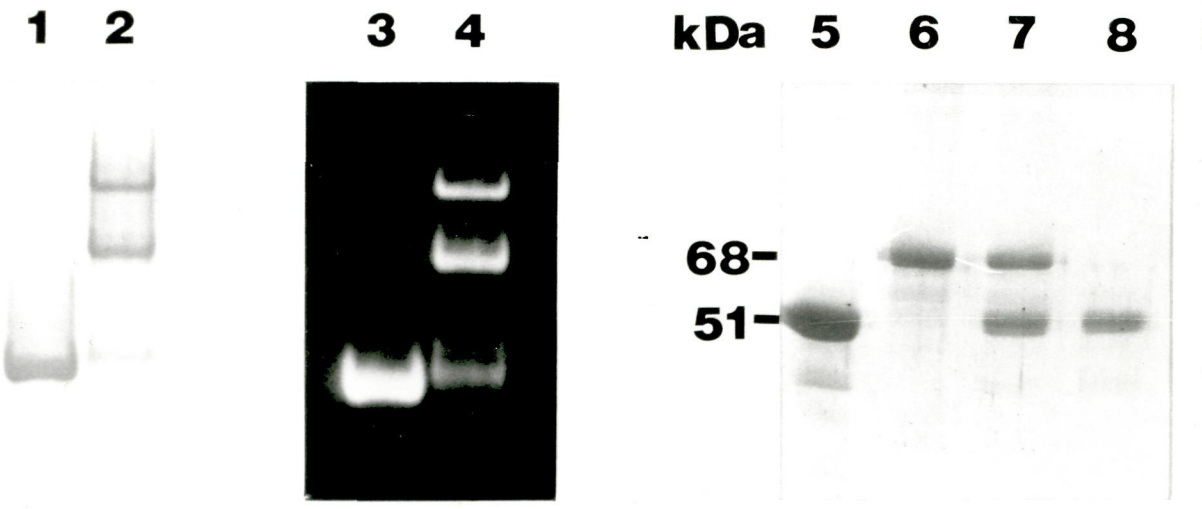

Figure 3.25 Detection of heterodimers in purified Abg-CBD_{Cex}. Abg and Abg-$CBD_{Cex}1$ were subjected to non-denaturing PAGE (lanes 1 and 2). Enzymatically active bands were detected by applying MUG to the gel, then examining it under long-wavelength UV light (lanes 3 and 4). Active bands were cut out and incubated overnight at 4° in 20 µL phosphate buffer. Then 45 µL 2x SDS-loading dye was added and the sample agitated on a vortex mixer. After centrifugation at 14,800g for 10 min at room temperature, the supernatants were analyzed by SDS-PAGE (lanes 5-8). Lanes 1, 3 and 5, purified Abg; 2 and 4, Abg-$CBD_{Cex}1$; 6, lane 4 upper band; 7, lane 4 middle band; 8, lane 4 lower band.

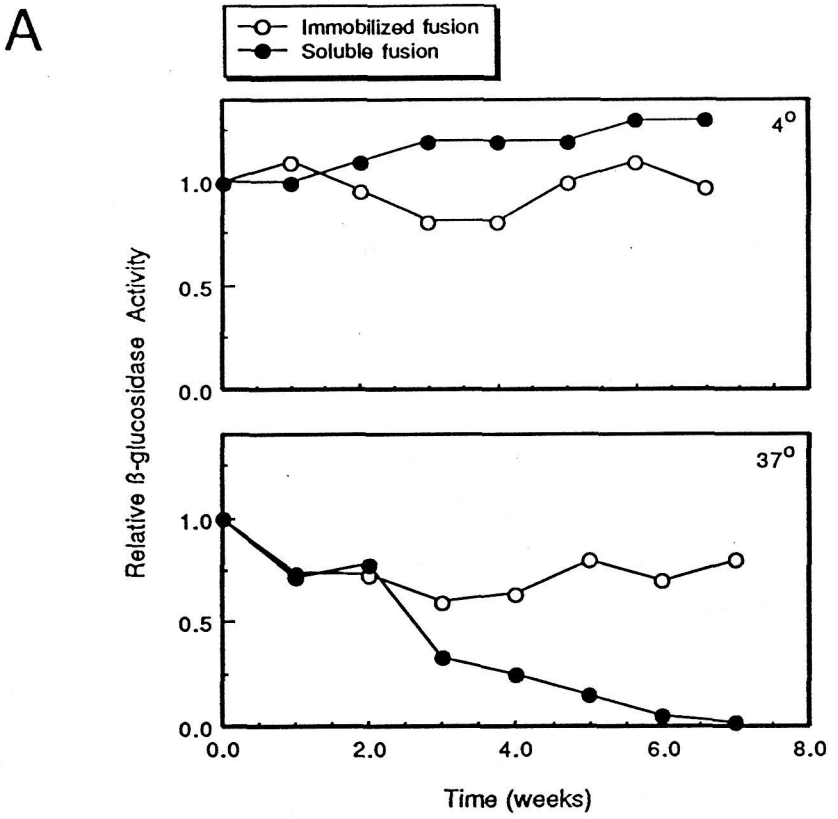

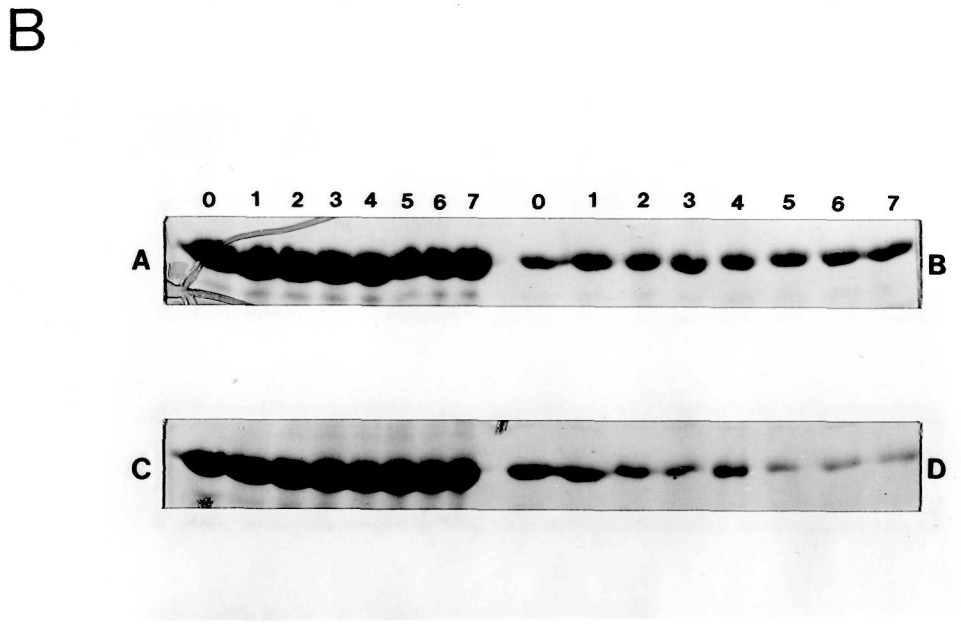

Figure 3.26 Stability of Abg-CBD$_{Cex}$1 adsorbed to Avicel. **A.** Residual ß-glucosidase activity of bound Abg-CBD$_{Cex}$1 expressed relative to initial activity at week 0. **B.** SDS-PAGE analysis of adsorbed Abg-CBD$_{Cex}$1. Numbers refer to time in weeks. Letters refer to different sets of samples: A, bound fusion at 4°; B, soluble fusion at 4°; C, bound fusion at 37°; D, soluble fusion at 37°. Experimental details are given in 2.15.3.

part of the Cex catalytic domain, Pro-Thr linker and the CBD (Abg-$CBD_{Cex}1$) or to the CBD directly (Abg-$CBD_{Cex}3$) did not alter significantly the activity of Abg. However, when the Pro-Thr linker was removed leaving Abg joined to CBD_{Cex} by 37 amino acids of the C-terminus of the catalytic domain of Cex (Abg-$CBD_{Cex}2$), the specific activity was decreased by almost 40%. Presumably this fusion polypeptide was unable to form a fully functional conformation. Abg-$CBD_{Cex}2$ was also unstable, being completely degraded to Abg and CBD_{Cex} during 6 months storage at 4° in the presence of 0.02% NaN_3 and protease inhibitors (data not shown). It was not studied further.

The K_{cat} values for the fusion polypeptides (Table 3.3) were very similar; thus the catalytic activity of Abg on pNPG was not affected significantly by the fusion of CBD_{Cex} to its C-terminus. The K_m values for Abg and Abg-$CBD_{Cex}1$ were almost identical, whereas the K_m for Abg-$CBD_{Cex}3$ increased by about 3-fold.

Table 3.3 Catalytic activities of Abg and the fusion polypeptides

Enzyme	K_m (μM pNPG)	K_{cat} (s^{-1})	K_{cat}/K_m ($\mu M^{-1}.s^{-1}$)
Abg	75	125	1.67
Abg-$CBD_{Cex}1$	70	143	2.04
Abg-$CBD_{Cex}3$	202	145	0.72

Immobilization of an enzyme may alter its catalytic activity (Hartmeier, 1988). The catalytic activity of Abg-$CBD_{Cex}1$ adsorbed to cellulose was examined. The specific mechanism-based inhibitor 2F-DNPG has been used to titrate the active sites of retaining glycosidases such as Abg and Cex (Withers *et al.*, 1987; Withers *et al.*, 1988; Tull *et al.*, 1991). The method is particularly useful for immobilized enzymes since it allows determination of V_{max} of the active, bound enzymes. K_{cat} for immobilized Abg-$CBD_{Cex}1$ was 113 s^{-1}. As this value was similar to the K_{cat} values of the enzymes in solution (Table 3.3), immobilization appeared not to affect catalytic activity. K_m for immobilized Abg-$CBD_{Cex}1$ in stirred suspension was 296 μM pNPG. This was 4-fold higher than K_m of the soluble enzyme suggesting that the transport of substrate to the active site of the immobilized enzyme was rate limiting, presumably due to external mass transfer resistance.

Ideally, the operation of an immobilized column should follow a plug-flow velocity profile wherein every element in the solution moves through the column at the same velocity (Lilly *et al.*, 1966). Under appropriate conditions, a column operated in a plug-flow would maximize catalytic conversion. The flow pattern of a reactor can be characterized from a plot of column product against effluent volume or residence time (Kohlwey & Cheryan, 1981). Plug flow is characterized by an abrupt change in the effluent after a given time equal to the residence time of the solution in the column. A deviation from this, like a gradual change of effluent over time, indicates significant relative fluid motion and mixing (Lilly *et al.*, 1966). The time distribution plot showed that the membrane column of immobilized Abg-$CBD_{Cex}1$ did not follow a plug-flow profile (Figure 3.27). This indicates that there was considerable variation in the perfusion velocity resulting in the differences in time distribution and the accessibility of substrates to or transport of products from the active site of the immobilized fusion polypeptide.

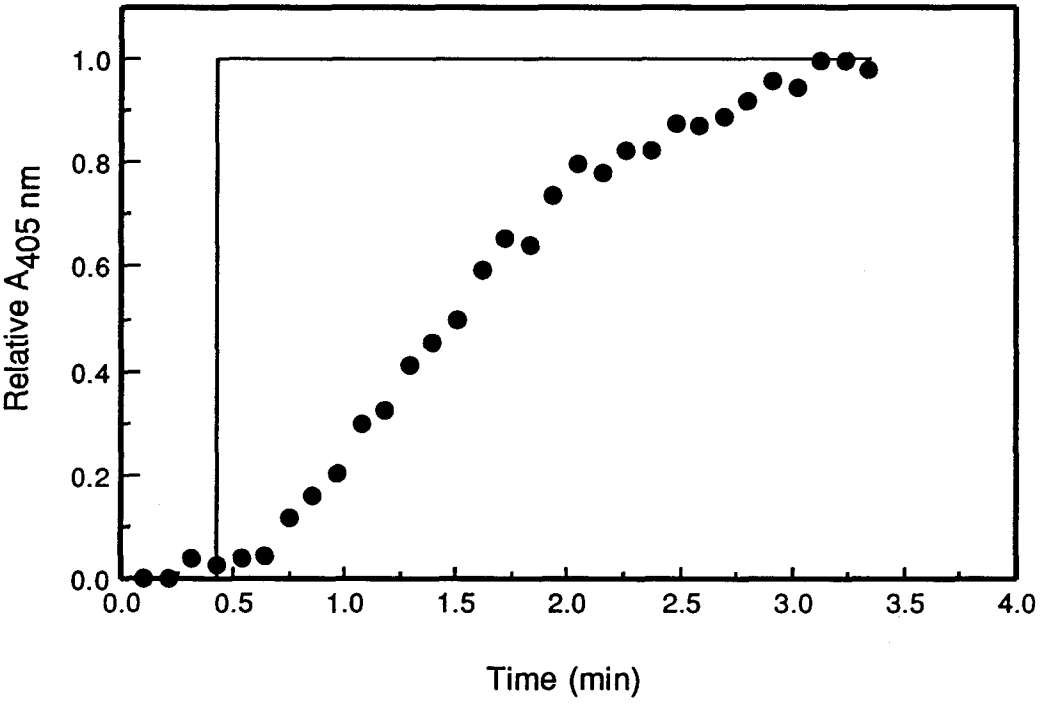

Figure 3.27 Column flow characteristics of pNP (●) produced from an immobilized Abg-$CBD_{Cex}1$ membrane column. Enzyme loading was 10 nmoles for 5 cellulose acetate membranes. Flow rate was 60 $mL.h^{-1}$. Temperature was 22°. (—), ideal plug-flow reactor.

The apparent K_m of Abg-$CBD_{Cex}1$ adsorbed to cellulose was determined in a continuous column reactor. An integrated Michaelis-Menten equation was used to express the total reaction occurring in the column (Lilly *et al.*, 1966; Ford *et al.*, 1972; Patwardhan & Karanth, 1982). The apparent K_m was 7-fold higher than that observed in a stirred suspension (data not shown), as would be expected with mass transfer limitation.

3.2.9 Immobilization yields for the fusion polypeptides

Immobilization yield is the percentage of the actual activity retained by the enzyme when immobilized. At near saturation of the cellulose the immobilization yield was about 30% for Abg-$CBD_{Cex}1$, and about 10% for Abg-$CBD_{Cex}3$. These values were higher when the Avicel™ was not saturated with enzyme (Figure 3.28). Abg did not adsorb to cellulose (data not shown). At least in this case the immobilization yield was improved by the presence of an extra 57 amino acids between the affinity "tag" and the fusion partner, presumably by extending the Abg portion of the fusion polypeptide into the solution. The decrease in immobilization yield as the amount of bound enzyme increased may be a result of steric hindrance at higher levels of immobilized polypeptide. However, the lower immobilization yield of Abg-$CBD_{Cex}3$ (lacking the 57 extra amino acids) at the same enzyme loading level as Abg-$CBD_{Cex}1$ (Figure 3.28) suggests that the proximity of the Abg to the cellulose surface may be significant.

The saturation levels were >2,000 U.g Avicel™$^{-1}$ (0.24 μmoles protein.g Avicel™$^{-1}$) for Abg-$CBD_{Cex}1$, and >3,500 U.g Avicel™$^{-1}$ (0.49 μmoles protein.g Avicel™$^{-1}$) for Abg-$CBD_{Cex}3$ (Figure 3.28). The level of actual

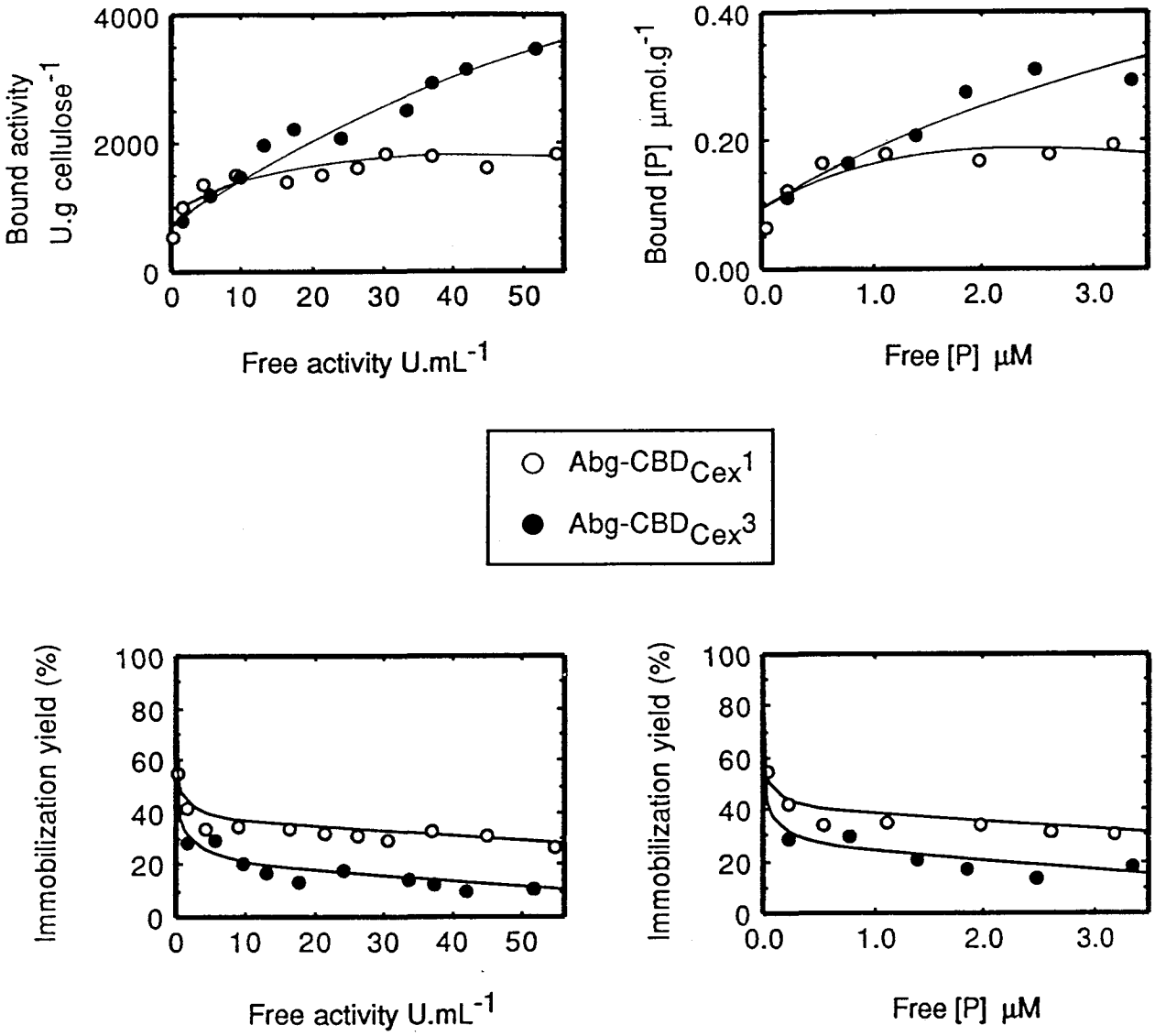

Figure 3.28 Adsorption equilibria (top) and immobilization yields (bottom) for Abg-CBD$_{Cex}$1 & 3 adsorbed to Avicel. Initial enzyme activity = 6-86 U.mL^{-1} (Abg-CBD$_{Cex}$1) and 6-81 U.mL^{-1} (Abg-CBD$_{Cex}$3). [P_o] = 0.7-10.3 µM (Abg-CBD$_{Cex}$1) and 0.8-11.3 µM (Abg-CBD$_{Cex}$3). The bound fusion protein was assayed for ß-glucosidase activity under standard conditions (M). The theoretical bound activity (T) was the difference between the activity added initially and the activity in the supernatant. Immobilization yield was (M/T)100.

bound ß-glucosidase activity exhibits an inverse relationship to the size of the bound polypeptide.

3.2.10 Stabilities of the immobilized enzymes

There are two aspects to the stability of an immobilized enzyme: its intrinsic stability and loss from the matrix. The latter was of particular interest for Abg-$CBD_{Cex}1$ because it was immobilized by simple adsorption to the cellulose surface. Abg-$CBD_{Cex}1$ was inactivated by prolonged incubation at or below pH 5.0, either in solution or adsorbed to cellulose (Figure 3.29A), but desorption was insignificant (Figure 3.29B). However, the enzyme was desorbed at pH 8-9 (Figure 3.29B). In solution it remained active at pH 7.5-9, but it was inactivated above pH 9. The pH stability of Abg-$CBD_{Cex}1$ in solution was similar to that reported for Abg (Han and Srinivasan, 1969).

As expected, Abg-$CBD_{Cex}1$ was desorbed from a cellulose column by a pH gradient from 7-12, but not by one from 7-2 (Figure 3.30). The enzyme desorbed at >pH 9 was inactive. Adsorbed Abg-$CBD_{Cex}1$ remained active and bound to cellulose during prolonged incubation at pH 6 to 7. *Trichoderma reesei* cellulase also desorbed at alkali pH (Otter *et al.*, 1989).

Abg-$CBD_{Cex}1$ in solution was stable for 24 h at 25°, pH 7.0 and ionic strengths from 0 to 1 M (Figure 3.31A). Immobilized Abg-$CBD_{Cex}1$ was also stable under these conditions but was largely desorbed from the cellulose in dH_2O (Figure 3.31A). Desorption of a column containing 70% of fusion polypeptide bound to cellulose with a linear NaCl gradient (0-1 M) confirmed this (Figure 3.31B). No desorption of the fusion polypeptide was observed indicating that the binding of Abg-$CBD_{Cex}1$ was stable up to 1 M NaCl.

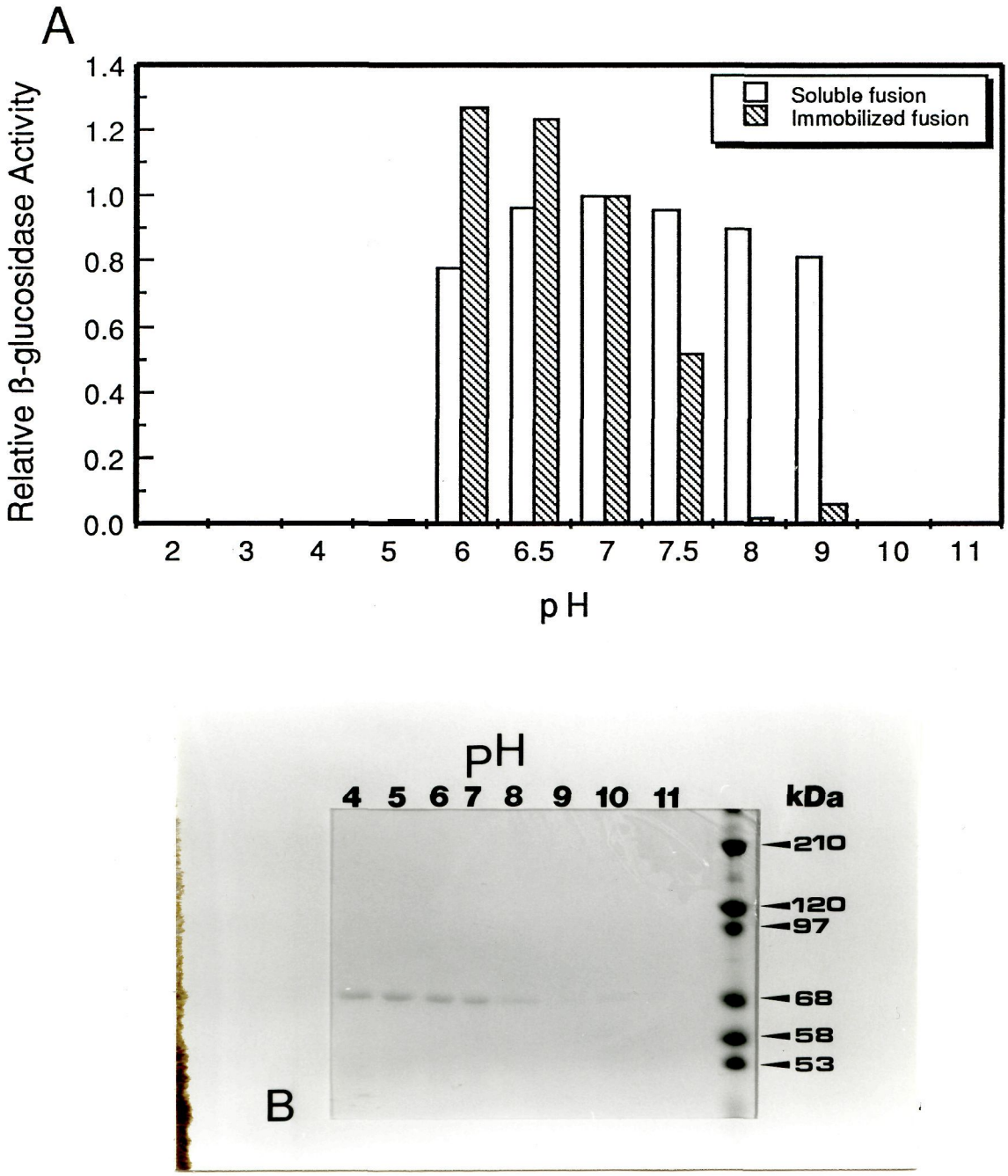

Figure 3.29 Stability of immobilized Abg-$CBD_{Cex}1$ as a function of pH. **A.** Activity. Residual ß-glucosidase activity of soluble Abg-$CBD_{Cex}1$ and adsorbed Abg-$CBD_{Cex}1$ assayed under standard conditions and expressed relative to the value obtained at pH 7. **B.** Binding. SDS-PAGE analysis of adsorbed Abg-$CBD_{Cex}1$ after incubation at different pH values. Arrow refers to Abg-$CBD_{Cex}1$. Last lane is molecular weight markers. Experimental details are given in 2.15.1.

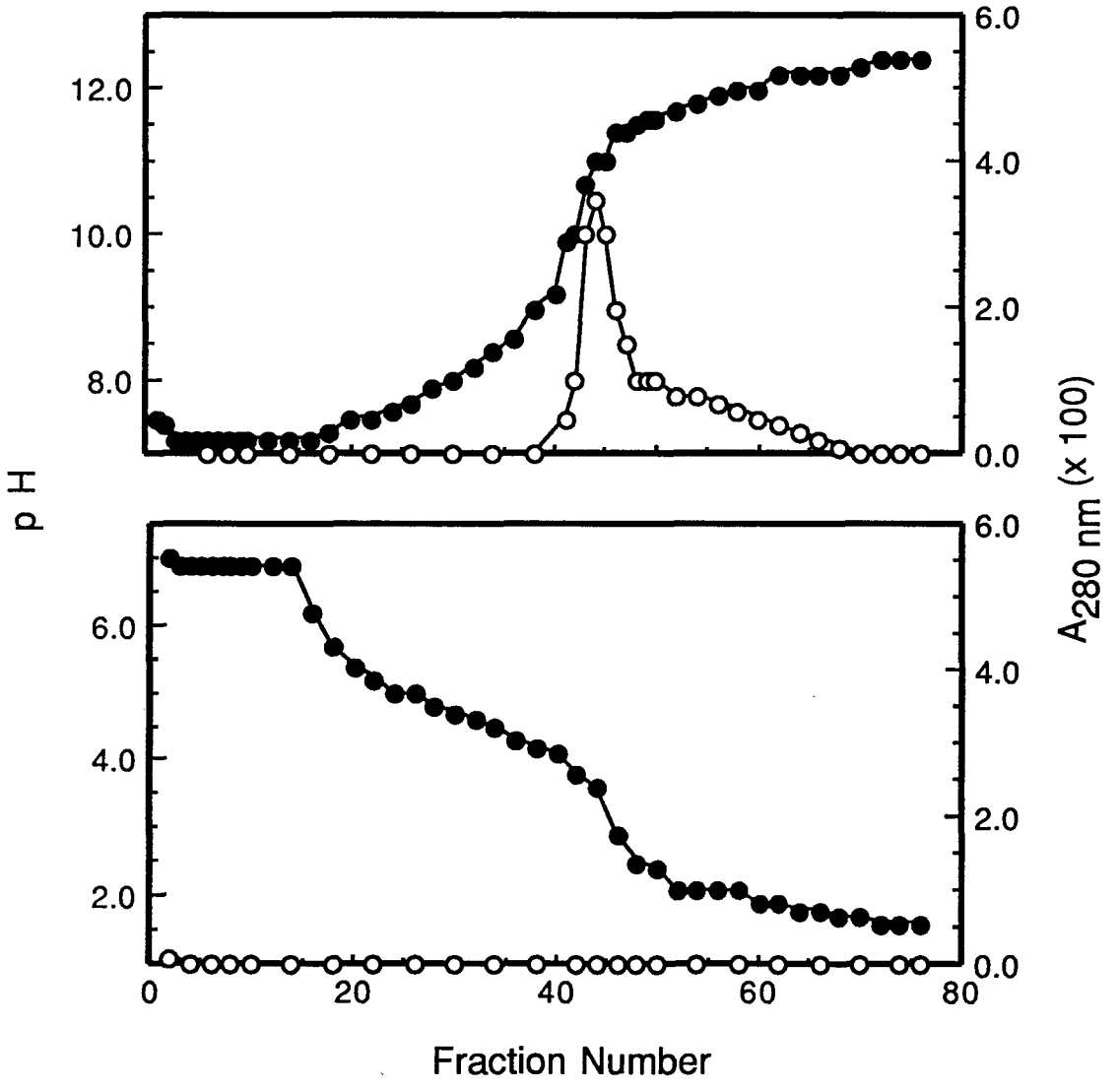

Figure 3.30 Desorption of Abg-CBD$_{Cex}$1 from cellulose with a pH gradient. Open circles indicate absorption at 280 nm. Closed circles indicate pH. Experimental details are given in 2.15.1.

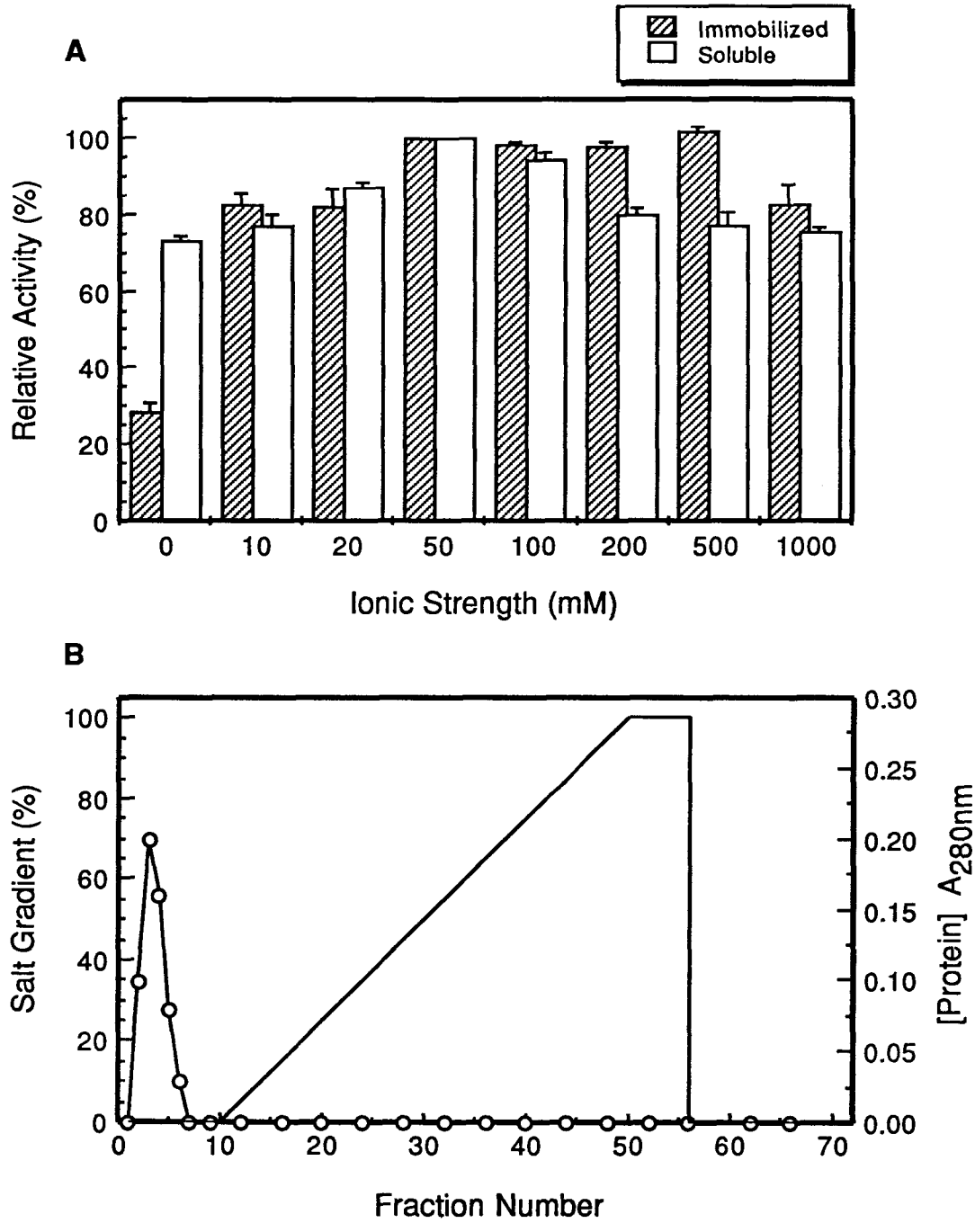

Figure 3.31 The influence of ionic strength on the stability of Abg-$CBD_{Cex}1$. **A.** Activity. Residual ß-glucosidase activity of soluble Abg-$CBD_{Cex}1$ and adsorbed Abg-$CBD_{Cex}1$ assayed under standard conditions and expressed relative to the value obtained at 50 mM NaCl in phosphate buffer. **B.** Binding. Stability of Abg-$CBD_{Cex}1$ in a salt gradient. Closed circles refer to A_{280nm} readings. Line is the salt gradient (0-1 M NaCl). Experimental details are given in 2.15.2.

3.2.11 Cellulose matrices

Since CBD_{Cex} adsorbed more strongly to crystalline than to amorphous cellulose (section 3.1.4), three types of cellulose were tested as matrices for Abg-CBD_{Cex} immobilization: CF1™ cellulose, cotton and cellulose acetate membrane. Abg-CBD_{Cex}1 was adsorbed to CF1™ cellulose, which was then packed into a column and equilibrated at 4°. A solution of pNPG was perfused through the column, and the amount of pNP released in the effluent was monitored. The conversion of pNPG to pNP dropped from 70% initially to 25% during the first 13 days of operation, but remained nearly constant during the following 8 days (Figure 3.32). When adsorbed to cotton fibres, enzyme activity decreased only 12% in the 15 day period (Figure 3.32). This suggested that, in the case of Abg-CBD_{Cex}1 adsorbed on the CF1™ cellulose, the enzyme bound to the amorphous regions of the cellulose was released gradually during the first 13 days of operation of the column. The enzyme tightly bound to the crystalline regions of the CF1™ cellulose was not released and accounted for the stably bound activity. When Abg-CBD_{Cex}1 was adsorbed to stacked cellulose acetate membranes, activity remained fairly constant throughout 14 days of continuous operation of the column (Figure 3.32). The substrate conversion rate was only 30% compared to 70% for cotton. This could be explained by the shorter residence time (4.8 min) in the cellulose acetate membrane column compared to 40 min in the column packed with either cotton or CF1™ cellulose.

Abg-CBD_{Cex}1 adsorbed to cotton was stable for at least 10 days continuous operation at 4°, 10° and 37° (Figure 3.33). It was inactivated completely in 3 days at 50°, but protein was not released from the column. Abg-CBD_{Cex}1 in solution was inactivated after 3 days at 50°. The activity of adsorbed Abg-CBD_{Cex}1 was highest at temperatures between 20° and 30° (Table

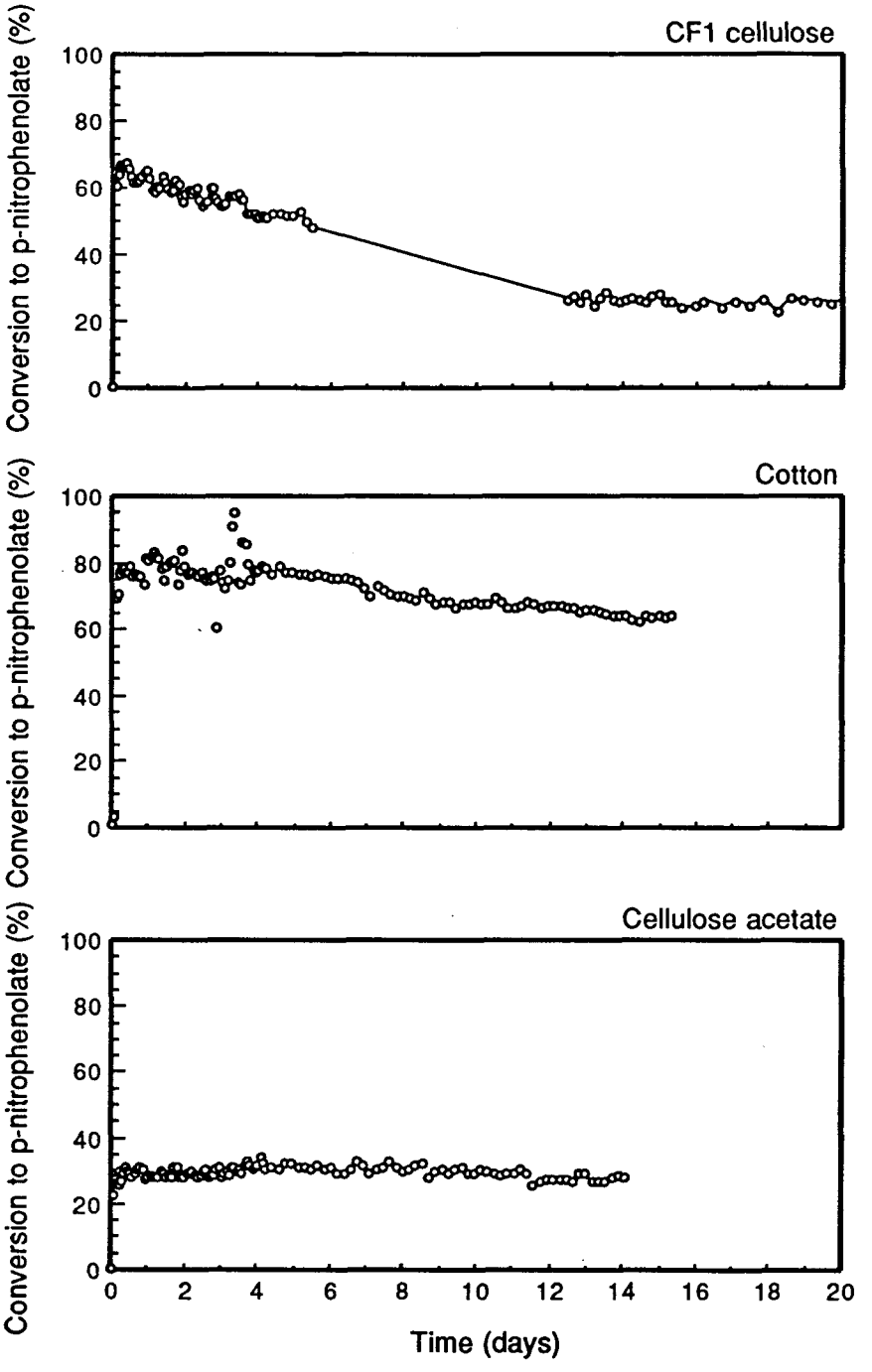

Figure 3.32 Performance of Abg-CBD$_{Cex}$1 immobilized enzyme columns: effect of cellulose structure. Amount of cellulose used was 1 g (CF1™ cellulose or cotton) or 5 cellulose acetate membranes (0.2 mm x 25 mm diameter). Enzyme loading was from 0.9-2.3 nmoles protein.g^{-1} cellulose or 3 nmoles protein.membrane^{-1}. Temperature of column run was 4° (CF1™ or cotton) or 22° (membrane). Flow rate was 7.8 mL.h^{-1}. Phosphate buffer only was passed through the CF1™ cellulose column from days 6 to 12. Further details are given in 2.16.

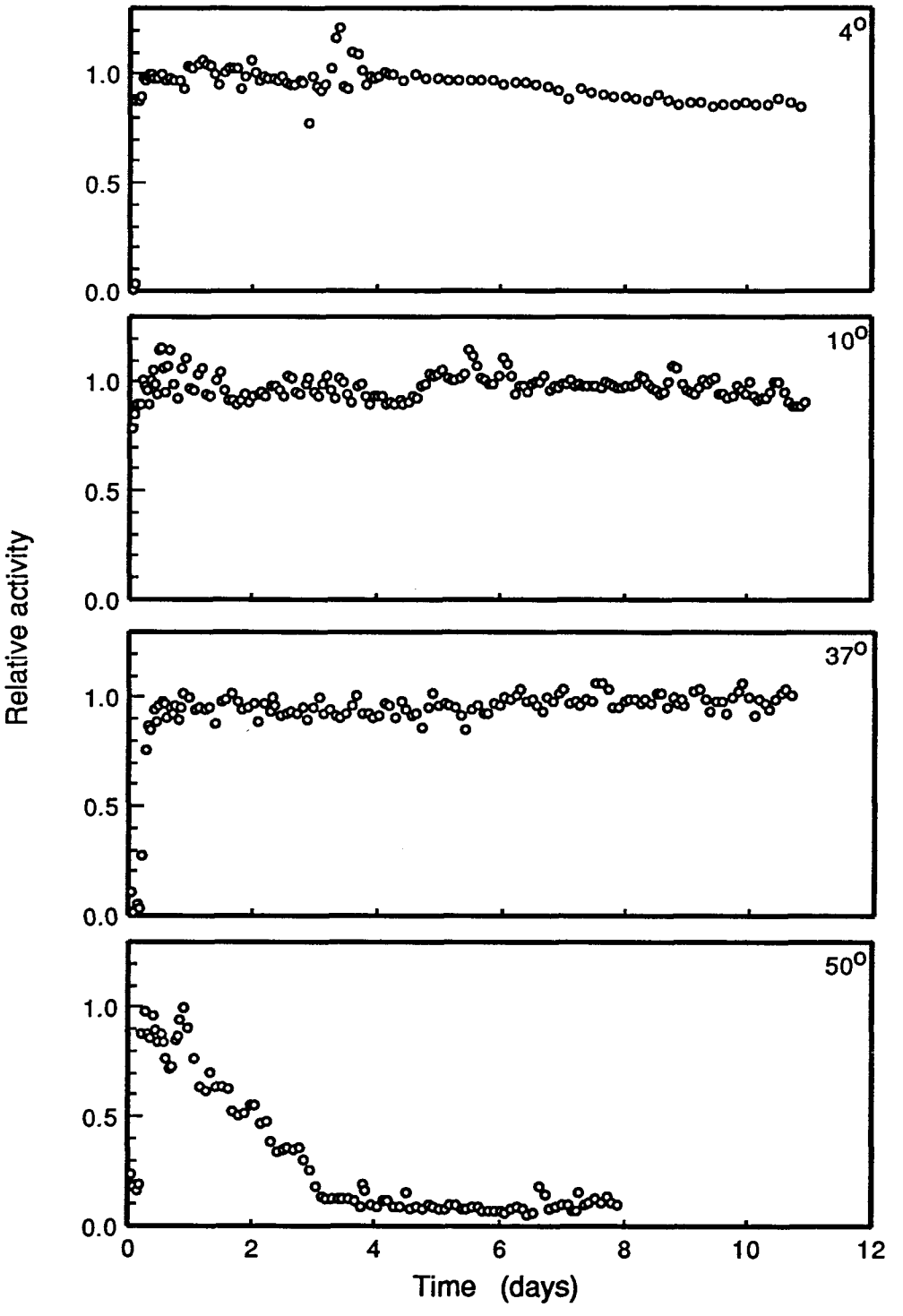

Figure 3.33 Performance of Abg-CBD$_{Cex}$1 immobilized enzyme columns: temperature stability. Amount of cotton used was 2 g. Enzyme loading was from 3.7-22 nmoles protein.g^{-1} cellulose. Flow rate was 7.8 mL.h^{-1}. Values are expressed relative to the initial, highest *p*-nitrophenol produced at that temperature. Further details are given in 2.16.

3.4). Conversion of pNPG to pNP was approximately 50% even after 20 h of operation. Although Abg-$CBD_{Cex}1$ remained bound at 50°, the Abg domain was inactivated.

Table 3.4 Activity of immobilized Abg-$CBD_{Cex}1$ at different temperatures

Temperature	Percent conversion to pNP	
°C	5h	20h
4	30	30
10	38	38
20	50	50
30	48	48
40	45	25

Amount of cotton used was 2 g. Enzyme loading was 0.013 μmoles protein.g^{-1} cotton. Flow rate was 7.8 mL.h^{-1}.

3.3 A fusion polypeptide comprising CBD_{Cex} fused to the C-terminus of a ß-glucosidase (Cbg) from *C. saccharolyticum* (Cbg-CBD_{Cex}; Figure 3.1)

3.3.1 Construction of a plasmid expressing *cbg-CBD_{cex}*

C. saccharolyticum is a thermophilic, cellulolytic bacterium (Love & Streiff, 1987). It produces a ß-glucosidase (Cbg) with a temperature optimum for hydrolysis of 70° (Love & Streiff, 1987). Furthermore, it shares 39% sequence identity with Abg and is virtually the same size. These properties emphasized the validity of comparing the two enzymes as fusion polypeptides with CBD_{Cex}. Cbg was fused at its C-terminus to CBD_{Cex} to examine its efficiency as an immobilized enzyme at temperatures at which Abg was inactivated. Construction of the plasmid expressing *cbg-CBD_{cex}* involved the introduction of two NheI sites at the sequences corresponding to the N- and C-termini of the mature Cbg. The 5' end of the *cbg* was ligated to the sequence encoding the Cex leader peptide. The sequence encoding CBD_{Cex} (without the Pro-Thr linker sequence) was ligated to the 3' end of *cbg* just before the stop codon. The gene fusion *cbg-CBD_{cex}* was expressed from the *lac* promoter with a consensus Shine-Dalgarno sequence located just upstream of the ATG of the coding sequence for the Cex leader peptide (Figure 3.34). The correctness of the construct was confirmed by restriction endonuclease analysis and DNA sequencing.

3.3.2 Purification of Cbg-CBD_{Cex}

The binding of Abg-CBD_{Cex}1 to cellulose was stable at 50° (section 3.2.11) and Cbg was known to be stable from 50°-70° (Love & Streiff, 1987). This made it likely that heat treatment could be used as an initial step in the purification of

Figure 3.34 Construction of pTZEO10. The HindIII fragment of pNZ1070 (Love *et al.*, 1988), containing the *cbg* coding sequence, was cloned into the HindIII site of pTZ18R. NheI sites were introduced just after the ATG and just before the TAA codons of *cbg* by *in vitro* mutagenesis. The resulting plasmid, pTZ18R-*cbg* (NheI), was digested completely with NheI and a 1.4 kbp fragment containing the *cbg* sequence was isolated. pTZEO7 (PTIS) was digested completely with NheI and ligated to the 1.4 kbp *cbg* fragment to give pTZEO10.

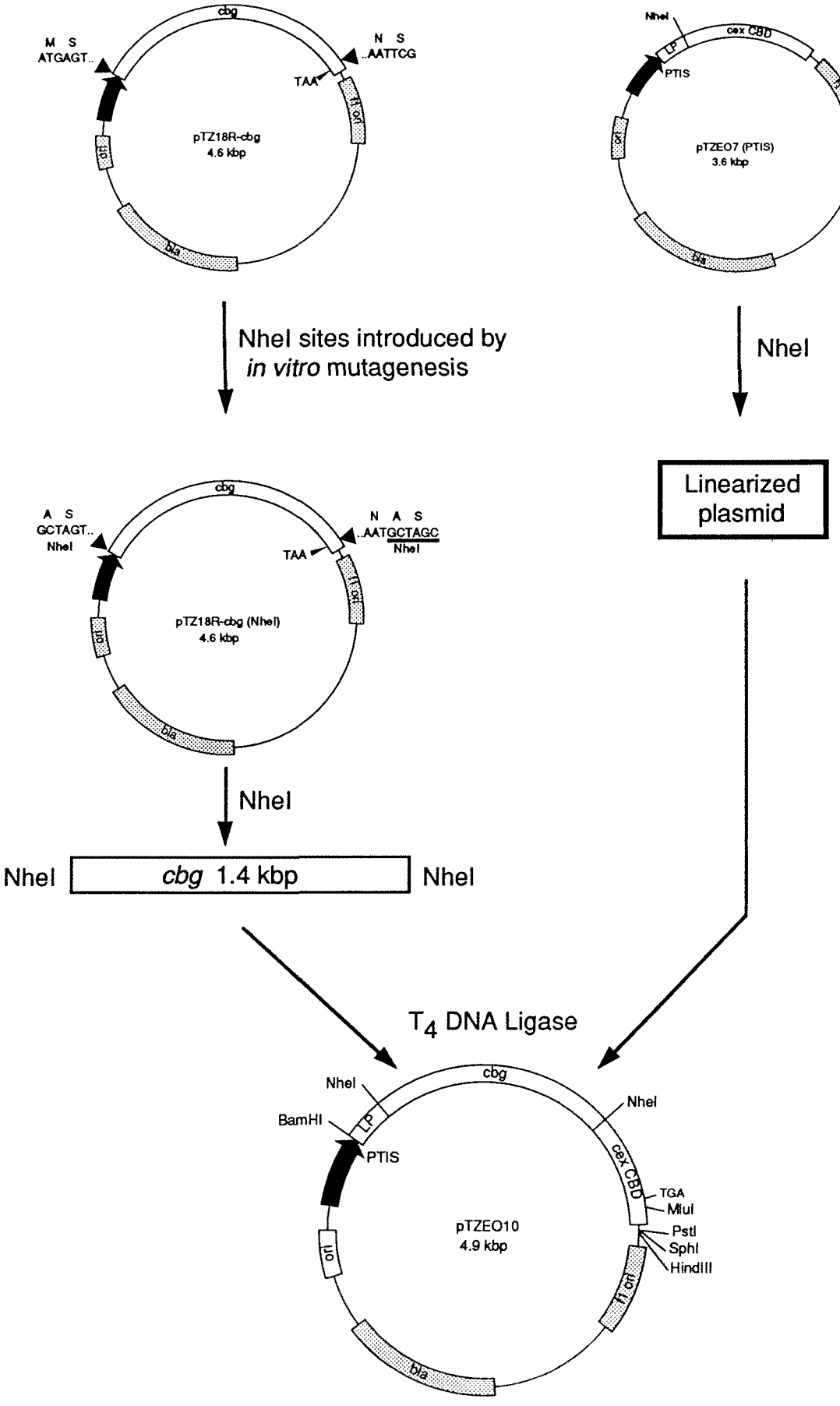
M S
ATGAGT..
N S
..AATTCG
cbg
TAA
pTZ18R-cbg
4.6 kbp
ori
T1 ori
bla
NheI sites introduced by
in vitro mutagenesis
NheI
A S
GCTAGT..
NheI
N A S
..AATGCTAGC
NheI
pTZ18R-cbg (NheI)
4.6 kbp
NheI
NheI
cbg 1.4 kbp
NheI
Linearized
plasmid
T4 DNA Ligase
NheI
BamHI
LP
PTIS
cbg
NheI
cex CBD
TGA
MluI
PstI
SphI
HindIII
pTZEO10
4.9 kbp
ori
T1 ori
bla
NheI
LP
PTIS
cex CBD
T1 ori
ori
pTZEO7 (PTIS)
3.6 kbp
bla

Cbg-CBD_{Cex}. Much of the protein in a crude cell extract was removed by heating at 50° for 30 min (Figure 3.35), without loss of Cbg-CBD_{Cex} activity. Cbg-CBD_{Cex} was recovered from the treated, clarified extract by adsorption to cellulose (Figure 3.35). Like Abg-CBD_{Cex}, Cbg-CBD_{Cex} was sensitive to proteolysis. The polypeptide reacting with anti-Cex antiserum had a similar M_r to that of Abg-$CBD_{Cex}3$, about 62 K.

Cbg-CBD_{Cex} could be desorbed from CF1™ cellulose either with dH_2O or 8 M GdmCl. However, when dH_2O was used, further Cbg-CBD_{Cex} could be released with GdmCl (Figure 3.36). The polypeptide desorbed with GdmCl comprised only the intact fusion polypeptide, whereas that desorbed by dH_2O also included degradation products (Figure 3.36). This suggested that adsorption of the intact homodimers (assuming that Cbg by analogy to Abg is also a dimer) was stronger than that of the heterodimers.

3.3.3 Properties of Cbg-CBD_{Cex}

The M_r of the intact fusion polypeptide was 64 K, in good agreement with that calculated from the predicted protein sequence (O'Neill *et al.*, 1986; Love *et al.*, 1988). The predicted pI was 5.6 (Skoog & Wichman, 1986). The N-terminal amino acid sequences of the Cbg-CBD_{Cex} desorbed with dH_2O or GdmCl, and of the degradation product were identical to that of Cbg (ASFPK). The intact fusion protein (both dH_2O- and GdmCl-desorbed) was recognized by the anti-Cex antiserum, whereas the degradation product was not (Figure 3.35). Thus Cbg-CBD_{Cex} appeared to be sensitive to proteolysis between the two domains. As with Abg-$CBD_{Cex}1$/Abg heterodimers, the resulting Cbg was purified as a heterodimer with Cbg-CBD_{Cex}.

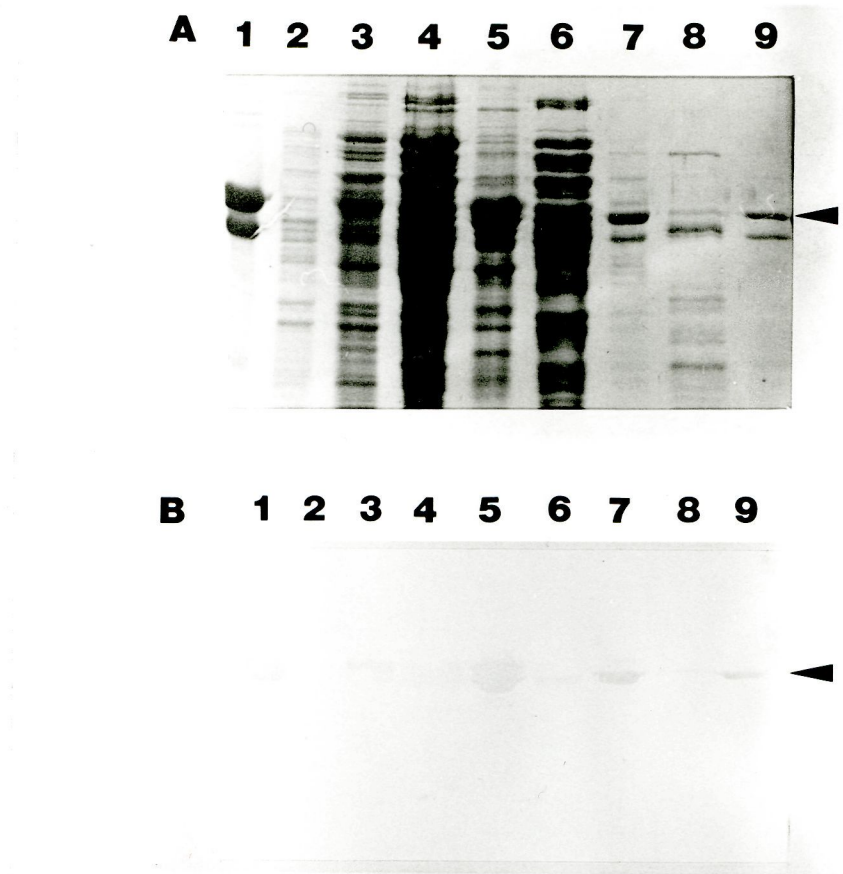

Figure 3.35 Purification of Cbg-CBD_{Cex}. Crude cell extracts were prepared as in Figure 3.5. Cell extracts were then heated to 50° or 70° for 30 min followed by centrifugation. The treated cell extract was allowed to bind to CF1™ cellulose for 2 h at 4°. Samples were treated as in Figure 3.5. Equivalent volumes were analyzed by SDS-PAGE (A). Lane 1, purified Abg-CBD_{Cex}3. Lane 2, JM101/pTZ18R cell extract. Lane 3, culture medium. Lanes 4, 6 & 8, unbound cell extracts incubated at 4°, 50° and 70°, respectively. Untreated (4°) and heat-treated (50° & 70°) CF1™ cellulose-bound proteins, lanes 5, 7 & 9, respectively. Arrow refers to the intact Cbg-CBD_{Cex}. B, Western blot of A. Primary antiserum used was rabbit anti-Cex.

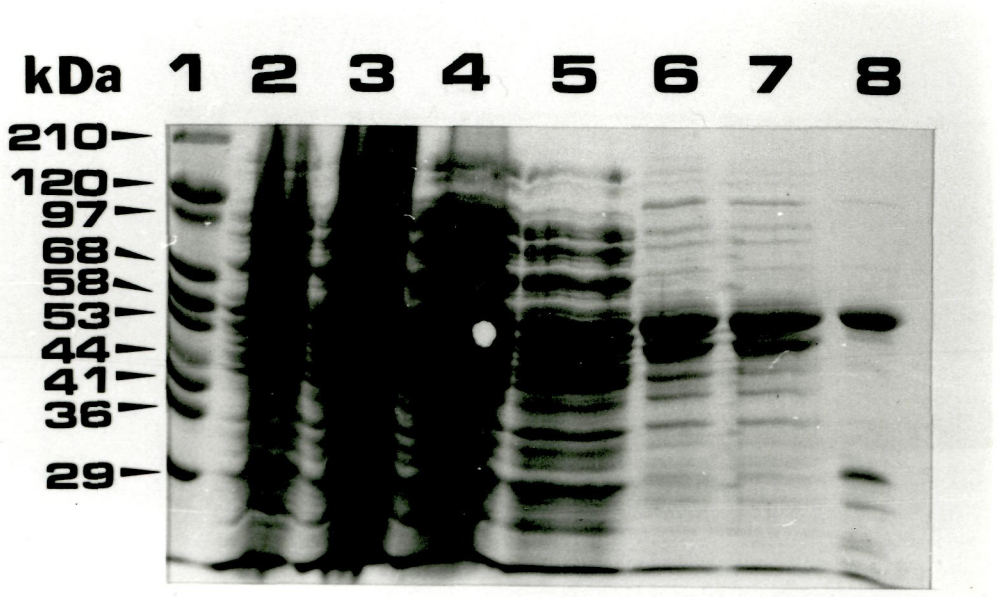

Figure 3.36 Purification of Cbg-CBD_{Cex}. Lane 1, molecular weight markers; lane 2, crude cell extract after rupture of cells with a French press; lane 3, crude cell extract after treatment with streptomycin sulfate and after ultracentrifugation; lanes 4 & 5, high and low salt buffer washes, respectively; lanes 6 & 7, dH_2O-desorbed before and after heat treatment at 50° for 30 min, respectively; lane 8, GdmCl-desorbed fusion polypeptide.

The fusion polypeptide was most active at 70° (192 pNPGase $U.mL^{-1}$) compared to 49.9 pNPGase $U.mL^{-1}$ at 50°. The specific activities of the dH_2O- and GdmCl-desorbed fusion polypeptides were 7,785 $U.\mu mol^{-1}$ and 13,323 $U.\mu mol^{-1}$, respectively. The almost 2-fold difference in specific activities could be the result of inactivation of a significant proportion of the dH_2O-desorbed preparation.

Cbg-CBD_{Cex} bound stably to CF1™ cellulose at 70° (Figure 3.37). Densitometric scan of the adsorbed fusion polypeptide incubated overnight at 70° showed a decrease of only 8% compared to the 4° control. Attempts to desorb the fusion polypeptide from CF1™ cellulose with dH_2O or high pH after incubation at 70° for 24 h were unsuccessful (data not shown). Most of the activity remained in the cellulose. Only a partial recovery of activity was obtained when GdmCl was used. This suggests that the CBD part of the fusion polypeptide may have become "fixed" on the cellulose surface as a result of its thermal denaturation.

3.3.4 Cbg-CBD_{Cex} as an immobilized enzyme

Cbg-CBD_{Cex} adsorbed to cellulose acetate membranes was stable during continuous operation at 70° for more than 70 h (Figure 3.38).

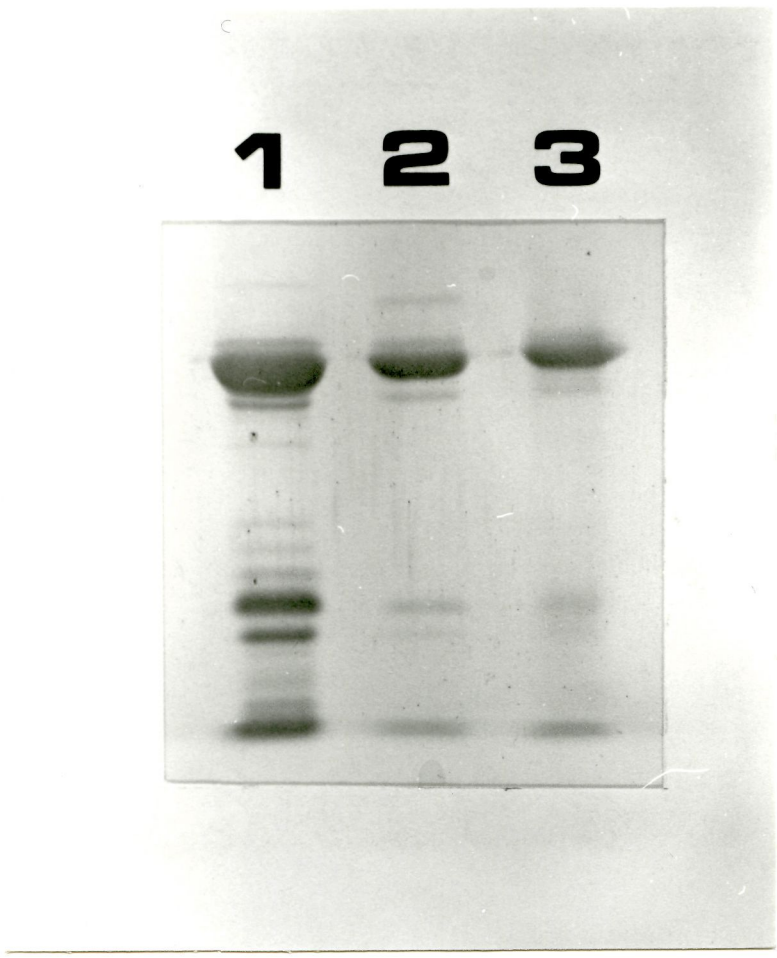

Figure 3.37 Binding of Cbg-CBD_{Cex} to cellulose. Cbg-CBD_{Cex} (0.32 nmoles) was added to 1 mg BMCC and allowed to bind overnight at either 4° or 70°. The samples were treated as in Figure 3.5. Lane 1, Cbg-CBD_{Cex} before binding to BMCC. Lanes 2 & 3, Cbg-CBD_{Cex} left in the cellulose pellet after incubation at 4° and 70°, respectively.

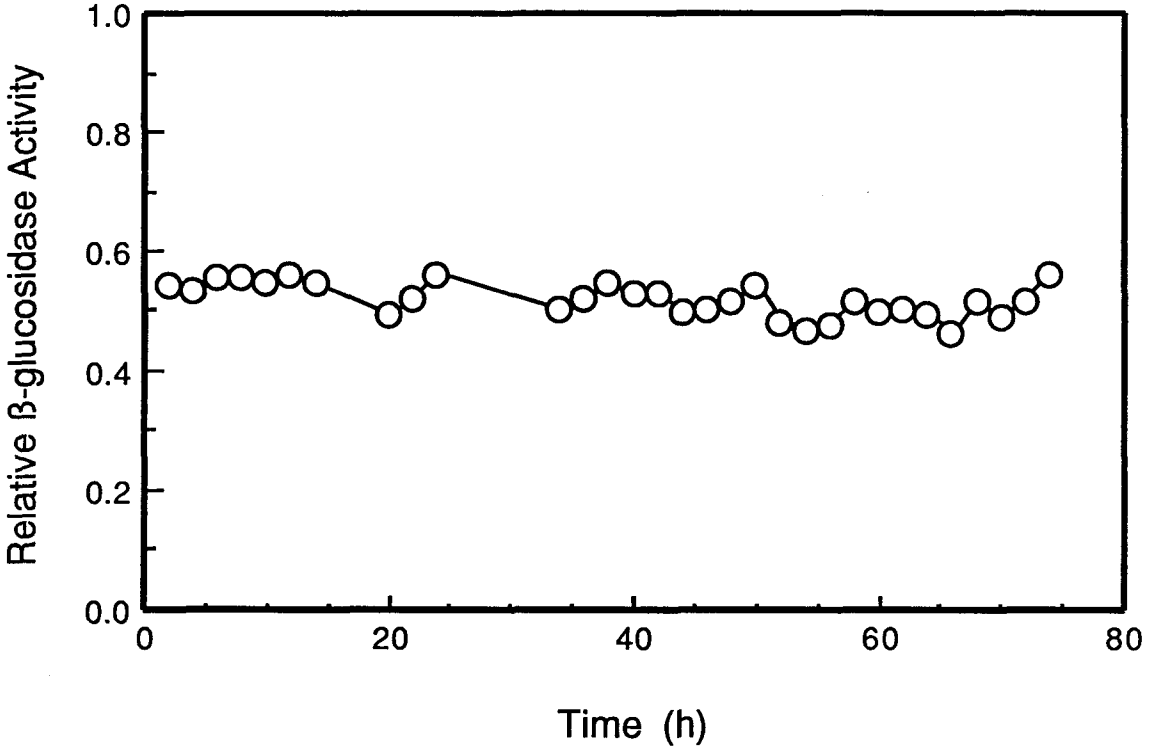

Figure 3.38 Temperature stability of Cbg-CBD_{Cex} immobilized enzyme column. Cellulose used was 5 stacked cellulose acetate membranes. Enzyme loading was 3.9 nmoles for 5 membranes. Flow rate was 8.8 $mL.h^{-1}$. Temperature of column run was 70°. Further details are given in 2.16.

4. DISCUSSION

The CBD of Cex was used to produce hybrid polypeptides for the purpose of enzyme immobilization. The high affinity of CBD_{Cex} for both native and modified cellulose allowed the strong and specific adsorption of fusion polypeptides without detectable leaching in an immobilized enzyme column. This work also demonstrated that CBD_{Cex} can be used as a "tag" for affinity chromatography on cellulose, thereby facilitating the purification of fusion polypeptides.

ß-glucosidase was chosen as a reporter enzyme for enzyme immobilization for the following reasons: (1) the genes for a mesophilic ß-glucosidase (Abg) from an *Agrobacterium* sp. and a thermophilic ß-glucosidase (Cbg) from *C. saccharolyticum* were available, and both had been sequenced and expressed in *E. coli* (Wakarchuk *et al.*, 1986; Wakarchuk *et al.*, 1988; Love *et al.*, 1988); (2) the enzymes had been characterized (Han & Srinivasan, 1969; Day & Withers, 1986; Love & Streiff, 1987); (3) a simple spectrophotometric assay using *p*-nitrophenol-ß-D-glucopyranoside as substrate was available to monitor activity.

Recombinant Abg does not have a leader peptide recognized by the *E. coli* leader peptidase, therefore Abg was found predominantly in the cytoplasm of the cells (Wakarchuk *et al.*, 1986). As with Abg, Abg-CBD_{Cex} was found in the cytoplasm of *E. coli*. Both CBD_{Cex} and Cbg-CBD_{Cex} had the Cex leader peptide at their N-termini; this allowed export of the polypeptide to the periplasm of *E. coli*. The production yield of CBD_{Cex} in *E. coli* was $\geq 6\%$ total cell protein, resulting in its accumulation in the periplasm and subsequent leakage into the culture supernatant. Non-specific protein leakage into the culture supernatant in *E. coli* is not uncommon (Gilkes *et al.*, 1984; Guo *et al.*, 1988; Shen *et al.*, 1991), but the exact mechanism is not clear. Lysis of cells was ruled out since cytoplasmic enzyme markers (e.g., glucose-6-phosphate dehydrogenase) were not

detected in the culture supernatant. However, significant levels of the periplasmic enzyme marker ß-lactamase were detected in the culture supernatant. It appears that the accumulation of polypeptides in the periplasm alters the integrity of the outer membrane, leading to non-specific leakage of both recombinant polypeptides. Unlike CBD_{Cex}, Cbg-CBD_{Cex} did not leak into the culture supernatant, probably because of its low synthesis level (< 0.05% of total cell protein). Abg-CBD_{Cex} and Cbg-CBD_{Cex} were therefore isolated from whole cell extracts.

Affinity chromatography is one of the most powerful procedures for purifying proteins (Ostrove, 1990). This procedure exploits the specific binding properties of the target protein. Unlike other chromatographic or filtration techniques, affinity chromatography relies on the highly specific interaction of biomolecules. Properties such as shape, conformational changes or recognition of certain regions in the molecule have all been used to effect separation. Different eluents (e.g. substrate analogs, chaotropic agents, and changes in pH, temperature or salt concentration) have been used to desorb the desired molecule from the matrix, but in some cases, irreversible denaturation of the target molecule results in poor yield. Affinity chromatography usually requires the use of ligands coupled chemically to matrices. As with similar supports used for immobilizing enzymes, the principal disadvantage is the expense of preparing such specialized matrices. The strategy employed for purifying polypeptides in this study utilized inexpensive and readily available cellulosic matrices, and water for desorption of the fusion polypeptides.

Like the intact exoglucanase Cex (Gilkes *et al.*, 1988), the fusion polypeptides were desorbed from cellulose with water with a recovery varying from 58-70%. CBD_{Cex}, however, was not desorbed with water but required 8 M GdmCl, with a recovery >90%. Surprisingly, in view of these differences in conditions for desorption, the relative affinities of Abg-CBD_{Cex}1 (7.8 $L.g^{-1}$) and

CBD_{Cex} (7.5 $L.g^{-1}$) for Avicel™ were similar. This suggests that the size of the polypeptide may influence the packing on the cellulose surface. The smaller CBD_{Cex} could pack more tightly, hindering the access of water molecules for desorption. Whereas for the larger hybrid polypeptides, the fusion partner might sterically block binding, resulting in lower and less dense surface packing (e.g. > 0.6 μmoles Abg-CBD_{Cex}1.g Avicel™$^{-1}$ compared to > 3 μmoles CBD_{Cex}.g Avicel™$^{-1}$). This in turn might facilitate the entry of water molecules to desorb the polypeptide much more readily. Cex is a monomer (Gilkes, unpublished results), whereas Abg (Day & Withers, 1986) and presumably Cbg are both dimers. The inability of water to completely desorb the fusion polypeptides from cellulose can also be attributed to the dimeric nature of the fusion partner. At least for Cbg-CBD_{Cex} the fusion polypeptides desorbed with water consisted of heterodimers with one partner bearing a CBD, whereas the unrecovered fusion polypeptides consisted of homodimers in which each partner had a CBD (Figure 3.36). It seems, therefore, that the homodimers bind more strongly to cellulose than the heterodimers because of the two-fold increase in the number of hydrogen bonds and van der Waals interaction between the homodimers and the cellulose matrix.

The different saturation levels of CBD_{Cex} to a number of substrates (Figure 3.8) relates at least in part to the difference in available surface area. Heterogeneity of the substrate structure may also play a role since the various cellulosic substrates employed differ in the extent and nature of their crystallinity. Regenerated cellulose is thought to be predominantly cellulose II (Figure 1.2; Blackwell, 1981; Sarko, 1986), although other workers have concluded that it is amorphous (Lee *et al.*, 1982; Ooshima *et al.*, 1983). The regeneration also results in a reduction in particle size and consequent increase in surface area (Lee *et al.*, 1982; Ooshima *et al.*, 1983). BMCC consists of uniform bundles of microfibrils, 20-50 nm wide and several μm long (Henrissat &

Chanzy, 1986; Ross *et al.*, 1991). The microfibrils are crystalline and consist of cellulose I. Avicel™, on the other hand, is a relatively heterogeneous cellulose preparation made from partially acid hydrolyzed wood fibres containing both crystalline and amorphous components (Ooshima *et al.*, 1983). It is a mixture of rod- and irregularly-shaped particles/aggregates with varying intraparticle pores (1-10 nm) and interparticle voids (≥ 5 μm) (Marshall & Sixsmith, 1974). CBD_{Cex} was also shown to adsorb to α-chitin. Chitin is a polymer of N-acetylglucosamine residues linked by ß-1,4-glycosidic linkages much like cellulose. Regenerated chitin (or α-chitin) forms an anti-parallel structure similar to cellulose II (Blackwell, 1981). The adsorption of CBD_{Cex} to chitin suggests a common recognition motif in both types of substrates. Adsorption is obviously not blocked by the 2-acetamido substitution of the glucosyl residues.

The CBD_{Cex} fusion polypeptides used for enzyme immobilization also bound to other cellulosic matrices (sections 3.2.4, 3.2.11, and 3.3.4). Cotton is one of the purest naturally occurring celluloses. It has a high crystallinity of 70-84% (Lee *et al.*, 1982; Wood, 1988). CF1™ cellulose is fibrous in nature with an average fibre length of 200 μm and diameter of 13.5 μm [E. Heilweil (Whatman, Inc.), personal communication]. It is made from highly purified cotton and has an α-cellulose content of at least 98%. CF1™ cellulose is therefore free of hemicelluloses and other polysaccharides. Its manufacture does not involve either acid or alkali swelling and regeneration, and is therefore characterized as cellulose I. The crystallinity of CF1™ cellulose is estimated at 75-85%. It is the preferred support for chromatographic application because of its good packing and flow rate characteristics. Cellulose acetate is made from wood pulp prepared with acids or organic solvents followed by acetylation and partial deacetylation. The pulping conditions generally hydrolyze amorphous cellulose, resulting in a high α-cellulose content (> 90%) (Klausmeier, 1986).

Depending on the manufacturing process, cellulose acetate contains regions of varying crystallinity. Cellufine™ consists of microcrystalline particles of 45-105 μm diameter, and is produced from cellulose triacetate after removal of the ester groups [D. Boyd (Amicon), personal communication].

It is evident that the nature of the substrate affects the reversibility of adsorption. The reasons for this are not immediately apparent but may be related to the crystallinity of, and available surface area on, the cellulose. For example, CF1™ cellulose allowed good recovery of CBD_{Cex} fusion polypeptides, and regenerated cellulose showed a very high capacity for binding CBD_{Cex}. By contrast, the use of a more crystalline cellulose (e.g. cotton; Cellufine™; BMCC; cellulose acetate) resulted in stable immobilization of the CBD_{Cex} fusion polypeptides. Protein purification by affinity chromatography requires reversible binding to the matrix, whereas for enzyme immobilization, a tight and irreversible binding is usually preferred. It is an advantage to have a choice of cellulosic supports with different affinities for CBD_{Cex} for particular biotechnological applications.

The saturation levels of CBD_{Cex} bound to BMCC (Figures 3.10) did not vary appreciably over the temperatures tested. The relative affinity values however did show a marked decrease at 50° (Figure 3.11), suggesting that a portion of the polypeptides could be denatured and therefore did not bind to BMCC. The portion of polypeptides that did bind probably adsorbed during the first few seconds of incubation before the temperature reached 50°, and remained bound subsequently. This is supported by the finding that CBD_{CenA} adsorbed to BMCC almost immediately at 30° (Gilkes *et al.*, 1992). More importantly, this also demonstrates that CBD_{Cex} could still be used for enzyme immobilization under operating conditions extending well beyond those normally encountered. Although Abg was inactivated at 50°, the fusion polypeptide remained bound to cellulose. Moreover, the stable and continuous operation of a

Cbg-CBD_{Cex} immobilized column confirmed unequivocably that CBD_{Cex} continued to bind at operating temperatures up to 70° with no apparent leaching of the fusion polypeptide (Figures 3.37 & 3.38). A possible explanation for the binding stability at elevated temperature is that the CBD_{Cex} part of the thermophilic fusion polypeptide was denatured *in situ* and "fixed" on the surface of the cellulose, with no obvious detrimental effect on the conformation of Cbg. Irreversible denaturation of the adsorbed CBD at high temperature would not be detrimental for enzyme immobilization as long as the enzyme retained catalytic activity.

The adsorption of CBD_{Cex} to cellulose at high pH can be explained partly by the pI of the polypeptide. At its pI, a protein exhibits the least intra- and intermolecular electrostatic repulsions, resulting in a more compact structure and greater surface packing. Glucoamylase adsorption to starch showed maximum saturation at its pI of 3.5, and decreased with increasing pH (Dalmia & Nikolov, 1991). The same trend was observed for CBD_{Cex} although the differences in the saturation levels were not large (Figure 3.11). The higher relative affinity of CBD_{Cex} at pH 9 could also be explained by the decreased electrostatic repulsion among polypeptides at this pH. The lower relative affinity of CBD_{Cex} at pH 3 could have resulted from an increased charge repulsion effect and/or changes in the conformation of the polypeptide. The desorption of the fusion polypeptide at a pH ($\geq$ 9) higher than its pI ($\sim$ 5) may have resulted from the electrostatic repulsions among fusion polypeptides on the cellulose surface. It is clear that no generalization can be made from the effect of temperatures and pHs on the binding of CBD_{Cex} to cellulose. Until more is known about the structure-function relations of CBD and its substrate, each fusion polypeptide constructed should be tested individually.

The immobilization yields for the two fusion polypeptides, Abg-CBD_{Cex}1 and 3 (section 3.2.9) were comparable to those reported for ß-glucosidases

immobilized by other methods (Table 1.1). An exception is the immobilization of ß-glucosidase through sugar moieties to concanavalin A-Sepharose. The activity retained was 90%. This difference in the performance of two analogous immobilization techniques might be due to denser packing of fusion polypeptides on the cellulose surface, resulting in steric hindrance of the bound molecules. Alternatively, the activity of the Abg fusion polypeptides might be reduced by the interaction of the active site of the fusion polypeptide with a cellobiosyl unit in the cellulose, to the exclusion of pNPG, i.e. cellulose could act as a competitive inhibitor of Abg-CBD_{Cex} under these conditions. In CenA, the Pro-Thr linker forms an extended, rigid segment connecting the ellipsoidal catalytic domain to the CBD (Pilz *et al.*, 1990; Shen *et al.*, 1991). It is not known if the Pro-Thr linker performs the same function in Cex. There is no model as yet for Cex, but the Cex paired distance distribution function from small-angle X-ray scattering analyses shows that the overall shape is similar to that of CenA (Schmuck & Gilkes, unpublished results). Moreover, the Pro-Thr linker-CBD amino acid sequence is very similar to that in CenA. The observation that Abg-$CBD_{Cex}3$ (lacking an intervening 57 amino acids) showed less activity than Abg-$CBD_{Cex}1$ is consistent with a role for the linker in reducing inhibitory interaction of Abg with the cellulose surface. The immobilization yield of Abg-CBD_{Cex} could be improved by reducing the enzyme loading. The enzyme loading and operational stability of the ConA-adsorbed ß-glucosidase were not reported, thus comparisons with the performance of Abg-CBD_{Cex} adsorbed to cellulose cannot be made.

Cex could be cleaved by a *C. fimi* serine protease (Gilkes *et al.*, 1988) and papain (Gilkes *et al.*, 1991a) into a stable core peptide (p33) corresponding to the catalytic domain and a shorter peptide (p8) corresponding to the CBD. p8 was resistant to further cleavage. CBD_{Cex} was resistant to cleavage by papain and the *C. fimi* protease (data not shown). Native CenA could be cleaved by trypsin at

sites inside the CBD producing p45 and p38 fragments, and, to a lesser extent, at the junction of the Pro-Thr linker and the catalytic domain producing a p30 fragment (Gilkes *et al.*, 1989). It was concluded that CBD_{CenA} had a rather open native conformation relative to the catalytic domain which resisted protease cleavage. Trypsin cleaved CBD_{Cex} in the presence of urea and DTT, albeit slowly. This suggests that CBD_{Cex} in solution adopts a more tightly folded conformation than CBD_{CenA} affording protection from proteolytic attack.

Pepsin is a carboxyl protease that hydrolyzes peptides with hydrophobic residues on either side of the scissile bond (Fersht, 1985). It is therefore a broad-spectrum protease capable of digesting polypeptides into very small fragments. It also requires a very acidic (pH 1-5) environment to function. CBD_{Cex} contaminated with xylan was rapidly digested by pepsin, whereas the xylan-free material was completely resistant (Figure 3.15). Xylan thus alters the sensitivity of CBD_{Cex} to pepsin presumably by changing the conformation of the polypeptide. It is possible that, under the conditions used for pepsin digestion (pH 4), the xylan associated with CBD_{Cex} was dissociated since xylan was removed during cation-exchange chromatography of CBD_{Cex} at pH 4 (Figure 3.7). However, the fact that pepsin digestion of the xylan-contaminated CBD_{Cex}, but not the purified material, still occurred at pH 4 argues against this possibility. This paradox could be explained by arguing that the low pH did not cause the dissociation of the xylan material from CBD_{Cex}. It did however allow the *displacement* of the xylan contaminant during cation-exchange chromatography favouring ionic interaction over hydrogen bonding. The strength of most ionic bonds is ~ 500 $kJ.mol^{-1}$, which makes them stronger than either hydrogen bonds (~25 $kJ.mol^{-1}$) or van der Waals interaction (~ 1 $kJ.mol^{-1}$) (Israelachvili, 1992). Charged residues (like lysine, arginine, glutamic and aspartic acids) have all been shown to participate in hydrogen bond formation in the arabinose-binding (Quiocho, 1988) and maltose-binding (Spurlino *et al.*, 1991) proteins. Further

confirmation of adsorption at acid pH comes from the observation that CBD_{Cex} bound stably to cellulose at pH 3 (Figure 3.11).

Detergents are a class of molecules with amphiphilic structure (Neugebauer, 1990). Each molecule has both hydrophobic and hydrophilic moieties and is capable of forming micelles with other detergent molecules. Non-ionic detergents (e.g. Triton X-100) act by disrupting hydrophobic interactions within and between molecules. In addition, ionic detergents (e.g. SDS) also bind to proteins causing gross structural changes and denaturation. The stable adsorption of CBD_{Cex} to cellulose in Triton X-100 (up to 2%; section 3.1.4) and SDS (up to 0.2%) suggests the potential use of CBD_{Cex} for fusion to polypeptides (e.g. membrane-associated lipoproteins) that require the presence of detergents for their solubilization and purification. More fundamentally, the ability of CBD_{Cex} to bind to cellulose in the presence of detergents suggests that the interaction between the CBD and cellulose is not mediated by hydrophobic interaction. However, hydrophobic interaction may well be involved in the structural stability of CBD_{Cex} because of the high aliphatic (24%) and aromatic (10%) amino acid contents of the polypeptide.

The adsorption plots of CBD_{Cex} (1/bound [P] vs. 1/free [P]; figures 3.9, 3.10 & 3.11) and Abg-CBD_{Cex}1 (bound [P]/free [P] vs. bound [P] (Scatchard); Ong *et al.*, 1991) were non-linear. Non-linearity is often indicative of binding site heterogeneity (i.e. the presence of two or more classes of binding sites) or cooperativity (i.e. ligand-ligand interaction) (Dahlquist, 1978). Classical Scatchard analysis is valid for small ligands interacting with independent binding but not for large biomolecules which can potentially occupy several binding sites at any given time (e.g. DNA-protein interaction [McGhee & von Hippel, 1974]). Since the dimensions of the CBD (Pilz *et al.*, 1990; Shen *et al.*, 1991) greatly exceed those of the repeating cellobiosyl units, the adsorption process may involve productive (binding) or non-productive (masking) or both interactions

with more than one lattice unit (Gilkes *et al.*, 1992). By extension of the DNA-protein interaction model (McGhee & von Hippel, 1974) the cellulose surface is viewed as a two-dimensional lattice with an array of overlapping potential sites (Gilkes *et al.*, 1992). Despite these considerations many previous studies on the adsorption of cellulases used a simple one- or two-site model based on the Langmuir adsorption isotherm (Lee *et al.*, 1982; Ooshima *et al.*, 1983; Stuart & Ristroph, 1985; Steiner *et al.*, 1988; Woodward *et al.*, 1988; Ståhlberg *et al.*, 1991). These analyses are further confounded by the use of very heterogeneous substrates like Avicel™. It is obvious that analysis of the adsorption process is inherently complex, and requires a better understanding of the structure of the CBD and the topology of cellulose.

The exact mechanism of CBD adsorption to cellulose is not known. A more thorough understanding of the adsorption process would allow the operating conditions and the choice of cellulosic matrix for purification and/or immobilization to be defined more precisely. Published results (Reese, E.T., 1982; Gilkes *et al.*, 1988; Owolabi *et al.*, 1988; Ong *et al.*, 1989b) strongly suggest that hydrogen bonding, together with van der Waals interactions, between the CBD and glucosyl units are the principal forces involved in the adsorption process. Binding does not appear to be mediated by salt linkages because native cellulose is uncharged and adsorbed CBD_{Cex} fusion polypeptides were stable at NaCl concentrations up to 1 M (section 3.2.4). Water molecules would compete with the hydrogen bond network between substrate and polypeptide, resulting in desorption of the polypeptide. The size and packing of the polypeptide on the cellulose surface, and the degree of crystallinity of the cellulose used also affect desorption, presumably by blocking access of water molecules or allowing tighter binding of the polypeptide to cellulose or both. A definitive explanation of the binding mechanism may be possible when the structure of the CBD, alone or bound to its substrate, is solved to a resolution

comparable to that of the maltose-binding protein (Spurlino *et al.*, 1991). X-ray crystallographic and two-dimensional nuclear magnetic resonance spectroscopic analyses of CBD_{Cex} are now underway.

In summary, the potential of fusion polypeptides containing CBD_{Cex} or related CBDs for affinity purification and/or enzyme immobilization on a commercial scale has been demonstrated. Simultaneous purification and immobilization would result in simplified downstream processing, improved recovery of proteins and significantly reduced purification costs. The simple and stable coupling of an enzyme-CBD fusion to a readily available, inexpensive and stable cellulosic support opens the possibility of using this technique as a generic method for immobilizing a complete range of proteins. Although this generic method for making fusion proteins necessitates the fusion partner tolerating the affinity "tag", the availability of other *C. fimi*-type CBDs (e.g. CBD_{CenA}) for fusion to the N-terminus of the fusion partner (Greenwood *et al.*, 1989) increases the flexibility of the method. This is especially important if fusion at the C-terminus of the protein is detrimental to its function.

5. REFERENCES

Aitken, A., M.J. Geisow, J.B.C. Findlay, C. Holmes & A. Yarwood. 1989. Peptide preparation and characterization. In J.B.C. Findlay & M.J. Geisow (ed.) *Protein Sequencing: A Practical Approach.* IRL Press, Oxford, pp. 43-68.

Alfani, F., L. Cantarella, A. Gallifuoco, L. Pezzullo, V. Scardi & M. Cantarella. 1987. Characterization of the ß-glucosidase activity associated with immobilized cellulase of *Aspergillus niger. Annals New York Acad. Sci.* **501**:503-07.

Atkinson, T. & M. Smith. 1984. Solid phase synthesis of oligodeoxyribonucleotides by the phosphite triester method. In N.J. Gait (ed.) *Oligonucleotide Synthesis: A Practical Approach.* IRL Press, Oxford, pp. 35-81.

Baker, J.O., K.K. Oh, K. Grohmann & M.E. Himmel. 1988. Thermal stabilization of fungal ß-glucosidase through glutaraldehyde crosslinking. *Biotechnol. Letters* **10**:325-330.

Baker, T.A., A.D. Grossman & C.A. Gross. 1984. A gene regulating the heat shock response in *Escherichia coli* also affects proteolysis. *Proc. Natl. Acad. Sci. USA* **81**:6779-6783.

Baneyx, F. & G. Georgiou. 1989. Expression, purification, and enzymatic characterization of a protein A-ß-lactamase hybrid protein. *Enzyme Microb. Technol.* **11**:559-67.

Baneyx, F., C. Schmidt & G. Georgiou. 1990. Affinity immobilization of a genetically engineered bifunctional hybrid protein. *Enzyme Microb. Technol.* **12**:337-42.

Bernath, F.R. & K. Venkatasubramanian. 1987. Methods of enzyme immobilization. In A. Demain & N. Solomon (ed.) *Manual of Industrial Microbiology and Biotechnology.* American Society for Microbiology, Washington, D.C., pp. 230-47.

Blackwell, J. 1981. The structures of cellulose and chitin. In R. Srinivasan (ed.) *Biomolecular Structure, Conformation, Function and Evolution. Vol. 1: Diffraction and Related Studies.* Pergamon, New York, pp. 523-35.

Bradford, M. 1976. A rapid and sensitive method for the quantitation of microgram quantities of proteins utilizing the principle of protein-dye binding. *Anal. Biochem.* **72**:248-254.

Buchholz, K. (ed.) 1979. *Characterization of Immobilized Biocatalysts.* Verlag Chemie, Weinheim.

Bülow, L. & K. Mosbach. 1991. Multienzyme systems obtained by gene fusion. *Trends Biotechnol.* **9**:226-31.

Caldwell, S.R. & F.M. Raushel. 1991. Detoxification of organophosphate pesticides using an immobilized phosphotriesterase from *Pseudomonas diminuta. Biotechnol. Bioeng.* **37**:103-09.

Cannon, J.J., L.F. Chen, M.C. Flickinger & G.T. Tsao. 1984. The development of an immobilized lactate oxidase system for lactic acid analysis. *Biotechnol. Bioeng.* **26**:167-73.

Cantor, C.R. & P.R. Schimmel. 1980. *Biophysical Chemistry Part II. Techniques for the Study of Biological Structure and Function.* Freeman, San Francisco, p. 380.

Chaplin, M.F. 1986. Monosaccharides. In M.F. Chaplin & J.F. Kennedy (ed.) *Carbohydrate Analysis: A Practical Approach.* IRL Press, Oxford, p. 2.

Chen, L., C. Ford, A. Kusnadi & Z.L. Nikolov. 1991. Improved adsorption to starch of a ß-galactosidase fusion protein containing the starch-binding domain from *Aspergillus* glucoamylase. *Biotechnol. Prog.* **7**:225-29.

Chen, L.F., C.S. Gong & G.T. Tsao. 1981. Immobilized glucose isomerase on DEAE cellulose beads. *Starch* **33**:58-63.

Chibata, I. (ed.) 1978. *Immobilized Enzymes: Research and Applications* Wiley, New York.

Chien, C.H., Y.H. Wei & J.F. Shaw. 1991. Immobilized enzyme system for determination of sialic acid in serum or urine. *Enzyme Microb. Technol.* **13**:45-52.

Coutinho, J.B., B. Moser, D.G. Kilburn, R.A.J. Warren & R.C. Miller, Jr. 1991. Nucleotide sequence of the endoglucanase C gene (*cenC*) of *Cellulomonas fimi*, its high-level expression in *Escherichia coli*, and characterization of its products. *Mol. Microbiol.* **5**:1221-33.

Creighton, T.E. 1989. Disulphide bonds between cysteine residues. In T.E. Creighton (ed.) *Protein Structure: A Practical Approach*. IRL Press, Oxford.

Dahlquist, F.W. 1978. The meaning of Scatchard and Hill plots. *Methods Enzymol.* **48**:270-99.

Dalmia, B.K. & Z.L. Nikolov. 1991. Characterization of glucoamylase adsorption to raw starch. *Enzyme Microb. Technol.* **13**:982-990.

Day, A.G. & S.G. Withers. 1986. The purification and characterization of a ß-glucosidase from *Alcaligenes faecalis*. *Biochem. Cell Biol.* **64**:914-22.

Domínquez, E., M. Nilsson & B. Hahn-Hägerdal. 1988. Carbodiimide coupling of ß-galactosidase from *Aspergillus oryzae* to alginate. *Enzyme Microb. Technol.* **10**:606-10.

Drickamer, K. 1988. Two distinct classes of carbohydrate-recognition domains in animal lectins. *J. Biol. Chem.* **263**:9557-60.

Dumitriu, S., M. Popa, V. Artenie & F. Dan. 1989. Bioactive polymers. 56: urease immobilization on carboxymethylcellulose. *Biotechnol. Bioeng.* **34**: 283-290.

Elving, P.J., J.M. Markowitz & I. Rosenthal. 1956. Preparation of buffer systems of constant ionic strength. *Anal. Chem.* **28**:1179-80.

Fersht, A. 1985. *Enzyme Structure and Mechanism*, 2nd ed. Freeman, New York.

Ford, J.R., A.H. Lambert, W. Cohen & R.P. Chambers. 1972. Recirculation reactor system for kinetic studies of immobilized enzymes. *Biotechnol. Bioeng. Symp.* **3**:267-84.

Fujikawa, S., T. Yokota & K. Koga. 1988. Immobilization of ß-glucosidase in calcium alginate gel using genipin as a new type of cross-linking reagent of natural origin. *Appl. Microbiol. Biotechnol.* **28**:440-41.

Gianfreda, L., M. Modaferri & G. Greco, Jr. 1985. Enzyme stabilization towards thermal, chemical and proteolytic deactivation. *Enzyme Microb. Technol.* **7**:78-82.

Gilkes, N.R., D.G. Kilburn, R.C. Miller, Jr. & R.A.J. Warren. 1984. A mutant of *Escherichia coli* that leaks cellulase activity encoded by cellulase genes for *Cellulomonas fimi*. *Bio/Technology* **2**:259.

Gilkes, N.R., D.G. Kilburn, R.C. Miller, Jr. & R.A.J. Warren. 1989. Structural and functional analysis of a bacterial cellulase by proteolysis. *J. Biol. Chem.* **264**:17802-08.

Gilkes, N.R., E. Jervis, B. Henrissat, B. Tekant, R.C. Miller, Jr., R.A.J. Warren & D.G. Kilburn. 1992. The adsorption of a bacterial cellulase and its two isolated domains to crystalline cellulose. *J. Biol. Chem..*, in press.

Gilkes, N.R., M. Claeyssens, R. Aebersold, B. Henrissat, A. Meinke, H.D. Morrison, D.G. Kilburn, R.A.J. Warren & R.C. Miller, Jr. 1991a. Structural and functional relationships in two families of ß-1,4-glycanases. *Eur. J. Biochem.* **202**:367-77.

Gilkes, N.R., B. Henrissat, D.G. Kilburn, R.C. Miller, Jr. & R.A.J. Warren. 1991b. Domains in microbial ß-1,4-glycanases: sequence conservation, function, and enzyme families. *Microbiol. Rev.* **55**:303-15.

Gilkes, N.R., R.A.J. Warren, R.C. Miller, Jr. & D.G. Kilburn. 1988. Precise excision of the cellulose-binding domains from two *Cellulomonas fimi* cellulases by a homologous protease and the effect on catalysis. *J. Biol. Chem.* **263**:10401-07.

Goldberg, A.L. & S.A. Goff. 1986. The selective degradation of abnormal proteins in bacteria. In W. Reznikoff and L. Gold (ed.) *Maximizing Gene Expression* Butterworths, Boston, pp. 287-313

Gomori, G. 1955. Preparation of buffers for use in enzyme studies. *Methods Enzymol.* **1**:138-46.

Greenwood, J.M., N.R. Gilkes, D.G. Kilburn, R.C. Miller, Jr. & R.A.J. Warren. 1989. Fusion to an endoglucanase allows alkaline phosphatase to bind to cellulose. *FEBS Letters* **244**:127-31.

Grossman, A.D., J.W. Erickson & C.A. Gross. 1984. The *htpR* gene product of *E. coli* is a sigma factor for heat-shock promoters. *Cell* **38**:383-90.

Guilbault, G.G. 1984. *Analytical Uses of Immobilized Enzymes.* Dekker, New York.

Guilbault, G.G. 1988. Enzyme electrode probes. *Methods Enzymol.* **137**:14-29.

Guilbault, G.G., J.M. Kauffman & G.J. Patriarche. 1991. Immobilized enzyme electrodes as biosensors. In R.F. Taylor (ed.) *Protein Immobilization.* Dekker, New York, pp. 209-62.

Guo, Z.M., N. Arfman, E. Ong, N.R. Gilkes, D.G. Kilburn, R.A.J. Warren & R.C. Miller, Jr. 1988. Leakage of *Cellulomonas fimi* cellulases from *Escherichia coli. FEMS Microbiol. Lett.* **49**:279-83.

Hahn-Hägerdal, B. 1984. An enzyme coimmobilized with a microorganism: the conversion of cellobiose to ethanol using ß-glucosidase and *Saccharomyces cerevisiae* in calcium alginate gels. *Biotechnol. Bioeng.* **26**:771-74.

Han, Y.W. & V.R. Srinivasan, V.R. 1969. Purification and characterization of ß-glucosidase of *Alcaligenes faecalis. J. Bacteriol.* **100**:1355-63.

Hanahan, D. & M. Meselson. 1983. Plasmid screening at high colony density. *Gene* **10**:63.

Hanahan, D. 1982. Studies on transformation of *Escherichia coli* with plasmids. *J. Mol. Biol.* **166**:557.

Harlow, E. & D. Lane. 1988. *Antibodies: A Laboratory Manual.* Cold Spring Harbor Laboratory Press, New York.

Hartmeier, W. 1988. *Immobilized Biocatalysts.* Springer-Verlag, Berlin.

Henrissat, B. & H. Chanzy. 1986. Enzymatic breakdown of cellulose crystals. In R.A. Young & R.M. Rowell (ed.) *Cellulose: Structure, Modification and Hydrolysis.* Wiley, N.Y., pp.337-47.

Henrissat, B., B. Vigny, A. Buleon & S. Perez. 1988. Possible adsorption sites of cellulases on crystalline cellulose. *FEBS Letters* **231**:177-82.

Hestrin, S. 1963. Bacterial cellulose. *Methods Carbohyd. Chem.* **3**:4-9.

Huang, Y.L., S.Y. Li, B.A.A. Dremel, U. Bilitewski & R.D. Schmid. 1991. On-line determination of glucose concentration throughout animal cell cultures based on chemiluminescent detection of hydrogen peroxide coupled with flow-injection analysis. *J. Biotechnol.* **18**:161-72.

Husain, Q. & M. Saleemuddin. 1989. An inexpensive procedure for the immobilization of glycoenzymes on Sephadex G-50 using crude concanavalin A. *Biotechnol. Appl. Biochem.* **11**:508-12.

Imai, K., T. Shiomi, K. Uchida & M. Miya. 1986. Immobilization of enzyme onto poly(ethylene-vinyl alcohol) membrane. *Biotechnol. Bioeng.* **28**:198-203.

Israelachvili, J. 1992. *Intermolecular and Surface Forces*, 2nd ed. Academic Press, London, p. 125.

Jayakumari, V.G. & N.R. Pillai. 1990. Peptide synthesis in a triphasic medium catalyzed by papain immobilized on a crosslinked polystyrene support. *Indian J. Chem.* **29**:514-17.

Jin, F. & K. Toda. 1988. Preparation of immobilized papain covalently bound on natural cellulose for treatment of beer. *Biotechnol. Letters* **10**:221-23.

Johnson, L.N., J. Cheetham, P.J. McLaughlin, K.R. Acharya, D. Barford & D.C. Phillips. 1988. Protein-oligosaccharide interactions: lysozyme, phosphorylase, amylases. *Current Topics Microbiol. Immunol.* **139**:81-134.

Karkare, S.B. 1991. Immobilized microbial and animal cells as enzyme reactors. In R.F. Taylor (ed.) *Protein Immobilization.* Dekker, New York, pp. 319-37.

Kierstan, M., A. McHale & M.P. Coughlan. 1982. The production of ethanol from cellobiose using immobilized ß-glucosidase coentrapped with yeast in alginate gels. *Biotechnol. Bioeng.* **24**:1461-63.

Kimura, T., M. Ogata, H. Kobayashi, M. Yoshida, K. Oishi & T. Nakakuki. 1990a. Continuous production of maltotetraose using a dual immobilized enzyme system of maltotetraose-forming amylase and pullulanase. *Biotechnol. Bioeng.* **36**:790-96.

Kimura, T., M. Ogata, M. Yoshida & T. Nakakuki. 1989. Stability of immobilized maltotetraose-forming amylase from *Pseudomonas stutzeri. Biotechnol. Bioeng.* **33**:845-55.

Kimura, Y., T. Yoshida, K. Muraya, K. Nakanishi & R. Matsuno. 1990b. Continuous synthesis of a tripeptide by successive condensation and transesterification catalyzed by two immobilized proteinases in organic solvent. *Agri. Biol. Chem.* **54**:1433-40.

Klausmeier, W.H. 1986. Economic analysis of an innovative process for cellulose acetate production. In R.A. Young & R.M. Rowell (ed.) *Cellulose: Structure, Modification and Hydrolysis.* Wiley, N.Y., pp. 187-201.

Kohlwey, D.E. & M. Cheryan. 1981. Performance of a ß-D-galactosidase hollow fibre reactor. *Enzyme Microb. Technol.* **3**:64-68.

Kraft, R., J. Tardiff, K.S. Krauter & L.A. Leinwand. 1988. Using mini-prep plasmid DNA for sequencing double-stranded template with Sequenase. *BioTechniques* **6**:544-48.

Kraulis, P.M., M.G. Clore, M. Nilges, T.A. Jones, G. Pettersson, J. Knowles & A.M. Gronenborn. 1989. Determination of the three-dimensional solution structure of the C-terminal domain of cellobiohydrolase I from *Trichoderma reesei.* A study using nuclear magnetic resonance and hybrid distance geometry-dynamical simulated annealing. *Biochemistry* **28**:7241-57.

Kunkel, T.A., J.D. Roberts & R.A. Zakour. 1987. Rapid and efficient site-specific mutagenesis without phenotypic selection. *Methods Enzymol.* **154**:367-82.

Laemmli, K. 1970. Cleavage of structural proteins during the assembly of the head of bacteriophage T4. *Nature* **227**:680-85.

Lee, J.M. & J. Woodward. 1983. Properties and application of immobilized ß-D-glucosidase coentrapped with *Zymomonas mobilis* in calcium alginate. *Biotechnol. Bioeng.* **25**:2441-51.

Lee, S.B., H.S. Shin, D.D.Y. Ryu & M. Mandels. 1982. Adsorption of cellulase on cellulose: effects of physicochemical properties of cellulose on adsorption and rate of hydrolysis. *Biotechnol. Bioeng.* **24**:2137-53.

Lilly, M.D., W.E. Hornby & E.M. Crook. 1966. The kinetics of carboxymethylcellulose-ficin in packed beds. *Biochem. J.* **100**:718-23.

Love, D.R. & M.B. Streiff. 1987. Molecular cloning of a ß-glucosidase gene from an extremely thermophilic anaerobe in *E. coli* and *B. subtilis*. *Bio/Technology* **5**:385-87.

Love, D.R., R. Fisher & P.L. Bergquist. 1988. Sequence, structure and expression of a cloned ß-glucosidase gene from an extreme thermophile. *Mol. Gen. Genet.* **213**:84-92.

Lowe, C.R. 1984. Biosensors. *Trends Biotechnol.* **2**:59-65.

Lund, B., F. Lindberg & S. Normark. 1988. Structure and antigenic properties of the tip-located P pilus proteins of uropathogenic *Escherichia coli*. *J. Bacteriol.* **170**:1887-94.

Marshall, K. & D. Sixsmith. 1974. Some physical characteristics of microcrystalline cellulose 1. powders for pharmaceutical use. *Drug Devel. Commun.* **1**:51-71.

Matsudaira, P. (ed.) 1989. *A Practical Guide to Protein and Peptide Purification for Microsequencing*. Academic Press, San Diego, CA.

Matsudaira, P. 1987. Sequence from picomole quantities of proteins electroblotted onto polyvinylidene difluoride membrane. *J. Biol. Chem.* **262**:10035-38.

Matsudaira, P. 1990. Limited N-terminal sequence analysis. *Methods Enzymol.* **182**:602-13.

Mattiasson, B. & R. Kaul. 1991. Determination of coupling yields and handling of labile proteins in immobilization technology. In R.F. Taylor (ed.) *Protein Immobilization.* Dekker, New York, pp. 161-79.

McClary, J.A., F. Witney & J. Geisselsoder. 1989. Efficient site-directed *in vitro* mutagenesis using phagemid vectors. *BioTechniques* **7**:282-89.

McGhee, J.D. & P.H. von Hippel. 1974. Theoretical aspects of DNA-protein interactions: co-operative and non-co-operative binding of large ligands to a one-dimensional homogeneous lattice. *J. Mol. Biol.* **86**:469-89.

Meacock, P.A. & S.N. Cohen. 1980. Partitioning of bacterial plasmids during cell division, a *cis*-acting locus that accomplishes stable plasmid inheritance. *Cell* **20**:529-42.

Meinke, A., C. Braun, N.R. Gilkes, D.G. Kilburn, R.C. Miller, Jr. & R.A.J. Warren. 1991. Unusual sequence organization in CenB, an inverting endoglucanase from *Cellulomonas fimi. J. Bacteriol.* **173**:308-14.

Merril, C.R. 1990. Gel staining techniques. *Methods Enzymol.* **182**:477-88.

Monsan, P. & D. Combes. 1988. Enzyme stabilization by immobilization. *Methods Enzymol.* **137**:584-98.

Mozhaev, V.V. 1990. Immobilization provides additional stabilization of an initially stable protease from *Thermoactinomyces vulgaris* (Thermitase). *Biotechnol. Techniques* **4**:255-56.

Nakakuki, T., T. Hayashi, M. Monma, K. Kawashiwa & K. Kainuma. 1983. Immobilization of the exo-maltohexaohydrolase by the irradiation method. *Biotechnol. Bioeng.* **25**:1095-107.

Nakanishi, K., R. Matsuno, K. Torii, K. Yamamoto & T. Kamikubo. 1983. Properties of immobilized ß-D-galactosidase from *Bacillus circulans*. *Enzyme Microb. Technol.* **5**:115-20.

Nelson, J.M. & E.G. Griffin. 1916. Adsorption of invertase. *J. Am. Chem. Soc.* **38**:1109-15.

Neugebauer, J.M. 1990. Detergents: an overview. *Methods Enzymol.* **182**:239-53.

O'Neill, G., S.H. Goh, R.A.J. Warren, D.G. Kilburn & R.C. Miller, Jr. 1986. Structure of the gene encoding the exoglucanase of *Cellulomonas fimi*. *Gene* **44**:325-30.

Oguntimein, G.B. & P.J. Reilly. 1980. Purification and immobilization of *Aspergillus niger* ß-xylosidase. *Biotechnol. Bioeng.* **22**:1127-42.

Ong, E., N.R. Gilkes, R.A.J. Warren, R.C. Miller, Jr. & D.G. Kilburn. 1989a. Enzyme immobilization using the cellulose-binding domain of a *Cellulomonas fimi* exoglucanase. *Bio/Technology* **7**:604-07.

Ong, E., J.M. Greenwood, N.R. Gilkes, D.G. Kilburn, R.C. Miller, Jr. & R.A.J. Warren. 1989b. The cellulose-binding domains of cellulases: tools for biotechnology. *Trends Biotechnol.* **7**:239-43.

Ong, E., N.R. Gilkes, R.C. Miller, Jr., R.A.J. Warren & D.G. Kilburn. 1991. Enzyme immobilization using a cellulose-binding domain: properties of a ß-glucosidase fusion protein. *Enzyme Microb. Technol.* **13**:59-65.

Ooshima, H., M. Sakata & Y. Harano. 1983. Adsorption of cellulase from *Trichoderma viride* on cellulose. *Biotechnol. Bioeng.* **24**:3103-14.

Ostrove, S. 1990. Affinity chromatography: general methods. *Methods Enzymol.* **182**:357-71.

Otter, D.E., P.A. Munro, G.K. Scott & R. Geddes. 1989. Desorption of *Trichoderma reesei* cellulase from cellulose by a range of desorbents. *Biotechnol. Bioeng.* **34**:291-98.

Owolabi, J.B., P. Beguin, D.G. Kilburn, R.C. Miller, Jr. & R.A.J. Warren. 1988. Expression in *Escherichia coli* of the *Cellulomonas fimi* structural gene for endoglucanase B. *Applied Environ. Microbiol.* **54**:518-23.

Patwardhan, V.S. & N.G. Karanth. 1982. Film diffusional influences on the kinetic parameters in packed-bed immobilized enzyme reactors. *Biotechnol. Bioeng.* **24**:763-80.

Peitersen, N., J. Medeiros & M. Mandels. 1977. Adsorption of *Trichoderma* cellulase on cellulose. *Biotechnol. Bioeng.* **19**:1091-94.

Pilz, I., E. Schwarz, D.G. Kilburn, R.C. Miller, Jr., R.A.J. Warren & N.R. Gilkes. 1990. The tertiary structure of a bacterial cellulase determined by small-angle x-ray scattering analysis. *Biochem. J.* **271**:277-80.

Price, N.C. & C.M. Johnson. 1989. Proteinases as probes of conformation of soluble proteins. In R.J. Beynon & J.S. Bond (ed.) *Proteolytic Enzymes: A Practical Approach.* IRL Press, Oxford.

Quiocho, F.A. & N.K. Vyas. 1984. Novel stereospecificity of the L-arabinose-binding protein. *Nature* **310**:381-86.

Quiocho, F.A. 1986. Carbohydrate-binding proteins: tertiary structures and protein-sugar interactions. *Ann. Rev. Biochem.* **55**:287-315.

Quiocho, F.A. 1988. Molecular features and basic understanding of protein-carbohydrate interactions: the arabinose-binding protein-sugar complex. *Current Topics Microbiol. Immunol.* **139**:135-48.

Reiken, S.R., R.J. Knob & D.M. Briedis. 1990. Evaluation of intrinsic kinetics in hollow fiber reactor systems. *Enzyme Microb. Technol.* **12**:736-42.

Roda, A., S. Girotti, B. Grigolo, S. Ghini, G. Carrea, R. Bovara, I. Zini & R. Grimaldi. 1991. Microdialysis and luminescent probe: analytical and clinical aspects. *Biosensors & Bioelectronics* **6**:21-30.

Ross, P., R. Mayer & M. Benziman. 1991. Cellulose biosynthesis and function in bacteria. *Microbiol. Rev.* **55**:35-58.

Rouvinen, J., T. Bergfors, T. Teeri, J.K.C. Knowles & T.A. Jones. 1990. Three-dimensional structure of cellobiohydrolase II from *Trichoderma reesei*. *Science* **249**:380-86.

Roy, F. & M.V. Hegde. 1987. Immobilization of ß-amylase on polystyrene cation exchange resin equilibrated with Al^{3+} ions (IR-120 Al^{3+}). *Enzyme Microb. Technol.* **9**:550-52.

Roy, S.K., S.K. Raha, S.K. Dey & S.L. Chakrabarty. 1989. Immobilization of ß-glucosidase from *Myceliophthora thermophila* D-14. *Enzyme Microb. Technol.* **11**:431-35.

Sambrook, J., E.F. Fritsch & T. Maniatis. 1989. *Molecular Cloning: A Laboratory Manual*, 2nd ed. Cold Spring Harbor Laboratory Press, New York.

Sanger, F., S. Nicklen & A.R. Coulson. 1977. DNA sequencing with chain terminating inhibitors. *Proc. Natl. Acad. Sci. USA* **74**:5463-67.

Sarko, A. 1986. Recent x-ray crystallographic studies of celluloses. In R.A. Young & R.M. Rowell (ed.) *Cellulose: Structure, Modification and Hydrolysis*. Wiley, New York, pp. 29-49.

Sassenfeld, H.M. 1990. Engineering proteins for purification. *Trends Biotechnol.* **8**:88-93.

Schägger, H. & G. von Jagow. 1987. Tricine-sodium dodecyl sulfate-polyacrylamide gel electrophoresis for the separation of proteins in the range from 1 to 100 kDa. *Anal. Biochem.* **166**:368-79.

Scopes, R.K. 1974. Measurement of protein by spectrophotometry at 205nm. *Anal Biochem.* **59**:277-82.

Sharma, S. & H. Yamazaki. 1984. Preparation of hydrophobic cotton cloth. *Biotechnol. Lett.* **6**:301-06.

Shen, H., M. Schmuck, I. Pilz, N.R. Gilkes, D.G. Kilburn, R.C. Miller, Jr. & R.A.J. Warren. 1991. Deletion of the linker connecting the catalytic and cellulose-binding domains of endoglucanase A (CenA) of *Cellulomonas fimi* alters its conformation and catalytic activity. *J. Biol. Chem.* **266**:11335-40.

Skoog, B. & A. Wichman. 1986. Calculation of the isoelectric points of polypeptides from the amino acid composition. *Trends Anal. Chem.* **5**:82-83.

Spurlino, J.C., G.Y. Lu & F.A. Quiocho. 1991. The 2.3-A resolution structure of the maltose- or maltodextrin-binding protein, a primary receptor of bacterial active transport and chemotaxis. *J. Biol. Chem.* **266**:5202-19.

Ståhlberg, J., G. Johansson & G. Pettersson. 1991. A new model for enzymatic hydrolysis of cellulose based on the two-domain structure of cellobiohydrolase I. *Bio/Technology* **9**:286-90.

Steiner, W., W. Sattler & H. Esterbauer. 1988. Adsorption of *Trichoderma reesei* cellulase on cellulose: experimental data and their analysis by different equations. *Biotechnol. Bioeng.* **32**:853-65.

Stoll, V.S. & J.S. Blanchard. 1990. Buffers: principles and practice. *Methods Enzymol.* **182**:24-38.

Strandberg, G.W. & K.L. Smiley. 1972. Glucose isomerase covalently bound to porous glass beads. *Biotechnol. Bioeng.* **14**:509-13.

Stuart, J.Y. & D.L. Ristroph. 1985. Analysis of cellulose-cellulase adsorption data: a fundamental approach. *Biotechnol. Bioeng.* **27**:1056-59.

Svensson, B., H. Jespersen, M.R. Sierks & E.A. MacGregor. 1989. Sequence homology between putative raw-starch binding domains from different starch-degrading enzymes. *Biochem. J.* **264**:309-11.

Tabor, S. & C.C. Richardson. 1987. DNA sequence analysis with a modified bacteriophage T7 DNA polymerase. *Proc. Natl. Acad. Sc. USA.* **84**:4767-71.

Taylor, R.F. (ed.) 1991. *Protein Immobilization.* Dekker, New York.

Taylor, R.F. 1991. Immobilized antibody- and receptor-based biosensors. In R.F. Taylor (ed.) *Protein Immobilization.* Dekker, New York, pp.263-318.

Tomar, M. & K.A. Prabhu. 1985. Immobilization of glucoamylase on DEAE-cellulose activated with chloride compounds. *Enzyme Microb. Technol.* **7**:557-60.

Tull, D., S.G. Withers, N.R. Gilkes, D.G. Kilburn, R.A.J. Warren & R. Aebersold. 1991. Glutamic acid 274 is the nucleophile in the active site of a "retaining" exoglucanase from *Cellulomonas fimi*. *J. Biol. Chem.* **266**:15621-25.

Vieira, J. & J. Messing. 1982. The pUC plasmids, an M13mp7-derived system for insertion mutagenesis and sequencing with synthetic universal primers. *Gene* **19**:259-68.

Wakarchuk, W.W., D.G. Kilburn, R.C. Miller, Jr. & R.A.J. Warren. 1986. The molecular cloning and expression of a cellobiase gene from an *Agrobacterium* in *Escherichia coli*. *Mol. Gen. Genet.* **205**:146-52.

Wakarchuk, W.W., N.M. Greenberg, D.G. Kilburn, R.C. Miller, Jr. & R.A.J. Warren. 1988. Structure and transcription analysis of the gene encoding a cellobiase from *Agrobacterium* sp. strain ATCC 21400. *J. Bacteriol.* **170**:301-07.

Webster, I.A., C.E. Schwier & F.S. Bates. 1985. Using the rotational masking concept to enhance substrate inhibited reaction rates: controlled pore supports for enzyme immobilization. *Enzyme Microb. Technol.* **7**:266-74.

Withers, S.G. & I.P. Street. 1988. Identification of a covalent α-D-glucopyranosyl enzyme intermediate formed on a ß-glucosidase. *J. Am. Chem. Soc.* **110**:8551-53.

Withers, S.G., I.P. Street & D.H. Dolphin. 1987. 2-deoxy-2-fluoroglucosides: a novel class of mechanism-based glucosidase inhibitors. *J. Amer. Chem. Soc.* **109**:7530-31.

Withers, S.G., K. Rupitz & I.P. Street. 1988. 2-deoxy-2-fluoro-D-glycosyl fluorides: a new class of specific mechanism-based glycosidase inhibitors. *J. Biol. Chem.* **263**:7929-7932.

Wong, W.K.R., B. Gerhard, Z.M. Guo, D.G. Kilburn, R.A.J. Warren & R.C. Miller, Jr. 1986. Characterization and structure of an endoglucanase gene *cenA* of *Cellulomonas fimi*. *Gene* **44**:315-24.

Wood, T.M. 1988. Preparation of crystalline, amorphous and dyed cellulase susbstrates. *Methods Enzymol.* **160**:19-25.

Woodward, J. & G.S. Zachry. 1982. Immobilization of cellulase through its carbohydrate side chains - a rationale for its recovery and reuse. *Enzyme Microb. Technol.* **4**:245-48.

Woodward, J., M.K. Hayes & N.E. Lee. 1988. Hydrolysis of cellulose by saturating and non-saturating concentrations of cellulase: implications for synergism. *Bio/Technology* **6**:301-04.

Yannish-Perron, C., J. Vieira & J. Messing. 1985. Improved m13 phage cloning vectors and host strains: nucleotide sequence of the m13mp18 and pUC19 vectors. *Gene* **33**:103-19.

Yoshida, Y., M. Kawase & T. Shiraishi. 1990. Synthesis of branched cyclodextrin with immobilized enzyme bioreactor. *Hakkokogaku Kaishi* **68**:197-204.